FACTORS AFFECTING THE RATE OF DIELECTRIC RECOVERY OF POWER ARCS IN LONG AIR GAPS

Thesis by

Harry M. Ellis

In Partial Fulfillment of the Requirements

For the Degree of

Doctor of Philosophy

California Institute of Technology

Pasadena, California

1950

ACKNOWLEDGMENT

The author wishes to express his sincere appreciation for the guidance given by Professor G. D. McCann. He is greatly indebted to Mr. J. E. Conner for his tireless efforts in helping obtain the data and for his encouragement during the preparation of the thesis. He also acknowledges the valuable assistance of Mr. Sol Matt and Mr. W. C. Duesterhoeft in obtaining the data and the laboratory assistants who helped with the equipment construction. The high-speed photographic study was made possible by the excellent photographic work of Mr. D. H. Peterson. The author wishes to acknowledge the valuable assistance rendered by the Kelman Electric and Manufacturing Co., the Southern California Edison Co., and the Department of Water and Power of the City of Los Angeles. Their interest in improving the insulation co-ordination of transmission lines made this research possible. The author is indebted to Miss Dorothy Denhard for preparing the figures and to Miss Mary Stockly for typing the thesis.

SUMMARY

A satisfactory testing technique is developed for investigating the recovery characteristics of various power system insulations.

Duration of the fault current, for a vertical test gap, has little effect on the dielectric recovery. Five cycle fault current duration decreases the initial rate of recovery, for a horizontal test gap, below that for a half cycle, but for longer time delays thermal convection increases the rate of recovery above that for a half cycle duration.

The 11 inch test gap has a lower percentage recovery than the 6 inch test gap. The lower the boiling point and the lower the ionization potential of the electrode material, the lower the rate of recovery.

The increase in the rate of recovery produced by winds up to 1000 feet per minute is mainly due to displacement of the ionized gases from the test electrodes. For recovery based on this displacement of the ionized gases from the electrodes, the axial wind recovery should be half of the perpendicular. However, the axial wind decreases the cross section of the arc, heat transfer away from the ionized gases is increased, and the axial recovery is greater than half of the perpendicular recovery. Wind velocities less than 100 feet per minute have a negligible effect on the dielectric recovery characteristics.

A 3000 frame per second camera is used to make a high speed photographic study of the arc. By using a system of mirrors, two mutually perpendicular views of the arc are obtained simultaneously, on each frame of the film. Breakdown occurs in the weakest path through the

ionized gases, even though this path is 2 to 3 times as long as the electrode separation.

The extent of ionization of the luminous gases is obtained with the aid of a microphotometer by taking density readings directly from the image of the arc on the 16 mm. negative film. The average density variation with time follows the general shape of the curve based on diffusion as the only important deionizing agent, for a short time after current zero.

The local coefficient of heat transfer obtained from the analogy of the arc to a hot cylindrical solid body increases with the wind velocity and the density of ionization of the luminous gases decreases with increasing wind velocity.

The diameter and density of the arc are obtained from the photographic study and the recovery voltage calculated, at various time delays, from Slepian's theory for the critical breakdown gradient of the arc column. The results are in general qualitative agreement with the experimental results.

The minimum reclosing time for high-speed automatic-reclosing circuit breakers on a transmission system can be reduced by a factor of five for a wind of 1000 feet per minute (15 miles per hour) blowing across the ionized fault path.

CONTENTS

ILLUSTRATIONS

I A REVIEW OF PREVIOUS INVESTIGATIONS

One of the most important design considerations of transmission and distribution engineers is to improve system reliability. Transmission and distribution line flashovers -- caused by direct or induced lightning strokes, switching surges or arcing grounds -- require removal of the line from service long enough so that the arc does not restrike when the line is re-energized. However, just as there is a minimum time for which the line must be de-energized to allow the arc path to recover sufficient dielectric strength, there is a maximum time after which the transient stability limit of the line is exceeded and the generating station loses synchronism with the rest of the electrical system.

In large industrial centers, it is very important to prevent power outages because of the expense incurred by the users of the power in loss of plant operation. The frequency of these outages has been reduced by improved insulation co-ordination of systems through knowledge of the impulse characteristics of station and line type insulations[1,2,3,4] and through the correct application of lightning arresters and de-ion protector tubes[5,6,7,8,9,10]. Greater dependability of transmission line operation has also been obtained by the application of high-speed automatic-reclosing circuit breakers. After the fault on the transmission line has been cleared the re-closing circuit breakers reconnect the two parts of the system before the angular

displacement between them becomes large enough to cause a major power outage[11,12].

Thus, the reliability of service to the customer is improved and the maximum power which can be safely transmitted over high voltage lines is increased. Originally the limitation in the application of automatic-reclosing circuit breakers was the operating speed of the reclosing mechanism which was about 35 cycles. Prince and Sporn[13] found that 12 cycles of de-energized time was required, for faults lasting 8 cycles, to prevent reignition of the arc when the breaker reclosed. As the pneumatic reclosing mechanisms of the high-speed circuit breakers were improved, reclosing times were reduced to less than 9 cycles. Then the limitation on reclosing time became the deionizing time required for the arc path to recover its dielectric strength. Boisseau, Wyman and Skeats[14] determined minimum insulator-flashover deionizing times at various currents and voltages by supplying the fault current from one voltage source and the re-energizing potential from a second voltage source. The required de-energized time was less than 10 cycles for 69KV to 230KV insulator strings at fault currents up to 10,000 amperes and it was independent of the fault current duration. The effect of capacitive current, induced from the other two phases, on the minimum time for single phase reclosure has been investigated by Maury[15]. He found that dielectric recovery is not seriously retarded by capacitive current for 220KV lines less than 100 miles in length.

Except for the determination of minimum reclosing times for high-speed automatic-reclosing circuit breakers very little work has been done on the study of the dielectric recovery characteristics of long arcs. Slepian has defined the long arc as that arc in which the larger part of the dielectric recovery strength, during extinction and deionization, resides away from the cathode space; thus differentiating it from the short arc which recovers instantly to 200 volts in the cathode space at current zero[16] while the remainder of the arc space contributes negligibly to the dielectric strength.

In his paper, "Extinction of the Long A. C. Arc", Slepian[17] gives the following theory for deionization and extinction of long arcs. If the arc column is to maintain its conductivity after current zero in the long a.c. arc the ionizing agents, which depend directly upon the gradient of the electric field, must produce ions sufficiently rapidly to replace those lost by diffusion to the boundary and by direct recombination of ions of opposite sign within the arc space. The critical electric field gradient, which varies inversely with the density of ionization of the arc space, is obtained when the conductivity of the arc space is just maintained, or when the rate of loss of energy from the arc just equals the rate of energy input from the applied electric field. The rate of energy input from the electric field per unit length of the arc column is

$$W_2 = XI$$

where X = electric field

I = total current produced by the ion motion.

$$= k\ X\ n\ e\ \frac{(\pi a^2)}{4}$$

where

k = a constant of the gas depending on temperature and pressure.

a = diameter of the arc section.

n = average density of ions of one sign per unit length of arc.

e = charge of the electron

therefore,

$$W_2 = k\ X^2\ e\ n\ \frac{(\pi a^2)}{4}$$

It is assumed that no thermal ionization occurs until the gas reaches a critical temperature, T_o, and that ionization increases rapidly with further increase of temperature[18,19]. During the extinction period of the a.c. arc the temperature of the arc column falls below the critical temperature, T_o, and thermal ionization ceases. Energy continues to be lost by recombination and diffusion of the ions and also by loss of energy of the unionized column of gas in the arc. This rate of thermal loss of energy per unit length of the arc column, W_3, is an increasing function of the temperature. The value of W_3 at the critical temperature, T_o, is W_o, which is proportional to the arc perimeter, or

$$W_o = C \pi a.$$

where

C = a constant for the gas.

If the electrical input, W_2, is greater than W_o, then the temperature may rise to T_o and the condition for arc reignition is satisfied. The critical breakdown gradient is determined from the condition,

$$W_2 = W_o$$

or

$$\frac{\pi a^2}{4} k X_c^2 e n = C \pi a$$

and

$$X_c = \frac{D}{a^{\frac{1}{2}} n^{\frac{1}{2}}} .$$

where

D = a constant for the gas.

If the principal rate at which ions continue to be lost after current zero is by recombination, then

$$-\frac{\pi}{4} a^2 \frac{dn}{dt} = \frac{\pi}{4} a^2 n^2$$

$$\frac{dn}{dt} = n^2 \alpha$$

and

$$n = \frac{1}{\alpha t}$$

where

α = the coefficient of recombination which varies inversely as the cube of the absolute temperature.

$\frac{1}{n_o}$ = the reciprocal of the initial density of ionization is neglected

therefore

$$X_c = \frac{D}{a^{\frac{1}{2}}} \alpha^{\frac{1}{2}} t^{\frac{1}{2}}$$

If the principal loss of ions is by diffusion, then

$$-\frac{\pi}{4} a^2 \frac{dn}{dt} = A\pi a n$$

$$\frac{dn}{dt} = -\frac{4A\ n}{a}$$

and

$$n = N_o e^{\frac{4A}{a} t}$$

therefore

$$X_c = \frac{D}{a^{\frac{1}{2}} N_o^{\frac{1}{2}}} e^{\frac{2A}{a} t}$$

According to Slepian's theory of diffusion[20] the function of an air blast in accelerating the deionization of the arc space is to create a high degree of turbulence prior to current zero which enhances thermal conduction and ion diffusion. Turbulence breaks up the highly ionized conducting gas into fine filaments interspersed with masses of much less intensely ionized gas which has been deionized by recent contact with the bounding walls or has been freshly introduced. At current zero the highly conducting regions rapidly lose their density of ionization by diffusion into the adjacent non-conducting gas, thus producing more uniform and much lower maximum density of ionization and therefore a higher breakdown gradient than without the air blast.

Browne[21] obtained evidence supporting this enhanced diffusion theory

of dielectric recovery. He produced turbulence in a cylindrical chamber by causing the arc to rotate under the influence of an external magnetic field. In experiments with air as the dielectric, he found that the rate of recovery was directly proportional to the speed of rotation of the arc (up to 600 meters per second). In later experiments to determine the recovery characteristics of air blast circuit breakers, Browne[22] found two stages of dielectric recovery. The very rapid recovery in the first stage was attributed to the enhanced diffusion of ions from high intensity to regions of low intensity. The rate of recovery in this stage was determined by the degree of turbulence in the arc prior to current zero. The recovery in the second stage was much slower and was due to diffusion of ions to surrounding surfaces and recombination of ions within the arc column. The above theory does not agree with the displacement theory of Prince[23] which states that the dielectric recovery characteristics of the oil blast circuit breaker are directly proportional to the velocity of the oil blast directed at the arc. Hence, recovery is the result of cool unionized oil driving a wedge of high dielectric strength into the arc.

II DESCRIPTION OF EQUIPMENT AND EXPERIMENTAL RESULTS

In order to investigate the dielectric recovery characteristics of long power arcs in various insulation media an extensive research program was instigated at the High Voltage Laboratory of the California Institute of Technology. This research was sponsored on a co-operative basis by the Department of Water and Power of the City of Los Angeles, the Southern

California Edison Company, and the Kelman Electric and Manufacturing Company.

2.1 Tests Using Actual System Recovery Voltage.

The first phase of this research program was to determine the dielectric recovery characteristics of air. An attempt was made to study directly the reignition characteristics of standard rod gaps up to 11 inches in length. A schematic diagram of the circuit used to obtain this data is shown in Fig. 1. The test procedure consisted of breaking down the test gap with a surge generator which then allowed power current to flow through the test gap at a magnitude determined by the system voltage and the current-limiting reactors. The length of the gap and the system natural frequency were then adjusted until the rate of recovery of dielectric strength of the air gap was just sufficient to extinguish the arc at the first current zero. A point on the recovery curve was then obtained by measuring the time to crest and the crest magnitude of the system recovery voltage.

This technique has been used earlier[24,25] in determining the recovery characteristics of short arcs, but because of the relatively slow rate of recovery of long arcs, the inflexibility of the testing equipment, and the difficulty in obtaining dependable results (see Appendix I for previous publication of these results), a new testing technique was developed.

2.2 Two Surge Generator Testing Technique.

This new testing technique, which is an adaptation of that used by McCann and Clark [26], makes possible accurate control of the

FIG. 1
SCHEMATIC DIAGRAM OF CIRCUIT
FOR OBTAINING NATURAL RECOVERY

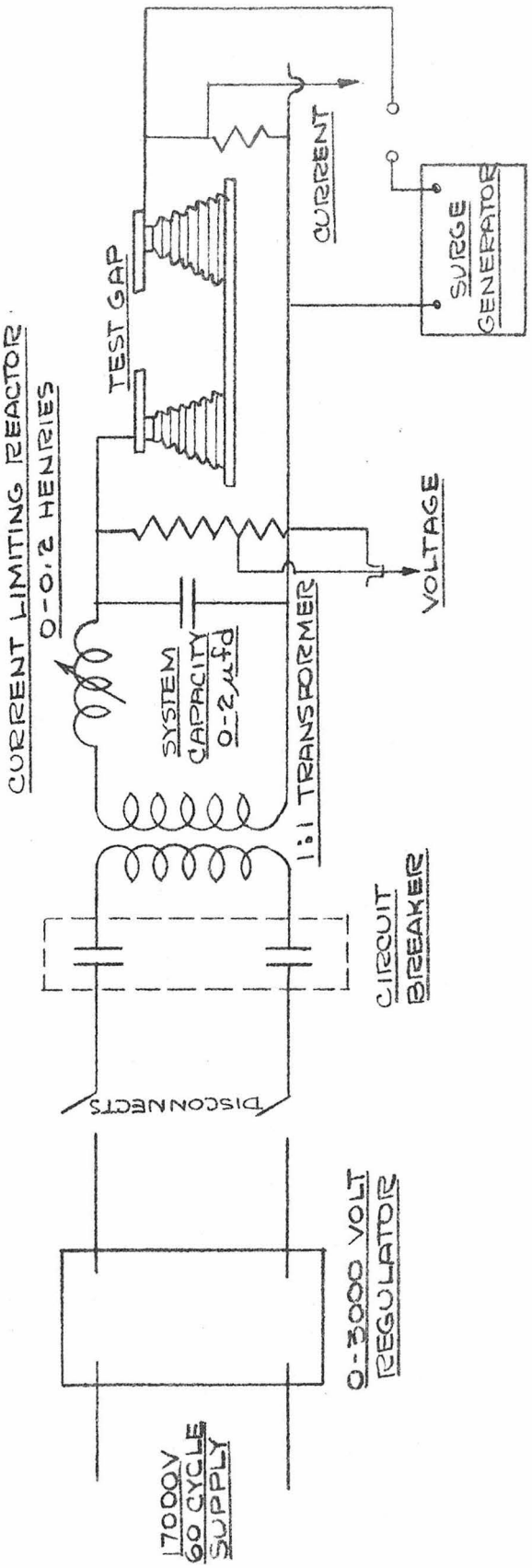

magnitude and duration of the fault current. This control is independent of the reignition test voltage and also eliminates the extra complication of varying the system natural frequency in conjunction with the magnitude of the fault current. The dielectric is first broken down by the No. 1 or constant-voltage surge generator, which then allows fault current to flow at the desired magnitude and for the required number of half- cycles of 60-cycle power; then the rate of dielectric recovery of the medium is tested over a wide range of time delays with the No. 2 or variable-voltage surge generator, and the dielectric recovery curve is obtained as shown schematically in Fig. 2.

A general schematic diagram of the test circuit is shown in Fig. 3, and a photograph of the main part of the power circuit is shown in Fig. 4. The 60-cycle power is supplied by a 17KV single phase line through an induction regulator to 4-150 KVA power transformers. By various connections of the power transformers, adjustment of the induction regulator voltage, and by varying the tap of the 0-60 ohm current-limiting reactors, fault currents up to 2000 amperes can be obtained.

The duration of the fault current is determined by the inverse-parallel ignitron circuit shown in Fig. 6. The control of the ignitrons is similar to that of an electric welder except that the auxiliary FG 105 thyratrons are biased to cut-off by the following timing control circuit. A pulse from No. 1 surge generator is applied to the single-shot multivibrator shown in Fig. 5. The plate-to-grid RC coupling time constant of the multivibrator, which controls the time delay for the output pulse, is varied by changing the value of the condenser. This output

FIG. 2

SCHEMATIC DIAGRAM OF TWO SURGE GENERATOR TEST TECHNIQUE

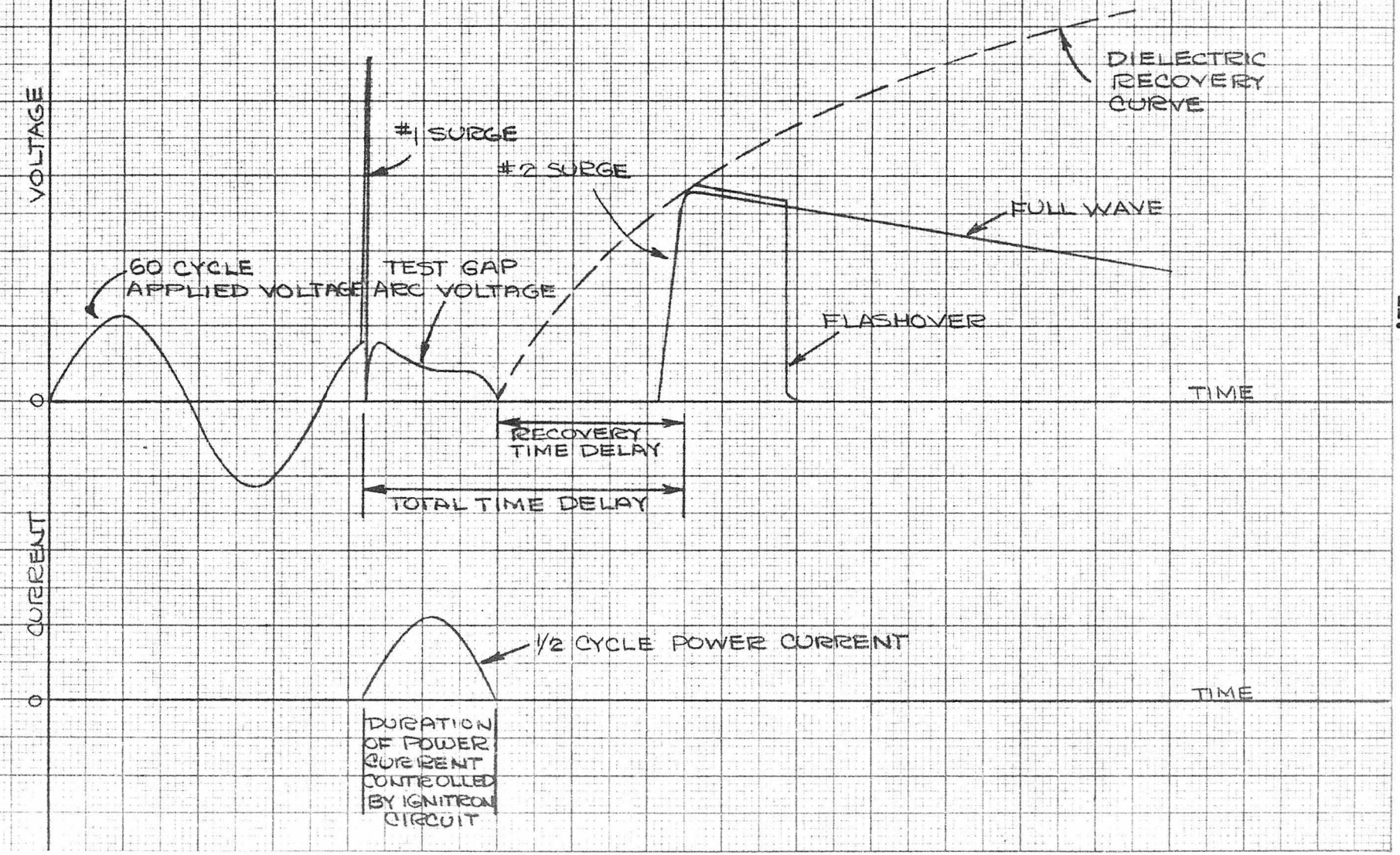

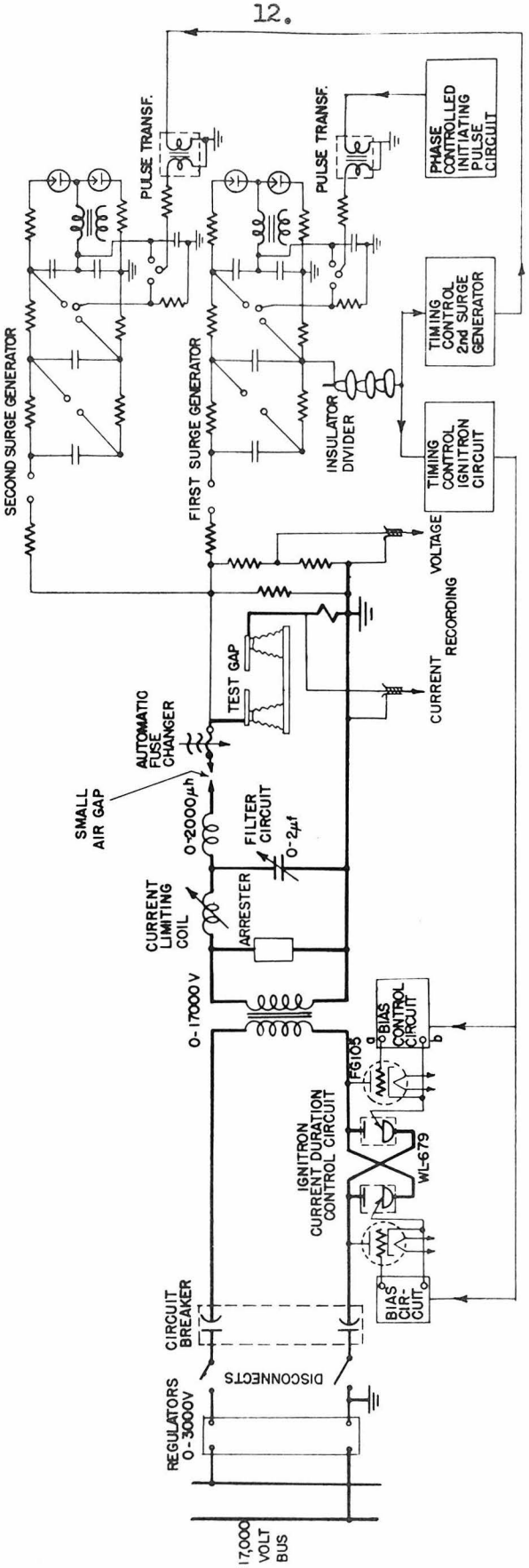

FIG. 3 SCHEMATIC DIAGRAM OF DIELECTRIC RECOVERY CIRCUIT FOR TWO SURGE GENERATOR TEST TECHNIQUE

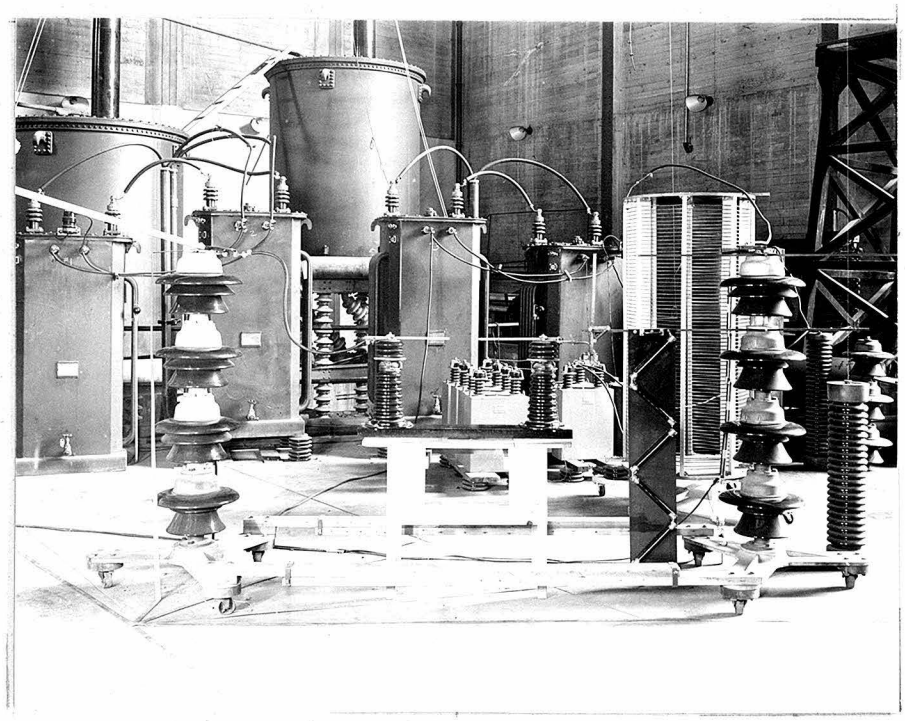

Fig. 4

Photograph of Main Part of
Power Circuit

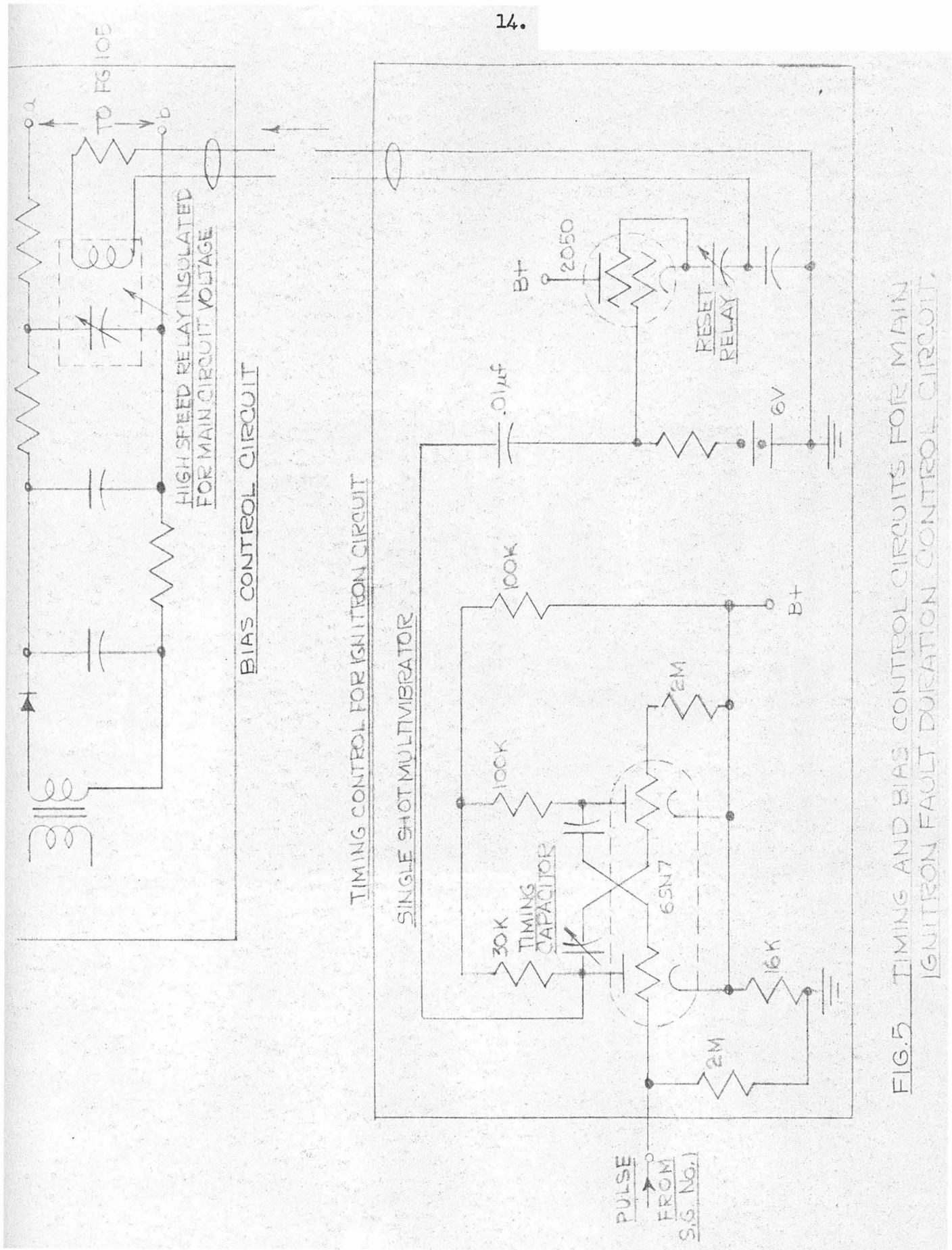

FIG.5 TIMING AND BIAS CONTROL CIRCUITS FOR MAIN IGNITRON FAULT DURATION CONTROL CIRCUIT.

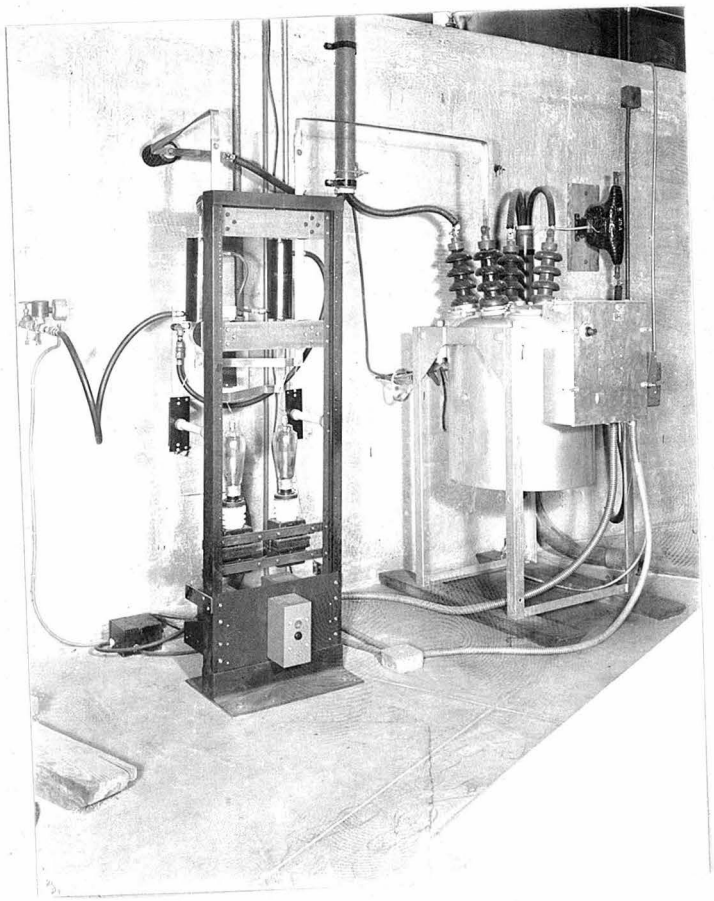

Fig. 6

Photograph of Ignitron Control Circuit

pulse is applied to the grid of a 2050 thyratron which supplies current to two high speed relays in its plate circuit. Normally-closed contacts on the relays open in less than 5 milliseconds and apply the negative bias directly to the FG 105 thyratrons. Thus, any number of half-cycles of power current can be obtained by suitable adjustment of the timing condenser. Originally 2050 thyratrons were tried in place of the high speed relays but induced pulses from the 60-cycle power circuit fired the 2050 thyratrons and biased the FG 105 thyratrons to cut-off, which prevented current flow in the ignitron tubes.

A typical test shot is initiated by tripping the No. 1 surge generator which breaks down the test gap. In order to accurately synchronize the tripping of the generator with the 60 cycle power source an electrical trip circuit, which has no appreciable time delay, is necessary. This electrical trip, shown in Fig. 7, consists of a phase-shifting selsyn and a peaking transformer, which apply an 8 KV pulse to the radar pulse transformer through a thyratron circuit. The pulse transformer, which has a ratio of 8 KV to 30 KV, and the triple sphere gap used to trip the surge generator are shown in Fig. 8. The two surge generators are basically identical, each, consisting of 10 capacitor banks of .25 microfarads each, connected in a modified Marx circuit. Charging voltages are supplied by two 100 KV voltage-doubling rectifier circuits. (See Fig. 9)

The No. 1 surge generator voltage is adjusted to break down the test gap on the front of the impulse. In order to protect the power transformers from this impulse voltage an L-C filter circuit is used as shown in Fig. 3. The filter circuit constants were determined

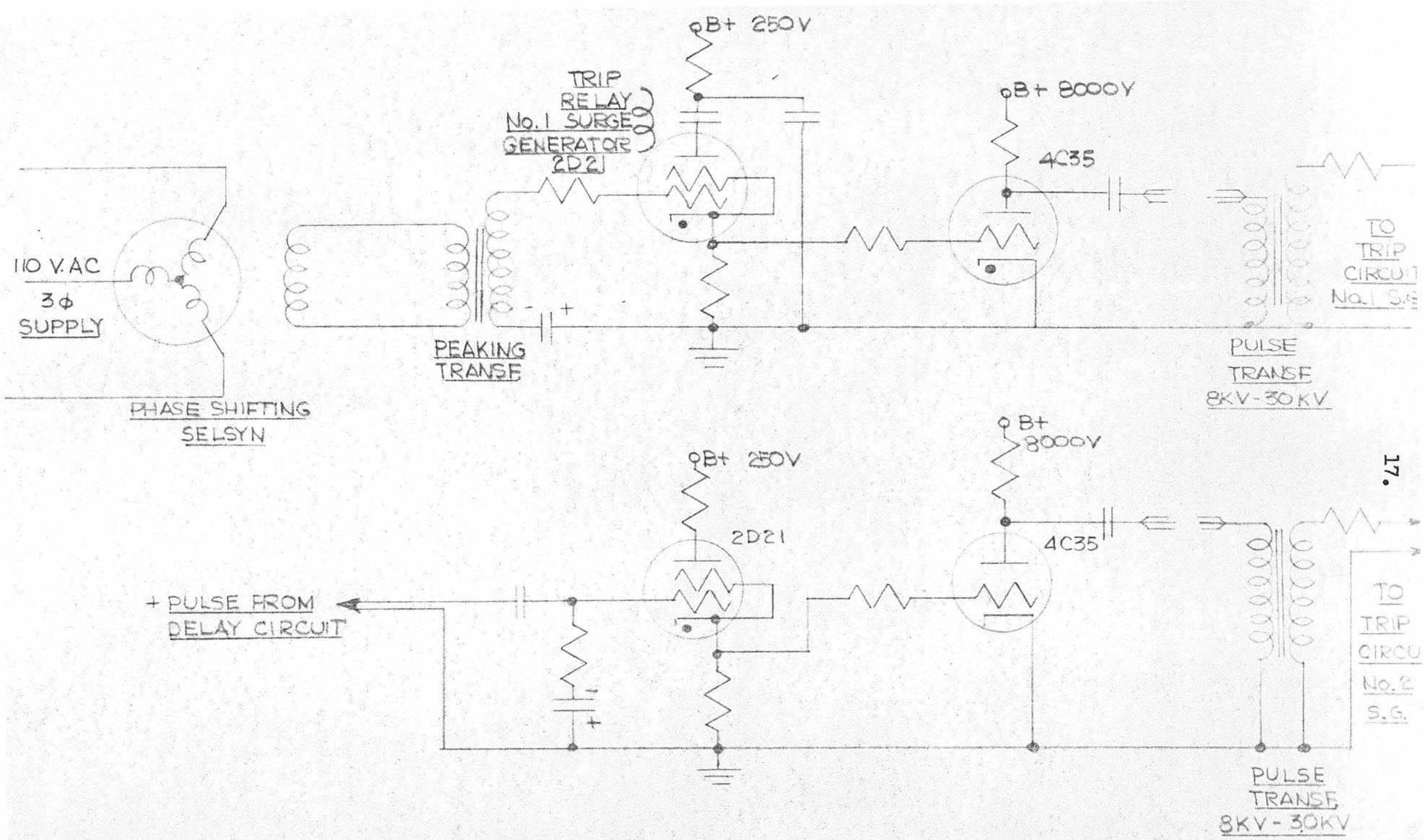

FIG. 7 CONTROL PULSE CIRCUITS FOR TIMING SURGE GENERATOR TRIP CIRCUITS

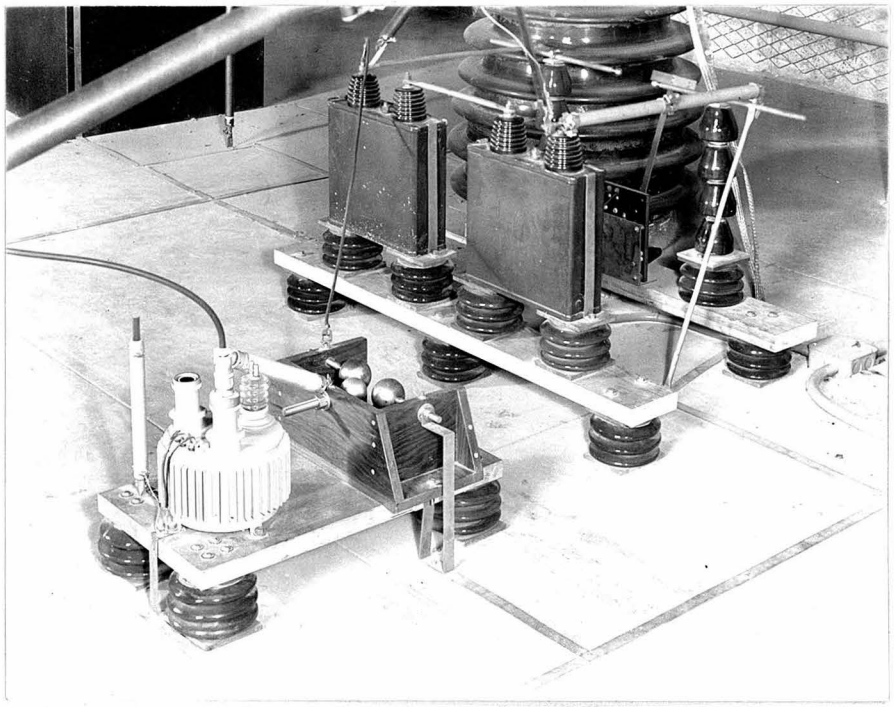

Fig. 8

Photograph of Pulse Transformer
and Triple Sphere Gap Trip
for Surge Generators

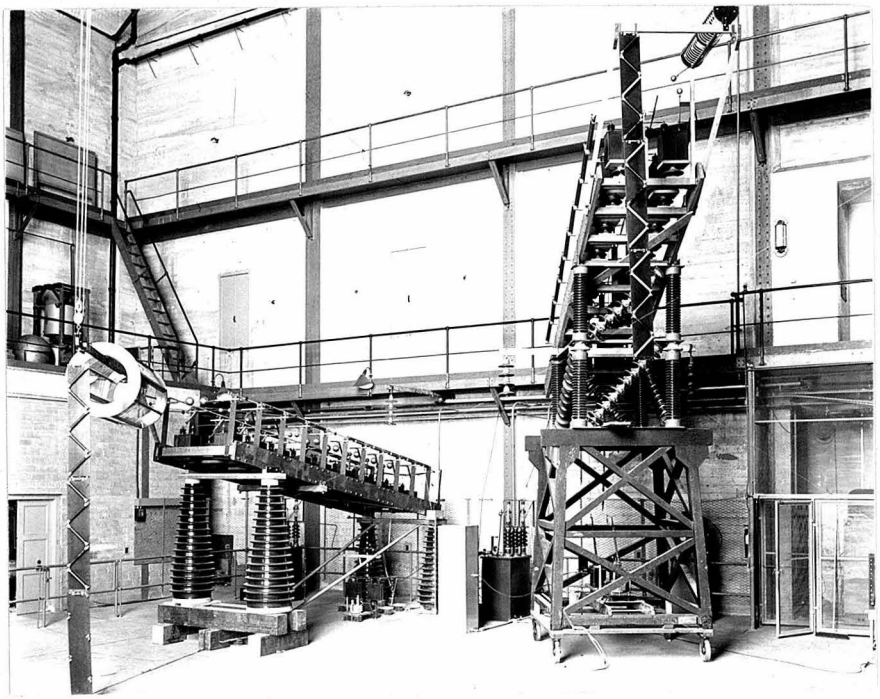

Fig. 9

Photograph of Surge Generators
Left - No. 2 Surge Generator
Right- No. 1 Surge Generator

by the lumped constant method on the analog computer such that the impulse transmitted to the transformer terminals is limited approximately to ten percent of that applied to the test gap.

When the main 60-cycle power circuit of Fig. 3 is energized, the test gap shunt resistors are isolated from the 60-cycle voltage by a small auxiliary air gap to reduce their required power rating. After the test gap has been broken down by No. 1 surge generator and power current has flowed until the specified current zero, the dielectric strength of the gap as a function of time is desired. To prevent distortion of the No. 2 surge generator voltage wave by the power circuit, an automatic fuse changer is placed in series with the main power circuit, as shown in Fig. 3. The fuse gap isolates the power circuit from the test gap when No. 2 surge generator voltage is applied to the gap. Effectively the fuse gap is in parallel with the main test gap and if it does not recover dielectric strength faster than the main gap, then No. 2 surge generator voltage breaks down the fuse gap. The voltage wave then has an oscillating wave tail produced by the L-C filter circuit (see oscillogram test numbers 26, 28, 29 and 32 of Fig. 11, Appendix I). The original fuse changer (see Appendix I) had a fuse length of 12 inches. Because its recovery rate was not sufficiently faster than the recovery of the 11 inch test gap, it was necessary to develop a 26 inch automatic fuse changer. To investigate the effect of wind on the recovery characteristics at a short time after current zero, it was necessary to increase the rate of recovery of the 26 inch fuse gap by directing an air blast across it and into a fiber arc chute, and by adding electrostatic shielding

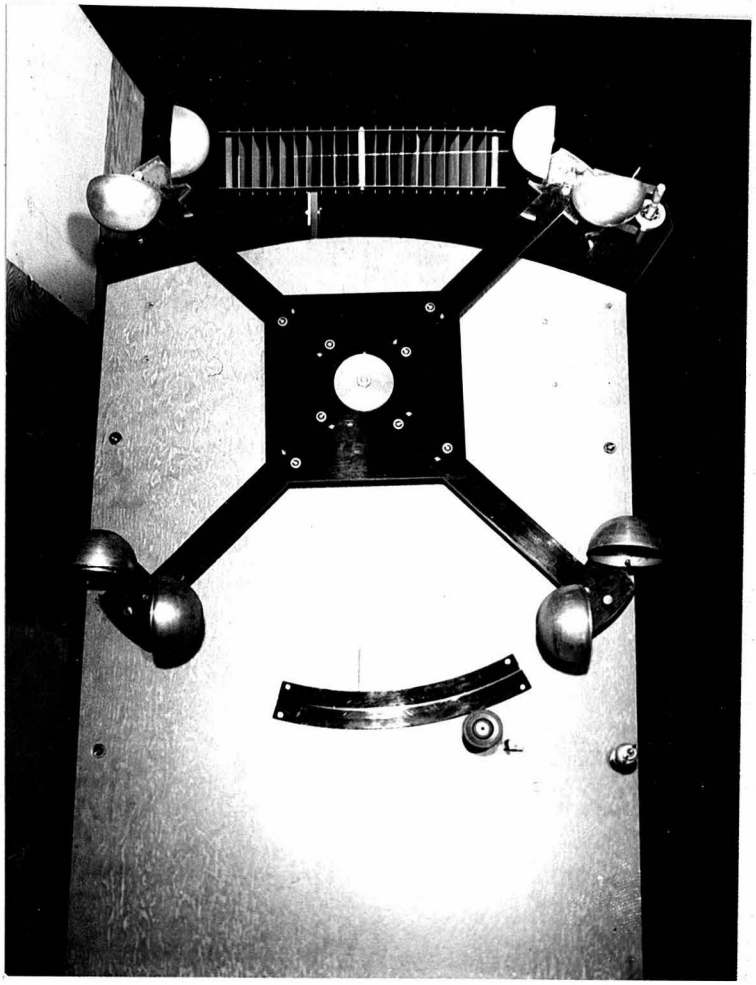

Fig. 10

Photograph of 26 Inch Automatic
Fuse Changer

spheres (see Fig. 10).

A wide range of time delay in tripping No. 2 variable-voltage surge generator is obtained by a delay circuit which is initiated by a pulse from the trip circuit of No. 1 surge generator (see Fig. 3). This time delay circuit, shown in Figs. 11 and 12, consists of a ten stage, scale-of-two, "flip-flop", or Higinbothom circuit. Each stage of this circuit consists of two tubes having two stable states which can be changed from one to the other by an appropriate trigger pulse. One negative pulse is produced by each stage for every two negative pulses applied to it, or for 10 stages a total of 2^{10} or 1024 negative pulses must be applied to the first stage to produce one negative output pulse. The delay time of this circuit can be adjusted from 13,000 microseconds to over one minute by varying the frequency of the oscillator from 80 kilocycles to 80 cycles. Smaller time delays can be obtained by decreasing the number of stages of the circuit.

The initiating pulse from No. 1 surge generator changes the stable state of the 6SN7 gate control tube, which applies a positive bias to the 6SL7 amplifier tube which in turn connects the oscillator to the "flip-flop" circuit (for details of operation, see Fig. 11). At the end of a complete operation of the delay circuit the gate control tube is returned to its cut-off state by a negative pulse from the delay circuit. The negative pulse from the delay circuit is also applied to the trip circuit of No. 2 surge generator through a phase inverter.

The first delay circuit which was constructed contained germanium diode coupling between stages. These diodes did not stand up

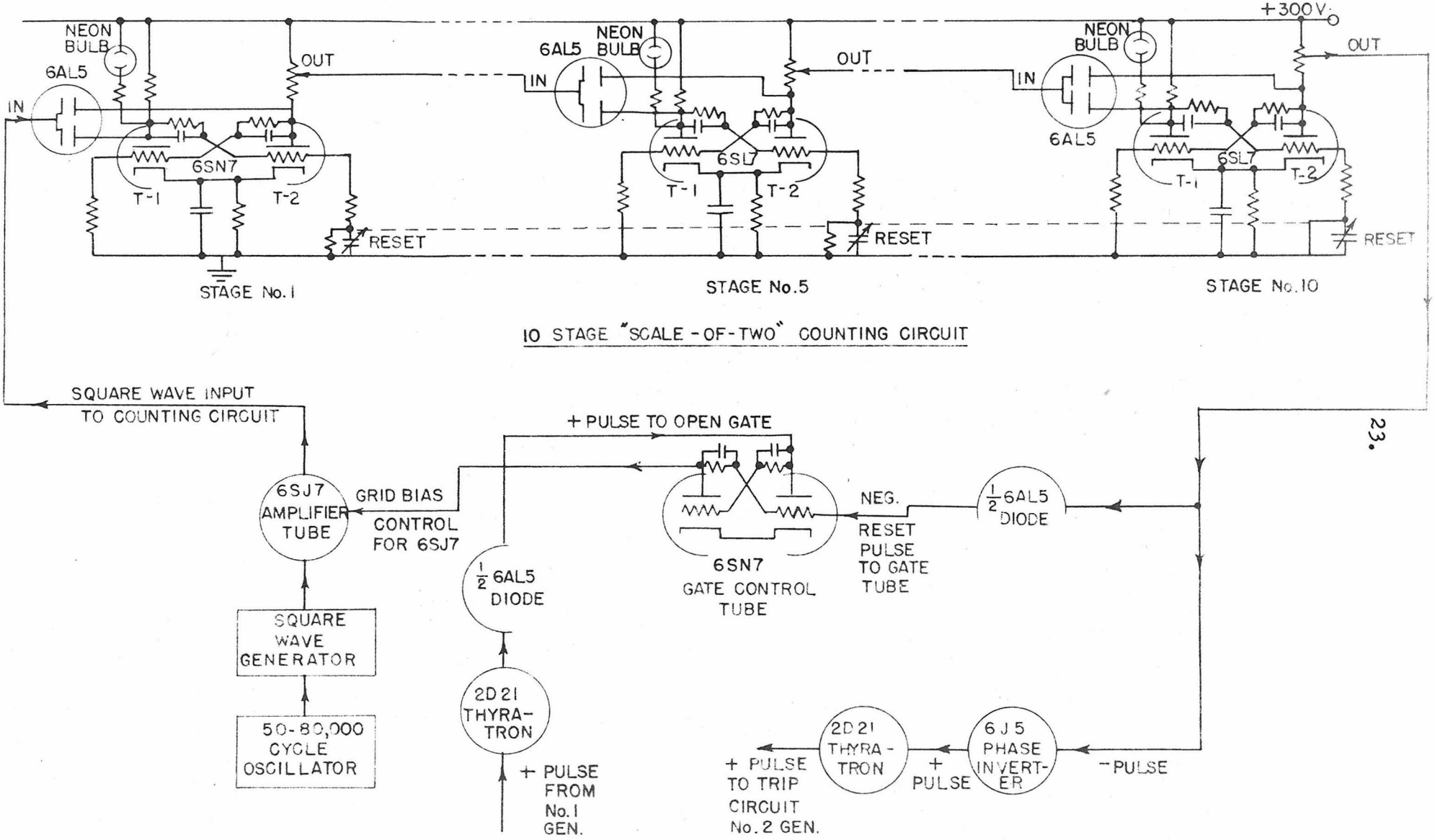

FIG. 11 SCHEMATIC DIAGRAM OF TIMING CONTROL CIRCUIT FOR NO. 2 GENERATOR

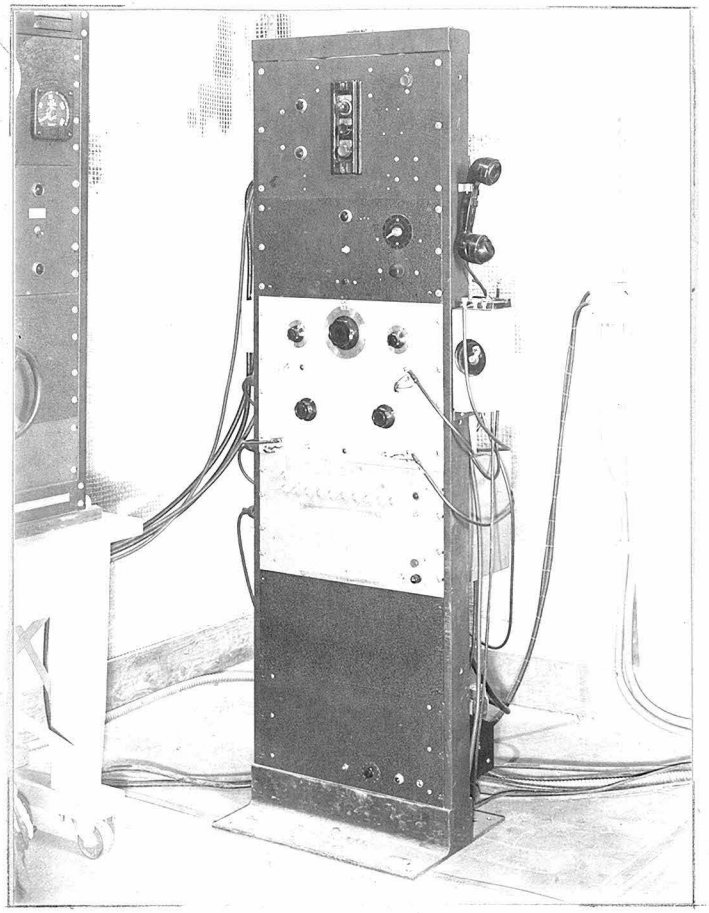

Fig. 12

Photograph of Components of
Time Delay Circuit

to service in the high voltage laboratory and the reason for their failure is probably because of incomplete shielding of the circuit from surges. The germanium diodes, type IN34 and IN38, were replaced by 6AL5 vacuum tube diodes and the Eccles-Jordan plate-to-grid interstage coupling was changed to the Higinbothom plate-to-plate coupling. Then the circuit operated satisfactorily.

No. 2 surge generator voltage is adjusted approximately to the critical value by changing the shunt and series discharge resistors shown in Fig. 3 and also by changing the number of capacitor banks in the generator. As the shunt discharge resistance determines the No. 1 surge generator voltage available to break down the test gap initially, its lower limit is such that the No. 1 surge generator voltage just breaks down the test gap. In order to obtain voltages as low as 5KV with No. 2 surge generator for short time delays after current zero, three banks of capacitors, each consisting of three banks in series, are used with a corresponding change in the discharge resistance to keep the time to half value of the voltage wave tail close to 40 microseconds. All the dielectric recovery data have been obtained with the impulse voltage wave as close to the standard $1\frac{1}{2}$ - 40 microsecond wave as possible. According to experiments performed by Bellaschi and Rademacher[27], the dielectric strength of air for switching transients from 600 to 1000 cycles per second is 90-95 percent of the strength for the $1\frac{1}{2}$ - 40 impulse wave. Therefore, the dielectric recovery curves obtained in this study can be directly applied to transients occurring on transmission and distribution systems.

After the critical breakdown voltage is approximately

determined, the test data, consisting of at least 40 separate records, are obtained over a limited voltage range by varying the 60-cycle charging voltage to the surge generator. Typical data establishing the critical voltage at one point on a dielectric recovery curve are shown in Fig. 13. At the critical voltage shown in the above figure there are an equal number of flashovers and full waves. Above this critical value flashovers predominate and below this value full waves predominate.

In order to study the effect of wind on the dielectric recovery characteristics of the ionized gases produced by the fault current, the main test gap is enclosed in a 14-inch square cross section duct as shown in Fig. 14. The central part of the duct is made of plexiglass so that a photographic study of the arc can be made. This size is selected for the duct because wind velocities up to 1000 feet per minute can be obtained in it with the centrifugal blower which is available, and because the longest electrode spacing to be used is 11 inches. By suitable adjustment of the armature series resistance of the d.c. motor supplying power for the blower, wind velocities of 100, 380, 660, and 1000 feet per minute can be obtained. The wind velocity is measured by means of a hot wire, bridge-type flow meter. By connecting the duct to the suction side of the blower a uniform wind velocity distribution is obtained to within one inch of the duct walls. The entrance end of the duct is flared out to decrease entrance disturbances, but no attempt is made to streamline the electrodes as it is assumed that turbulence produced by them has little effect on the recovery characteristics. For the data obtained with no wind in the duct, the duct was blown out for

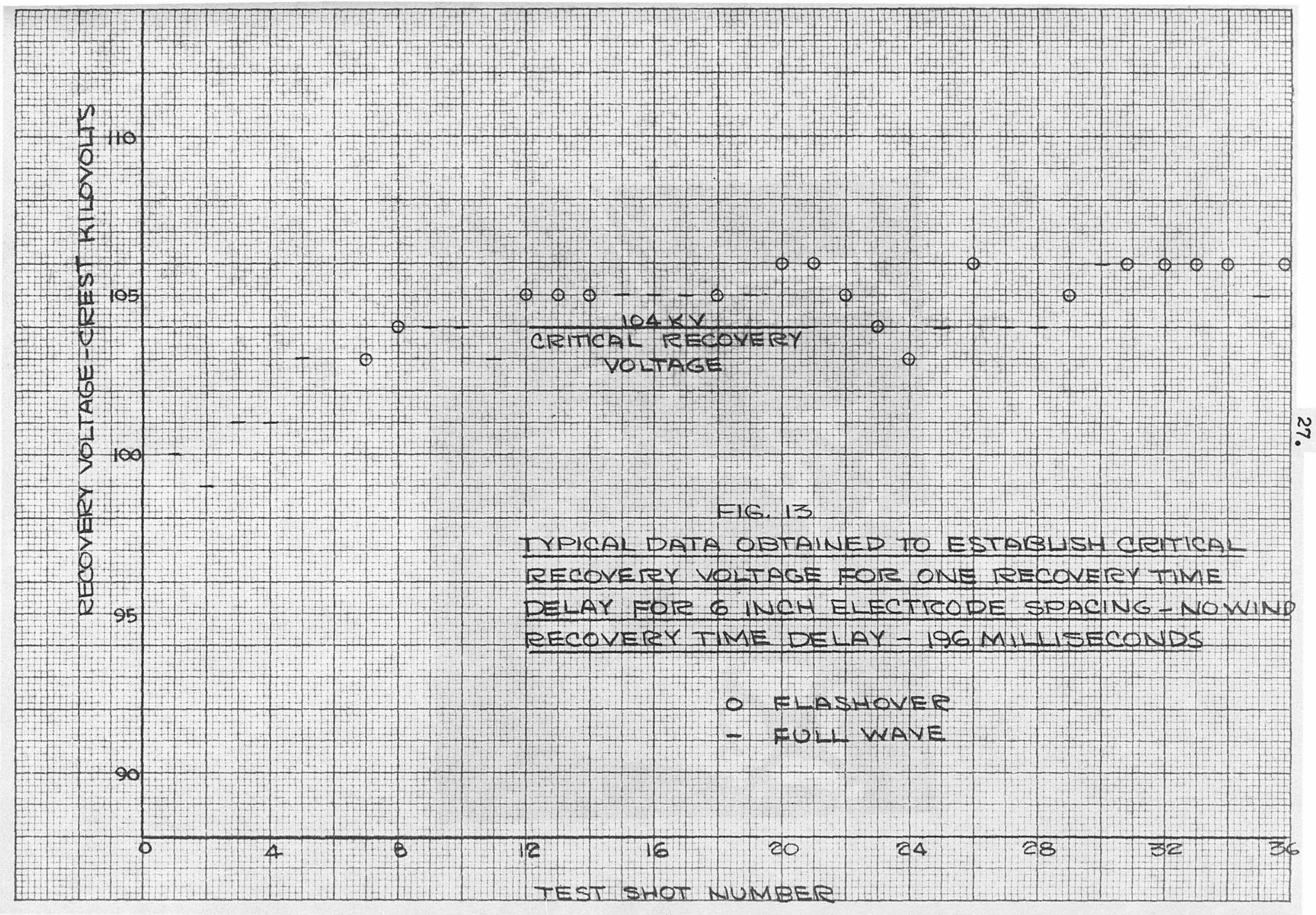

FIG. 13

TYPICAL DATA OBTAINED TO ESTABLISH CRITICAL RECOVERY VOLTAGE FOR ONE RECOVERY TIME DELAY FOR 6 INCH ELECTRODE SPACING - NO WIND

RECOVERY TIME DELAY - 196 MILLISECONDS

O FLASHOVER

\- FULL WAVE

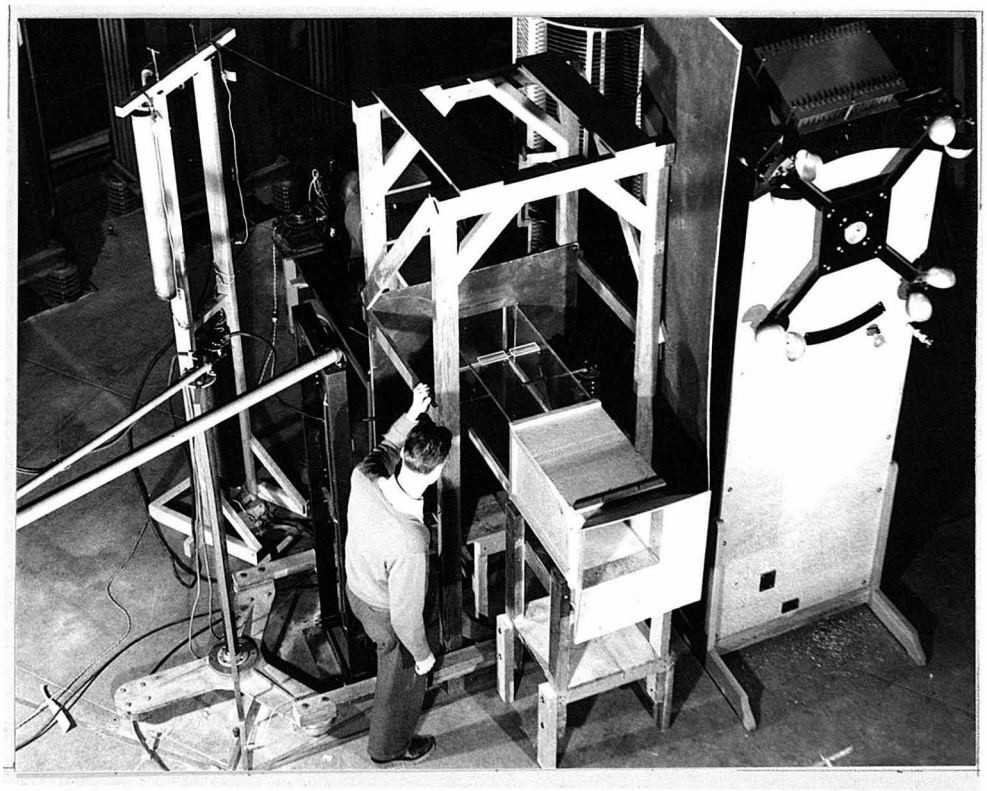

Fig. 14

Photograph of Main Test Circuit
with Duct in Place

15 seconds following each test shot, in order to insure that no residual ionization remained in the test gap to influence the recovery voltage for the following test shot.

The recovery voltage measuring circuit consists of potential dividers, each of which is 3000 ohms of non-inductive resistance, used in series and parallel combinations to obtain divider ratios of 1500-6000 ohms to 75 ohms. The 75 ohms is the terminating impedance for a Westinghouse cold cathode electronic oscillograph, (shown in Fig. 15), which is connected to the low voltage end of the potential divider through a 75 ohm characteristic impedance coaxial cable. The voltage across the 75 ohm impedance is applied to the deflecting plates of the oscillograph through a decade resistance which is adjusted to obtain convenient deflections in the oscillograph. A typical group of recovery voltage oscillograms are shown in Fig. 16.

A General Electric six-element magnetic oscillograph was used to record 60-cycle current and voltage. Magnetic oscillograms have been taken for approximately ten percent of the test records to check the magnitude and duration of the fault current and also the time delay between the tripping of the two generators. Oscillographic records of one half and five cycle current duration are shown in Fig. 17.

Some difficulty was encountered in preventing No. 2 surge generator tripping with No. 1 as both have a common connection in the discharge circuit at the test gap, and also a common ground connection. By adjusting the trip gap and the last gap in the No. 2 surge generator as large as possible, the disturbances produced when No. 1 surge generator

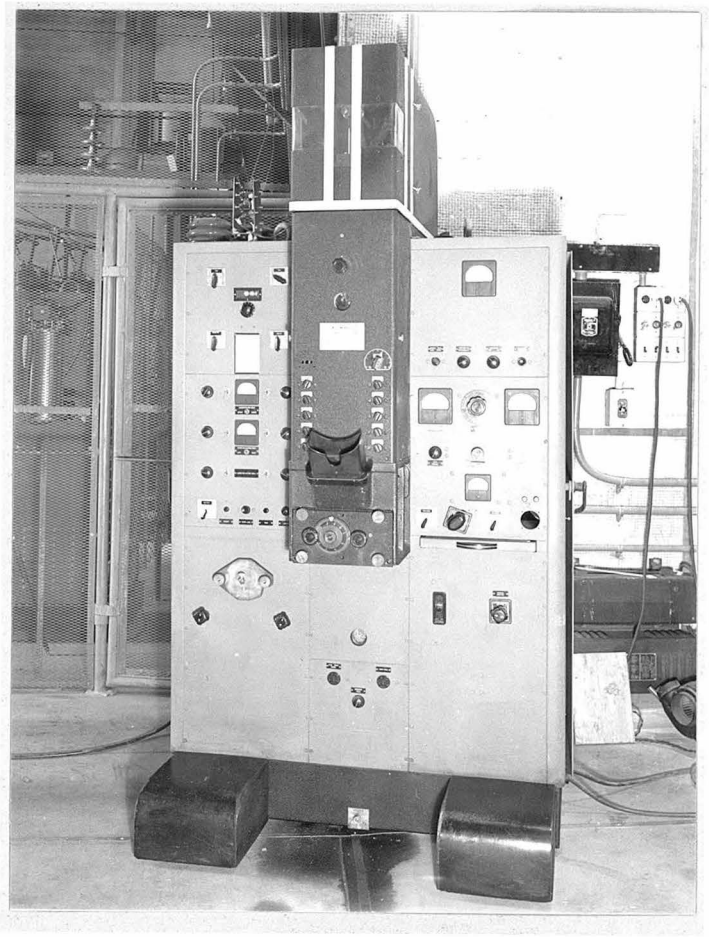

Fig. 15

Photograph of Westinghouse Cold Cathode
Electronic Oscillograph

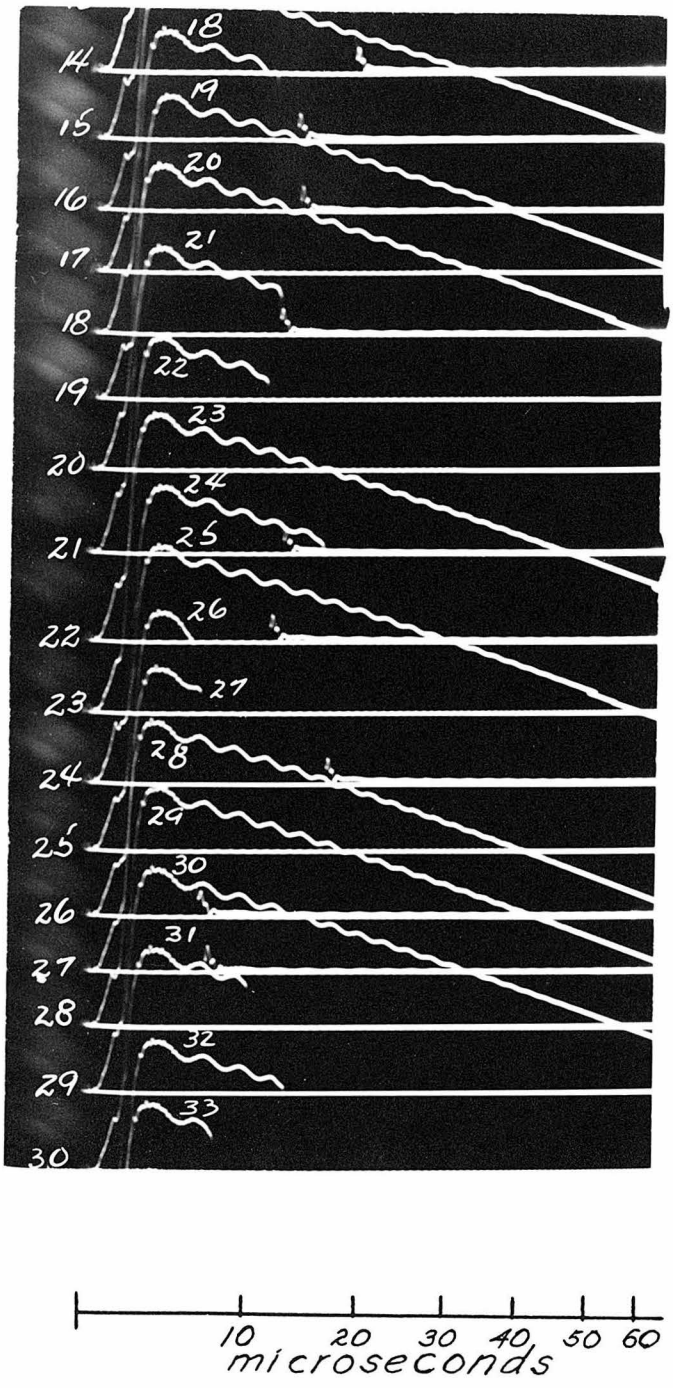

Fig. 16

Typical recovery voltage oscillograms of second surge generator discharge voltage wave for an 11 inch gap, 300 amperes, 1/2 cycle fault current. Recovery time delay is 120 milliseconds.

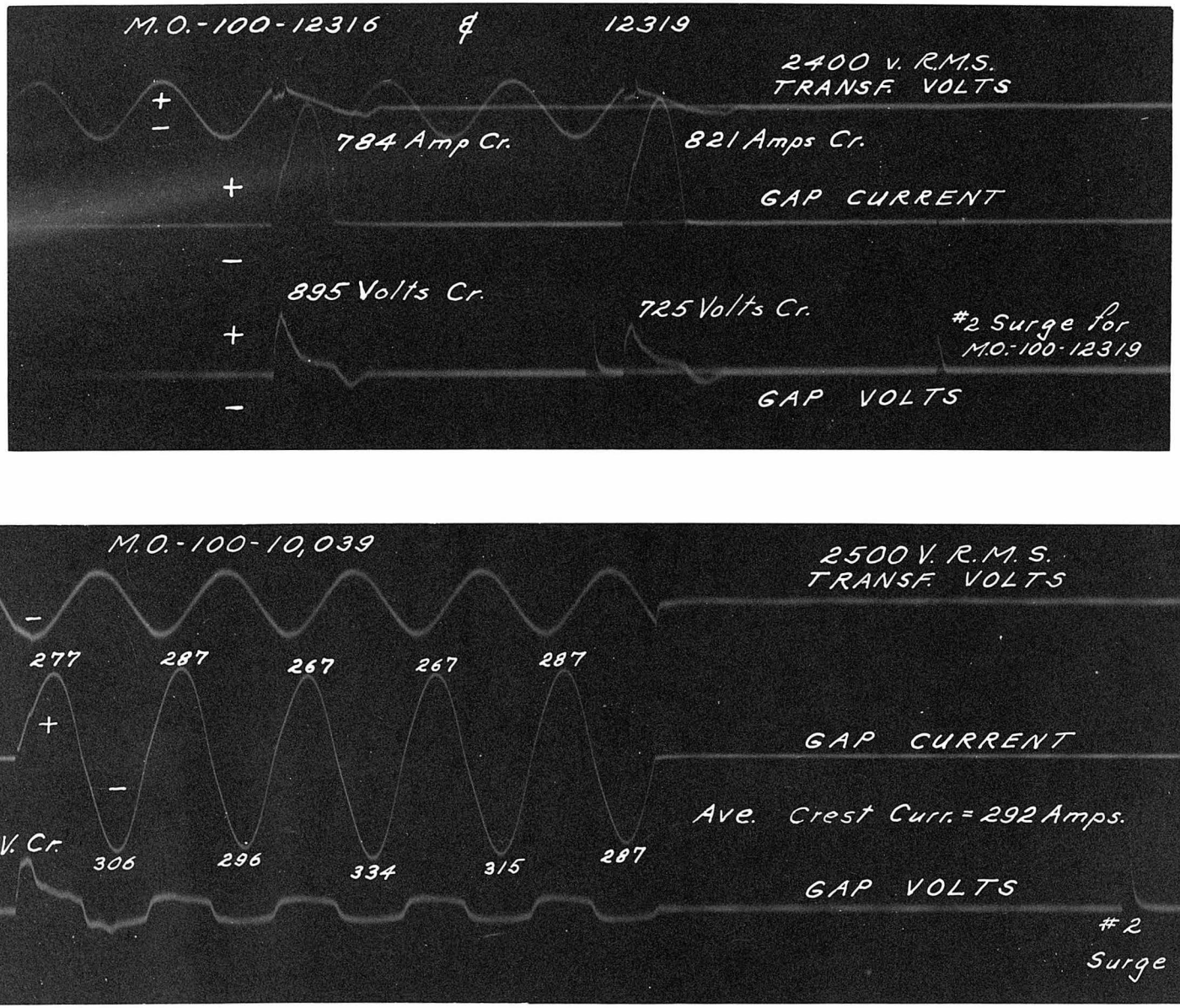

Fig. 17 Typical magnetic oscillograms of one-half cycle and five cycle power fault currents.

is tripped do not trip No. 2 surge generator. Because of induced pulses in the 40 foot trip lead running from No. 2 surge generator to the cathode ray oscillograph, the timing sweep of the oscillograph tripped from the firing of No. 1 surge generator. By running this trip lead as close to the ground plane as possible the oscillograph tripped only from the No. 2 surge generator trip signal.

The Westinghouse cathode ray oscillograph mentioned previously was continuously evacuated to a pressure less than 0.001 mm. of mercury by a high speed molecular pump. This pump gave some bearing trouble. A small misalignment of the bearings, which was serious because of the limited stator-rotor clearance (.006 inches) and which could not be eliminated because of the design of the bearing supports, caused the pump to stall after new bearings had been installed less than a week. An oil diffusion pump replaced it satisfactorily after a large baffle was added between the pump and the oscillograph chamber. The baffle eliminated contaminating oil molecules from the vacuum chamber of the oscillograph.

2.3 Photographic Study.

A photographic study of the arc is co-ordinated with the dielectric recovery characteristics for both axial and perpendicular winds across 6 and 11 inch test gaps. So as to obtain a more detailed picture of the geometrical structure of the ionized gases in the arc, mutually perpendicular views of the arc are taken simultaneously by means of the mirror system shown in Figs. 18 and 19. Twenty-five hundred feet of 16 mm. super XX film have been used in making this extensive photographic study with a 3000 frame per second camera. Previous experimenters[28] used a

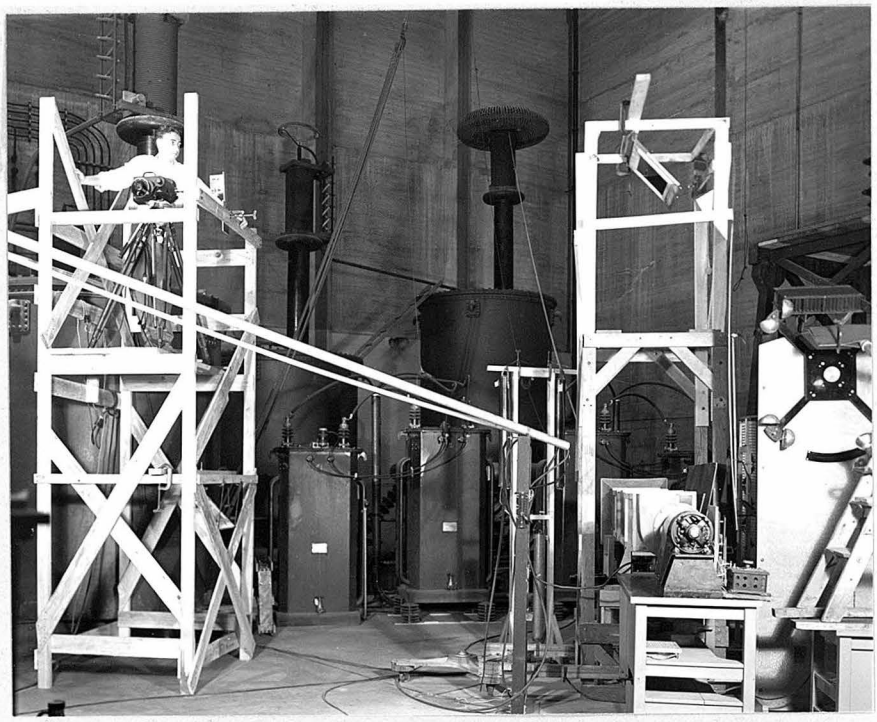

Fig. 18

Photograph of Mirror System
Used for Photographic Study

FIG. 19

SCHEMATIC OF MIRROR SET-UP FOR MUTUALLY PERPENDICULAR VIEWS OF ARC TAKEN SIMULTANEOUSLY

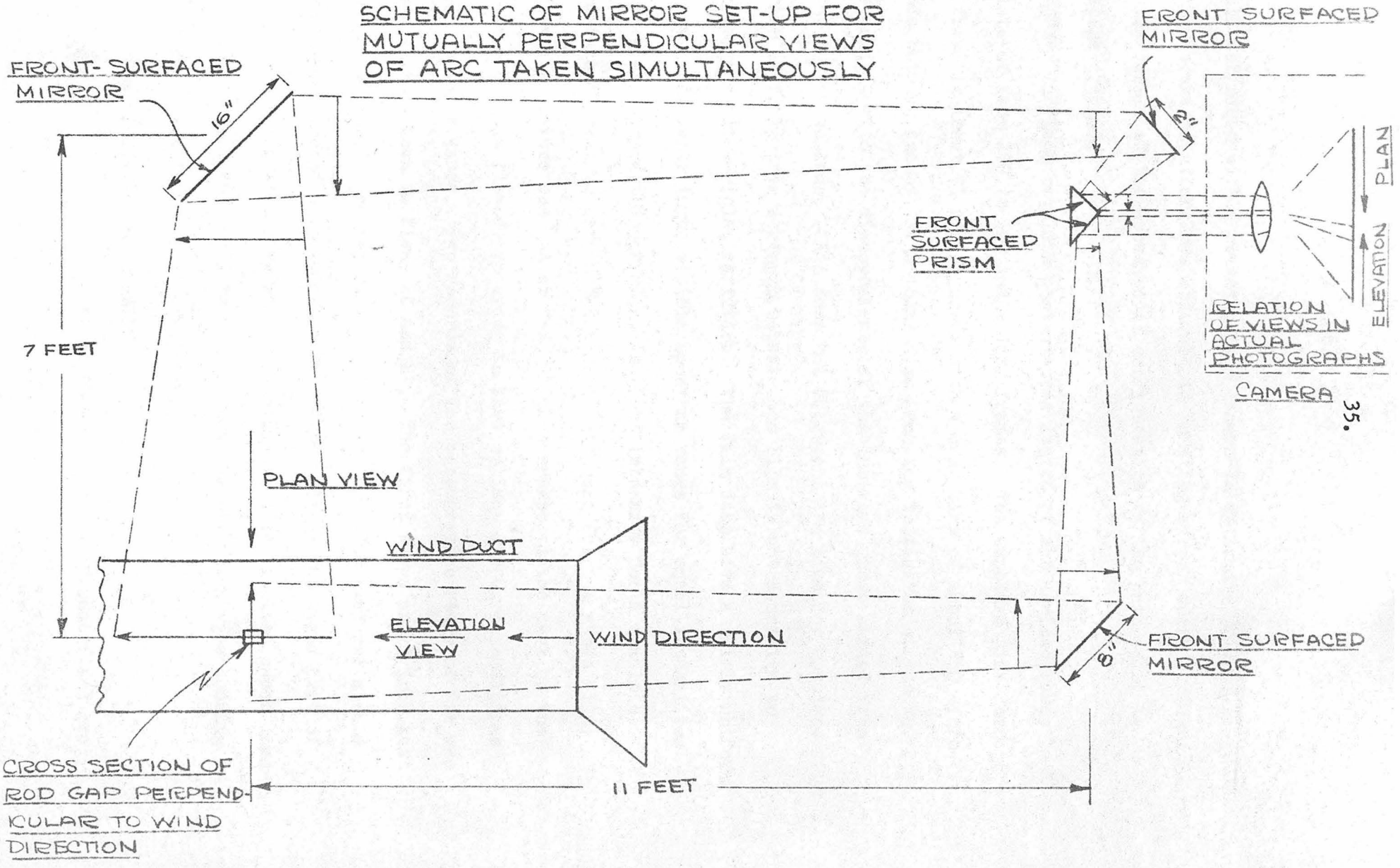

similar technique with a rotating drum camera to determine whether or not the localized afterglows observed in rotating-mirror spark photographs were the result of the geometrical configuration of the path taken by the spark channel.

Each complete photographic record of the ionized gases consists of from 200 to 400 individual frames. The exposure time for each frame is about 75 microseconds with a dead time of about 260 microseconds between frames. The total time from the initiation of the No. 1 surge generator to the disappearance of the luminous gases varied from 0.067 to 0.150 seconds. This does not represent the time for complete recovery of dielectric strength because the film is not sensitive to infra-red and ultra-violet radiation. The film does have a fairly uniform exposure sensitivity in the visible spectrum range for equal intensities of radiation. Since the variation in light intensity for a complete record is too great to obtain the correct exposure for the whole film, the camera aperature was set at f-8, (which overexposed the part of the film where current flowed) in order to have optimum exposure conditions for the luminous gases. Two records of the photographic study of the arc phenomenon are shown in Figs. 20 and 21. The first shows an 11 inch test gap for no wind and the second an 11 inch gap for 1000 feet per minute wind directed perpendicularly across the electrodes. The upper part of the frame shows the plan view where the wind blows the ionized gases downward in the picture and the lower part shows the elevation view looking into the wind duct as shown schematically in Fig. 19.

2.4 Experimental Results.

Dielectric recovery characteristics of an unconfined arc

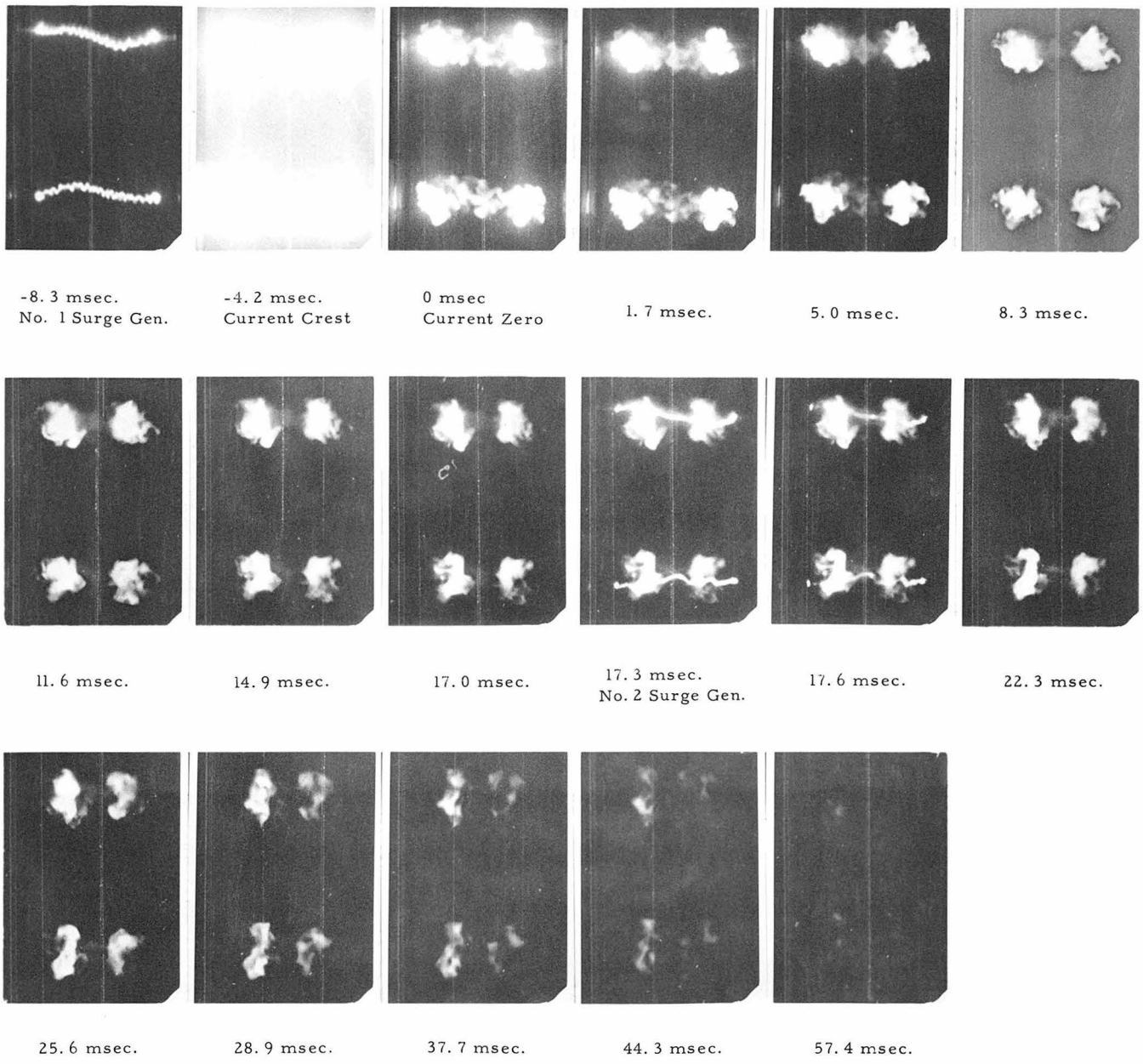

Fig. 20

Typical photographic record taken at 3000 frames per second showing two mutually perpendicular views of the arc for 300 amperes, half cycle, 11-inch test gap mounted horizontal with no wind.

Upper Picture - Plan View

Lower Picture - Elevation

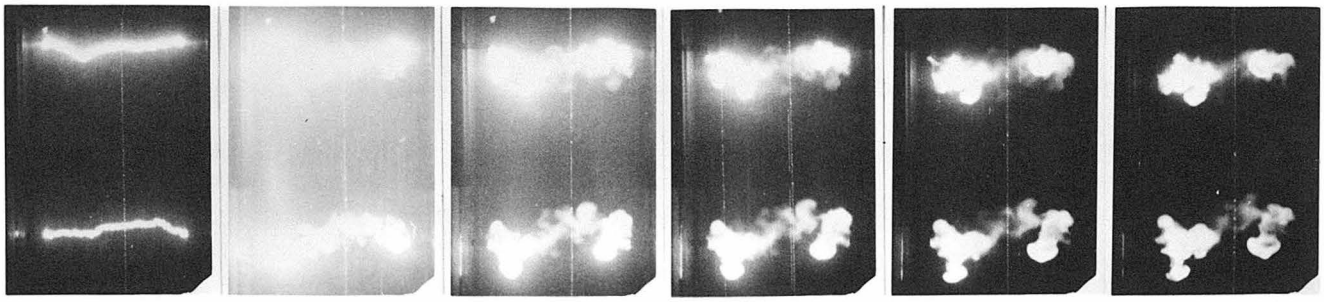

-8.3 msec. No. 1 Surge Gen. | -4.2 msec. Max. Current | 0 msec. Current Zero | 1.7 msec. | 5.1 msec. | 8.5 msec.

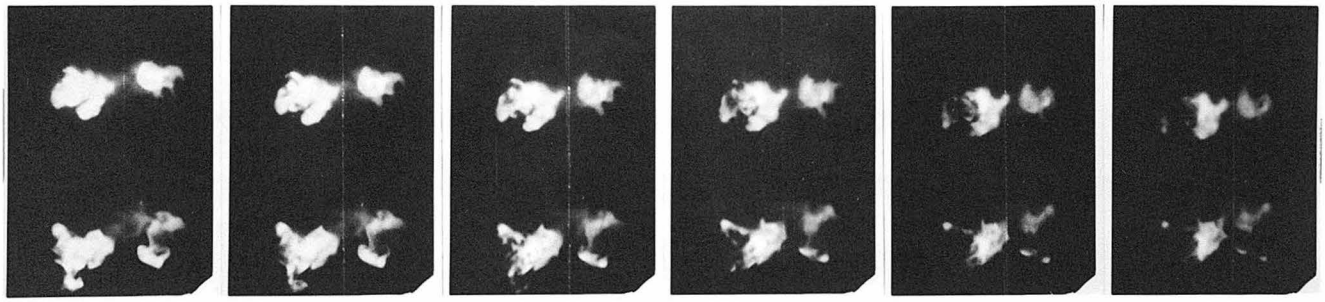

11.9 msec. | 15.3 msec. | 18.7 msec. | 22.1 msec. | 25.4 msec. | 28.7 msec.

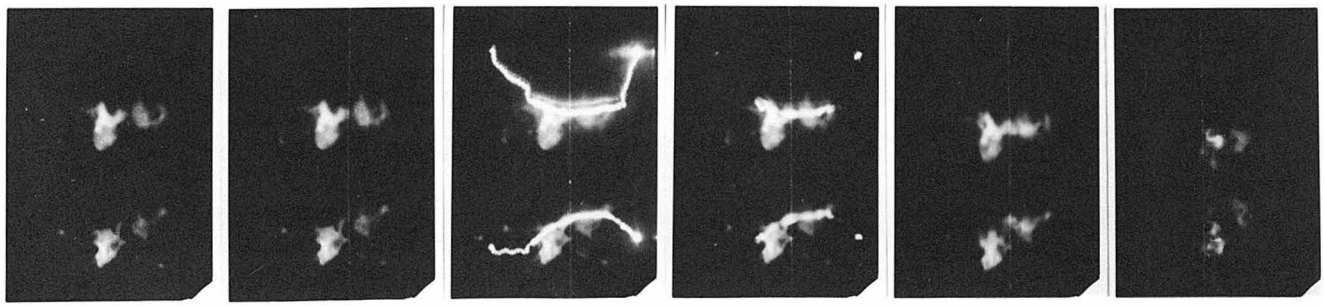

32.0 msec. | 32.3 msec. | 32.6 msec. No. 2 Surge Gen. | 32.9 msec. | 35.3 msec | 55.3 msec

Fig. 21

Typical photographic record taken at 3000 frames per second showing two mutually perpendicular views of the arc for 300 amperes, half-cycle, 11-inch test gap mounted horizontal. With wind of 1000 ft./min. directed perpendicular to electrodes in top view.

Upper Picture - Plan view

Lower Picture - Elevation

in still air have been investigated and the results published in an earlier paper (see Appendix I). Test gaps of 3, 6 and 11 inches were used, and because of electrode configuration and cooling effects the 3 inch gap recovered proportionately more rapidly than the 6 and 11 inch gaps. For 3 to 11 inch gaps the initial slope of the recovery voltage varied from 1 to 3 volts per microsecond. These initial rates of recovery for long a.c. arcs correspond to the following initial rates of recovery for short a.c. arcs; the initial rate of recovery of the 11 inch gap is approximately the same as for the 4 mm. electrode separation used by Browne and Todd[29], and the 3 inch gap the same as for the 8 mm. gap spacing of the short a.c. arc. The above initial recovery voltage rates show very clearly why so much difficulty was experienced in obtaining natural recovery (see Table I, Appendix I for summary of recovery tests) for long arcs using voltages greater than for the corresponding short arcs in the above reference.

Since publishing the results given in Appendix I, the effect of current duration in unconfined arcs for an 11 inch vertical test gap has been investigated. A comparison of recovery rates for 300 amperes of half and five cycle duration, shown in Fig. 22, indicates that current duration has little effect on the rate of dielectric recovery of a vertical test gap. Boisseau, Wyman, and Skeats[14] found that the duration of fault current has no effect on the deionization time required for successful reclosure of circuit breakers. The above figure also shows that there is little difference in recovery between the horizontal and vertical test gap configurations for a half cycle of fault current.

FIG. 22

COMPARISON OF DIELECTRIC RECOVERY FOR 11 INCH HORIZONTAL AND VERTICAL ROD GAPS FOR NO DUCT

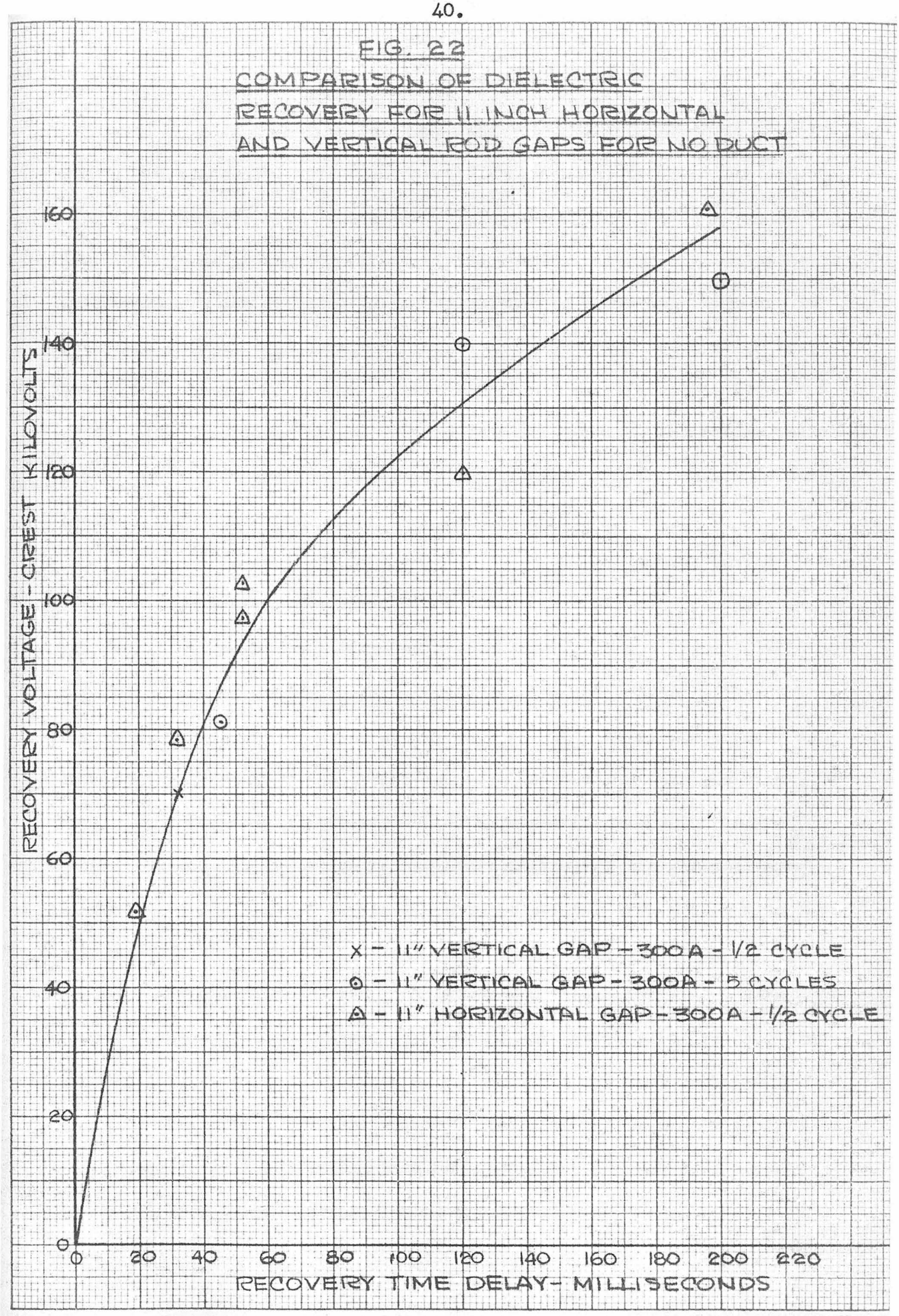

In obtaining recovery data, it is quite common to take 200 to 300 successive test records with the same electrodes. The condition of the electrode tips after varying amounts of use is shown in Fig. 23. To determine the effect of electrode condition on the dielectric recovery, the critical breakdown voltage of a six inch test gap is obtained, without predischarge, for new electrodes and those which have been used for some 80 recovery tests with fault current. The difference in critical breakdown voltage is less than one percent, indicating that the recovery data are independent of the condition of the electrode surfaces.

To determine the effect of electrode material on the recovery characteristics, recovery data have been obtained for carbon and iron electrodes under identical circuit conditions. For a 3 inch test gap the recovery with carbon electrodes is 30 to 40 percent higher than for iron, for a recovery time delay range of 30 to 80 milliseconds. The low-boiling-point iron electrodes vaporize much easier than the high-boiling-point carbon electrodes[30]. The electrode vapor in the arc column changes the effective ionization potential of the gas and vapor mixture. Carbon is more difficult to vaporize than iron and it also has a higher ionization potential than iron; 11.22 volts for carbon as compared with 7.83 volts for iron. Since both of these ionization potentials are lower than nitrogen (15.6 volts) and oxygen (12.5 volts), the effect of their vapor in the gas is to lower the critical breakdown voltage. Therefore, the more volatile lower-ionization-potential iron electrodes lower the critical breakdown considerably more than the carbon electrodes. Spectrograms for both carbon and iron electrodes at arc

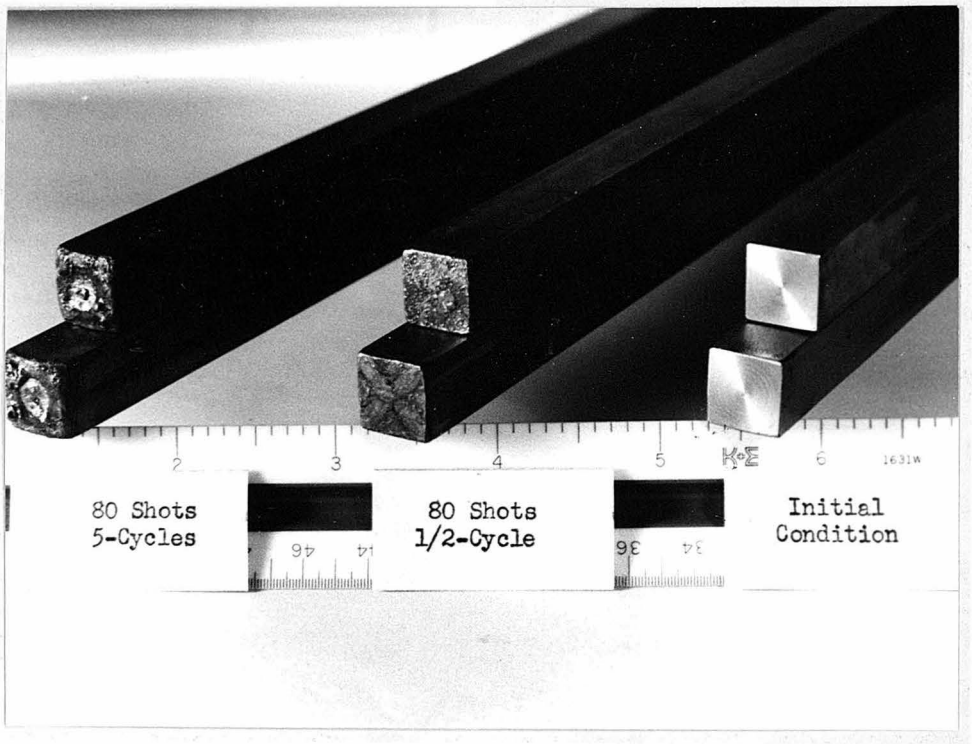

Fig. 23

Photograph of Test Electrodes
After Varying Amounts of Use

lengths of 6 and 11 inches show that these electrode materials are present in various states of excitation in the arc; but as the arc length is increased it is expected that the electrode material has a smaller effect on the critical recovery voltage.

For short arcs Browne[25] found that the critical reignition voltage is higher for low-boiling-point electrodes than for high-boiling-point electrodes. This is in contrast with long arcs where the reignition voltage is lower for the low-boiling-point steel electrodes than for the high-boiling-point carbon electrodes. If it is assumed that the temperature of the electrodes can not be higher than their respective boiling points, then the low-boiling-point electrodes are at a lower temperature than the high-boiling-point electrodes at current zero. Electrode cooling effects are much more important for short arcs than for long arcs (the greater relative rate of recovery of dielectric strength, noticed in Appendix I, for the 3 inch test gap over the 6 and 11 inch gaps is attributed to the electrode cooling effect). Hence, the increased arc reignition voltage for low-boiling-point electrodes for short arcs can probably be attributed to the greater cooling effect of these electrodes over that for the high-boiling-point electrodes.

The main subject of this thesis is the effect of wind on the dielectric recovery characteristics of air gaps. The first experimental results show the effect of wind velocities up to 1000 feet per minute directed perpendicular to the axis of the test electrodes, as shown in Fig. 24, on the recovery characteristics of a six inch test gap

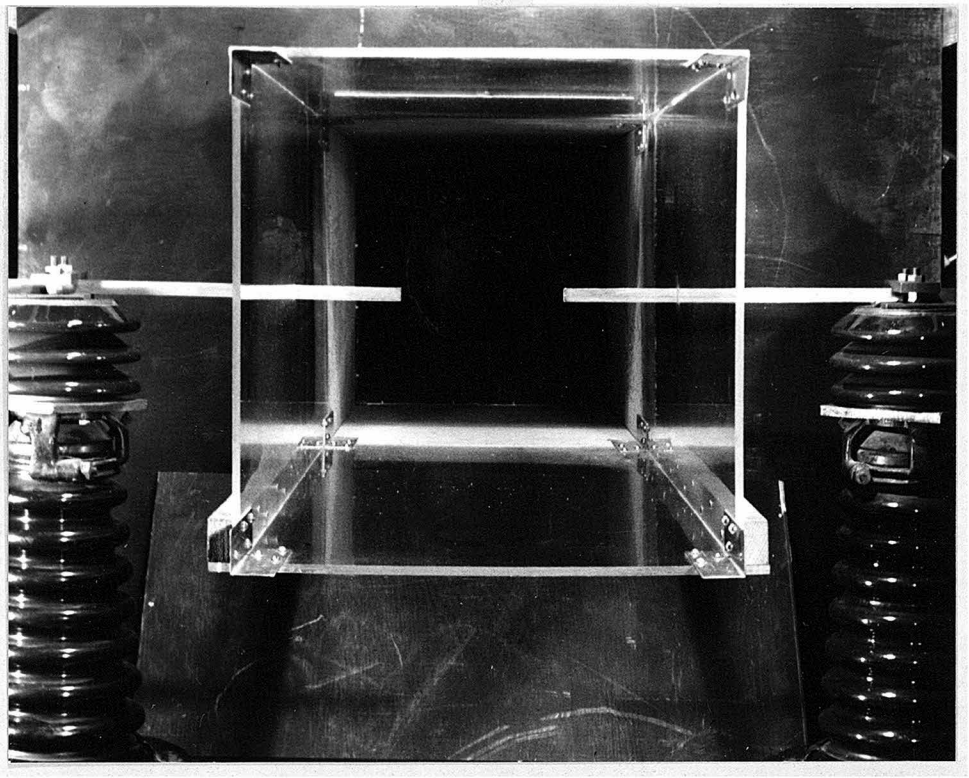

Fig. 24

Photograph of Test Gap for Electrodes Perpendicular to Wind Direction

with 300 amperes fault current of a half cycle duration. The curves obtained for wind velocities of zero, 380, 660 and 1000 feet per minute are shown in Fig. 25. The effect of current magnitude and duration on the rate of recovery of dielectric strength with wind perpendicular to the electrode axis is presented in Figs. 26 and 27 for 800 amperes fault current of a half cycle duration and 300 amperes fault current of five cycles duration, respectively. Because only a small air blast could be used on the fuse gap without affecting the magnitude of the five cycle fault current, the rate of recovery of the test gap is greater than that for the automatic fuse changer at this current duration and for wind velocities greater than 380 feet per minute. Therefore, data could not be obtained for the higher wind velocities with 5 cycles of fault current. The recovery characteristics for an 11 inch test gap at the various wind velocities are shown in Fig. 28 for 300 amperes fault current of a half cycle duration.

Initially it was intended to include data for 100 feet per minute wind velocity in the above curves but the recovery characteristics for this wind are about the same as for no wind. A comparison of recovery characteristics for no wind and 100 feet per minute wind for 300 and 800 ampere currents of a half cycle duration are shown in Fig. 29 A. and B. Because the 100 feet per minute recovery voltages are slightly lower than the no wind voltages and because for short times after current zero the 380 feet per minute wind curves have lower recovery rates than no wind (see Figs. 25 and 26), the possible motion of the arc due to magnetic fields, produced by unsymmetrical leads and other current

FIG. 25

EFFECT OF PERPENDICULAR WIND ON DIELECTRIC RECOVERY CURVES FOR SIX INCH STANDARD ROD GAP

300 AMPERES CREST CURRENT OF 1/2 CYCLE DURATION

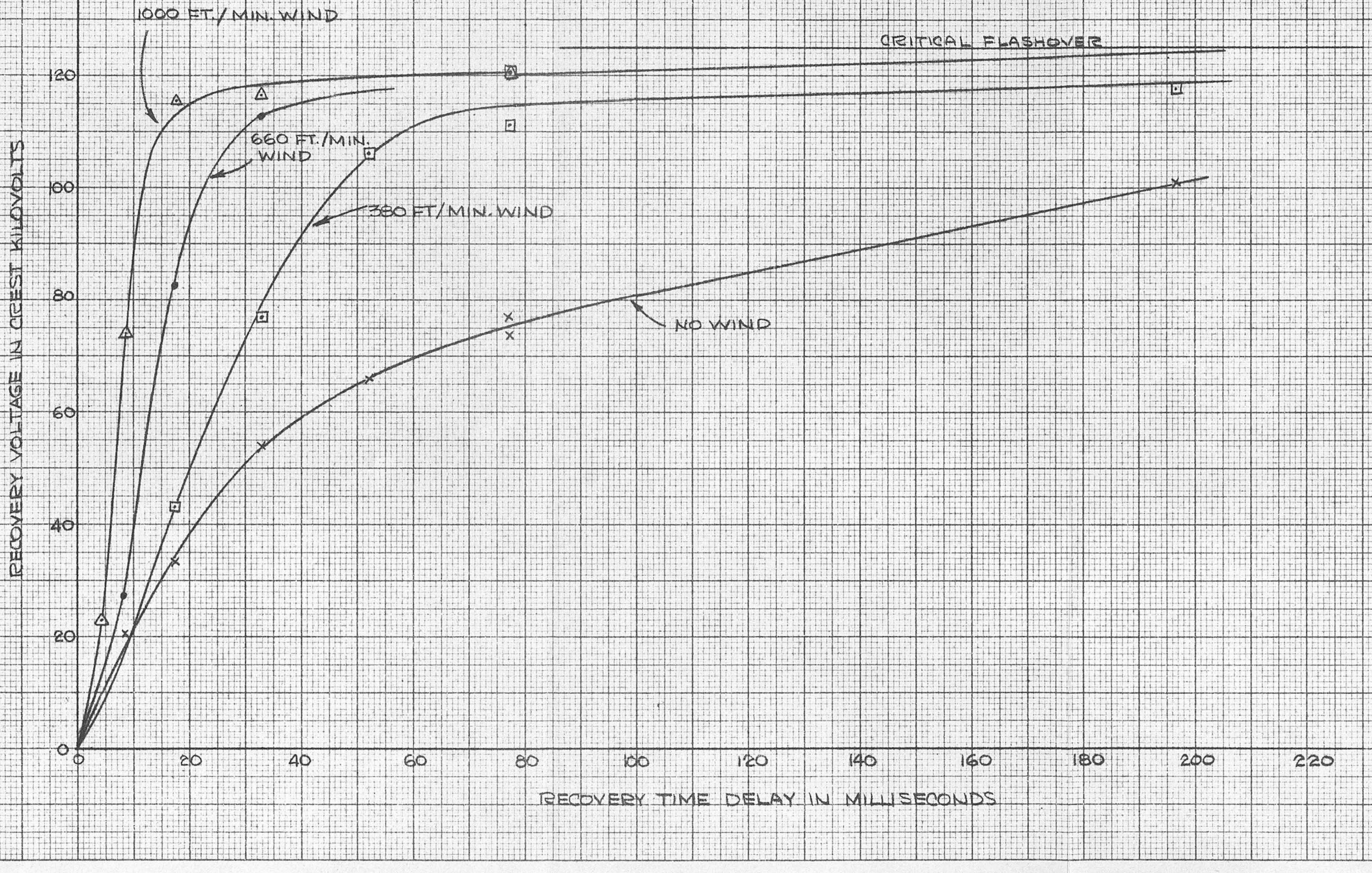

FIG. 26

EFFECT OF PERPENDICULAR WIND ON DIELECTRIC RECOVERY CURVES FOR SIX INCH STANDARD ROD GAP 800 AMPERES CREST CURRENT 1/2 CYCLE DURATION

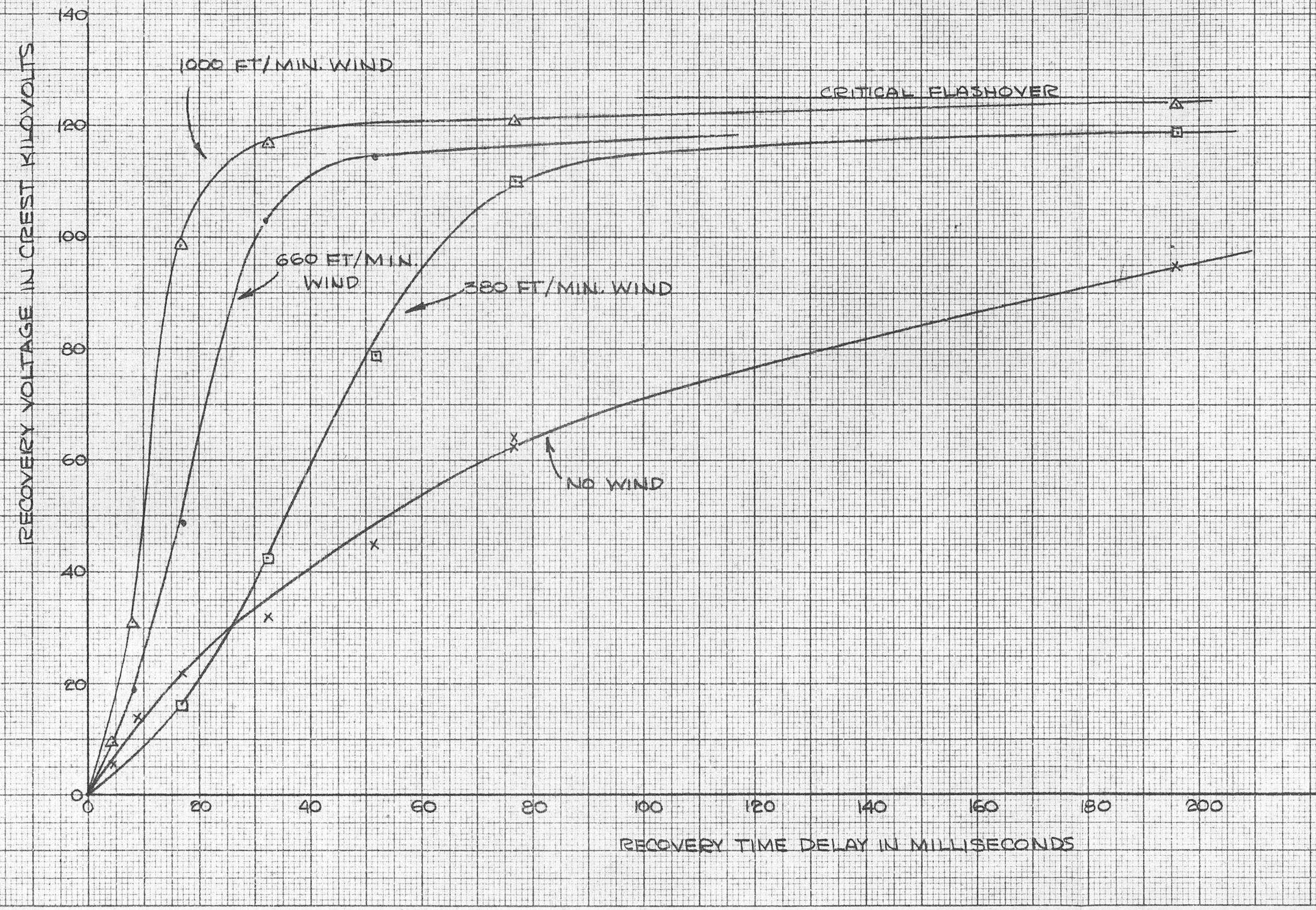

FIG. 27

EFFECT OF PERPENDICULAR WIND ON DIELECTRIC RECOVERY CHARACTERISTICS OF SIX INCH STANDARD ROD GAP FOR 300 AMPERES CREST 5 CYCLES DURATION

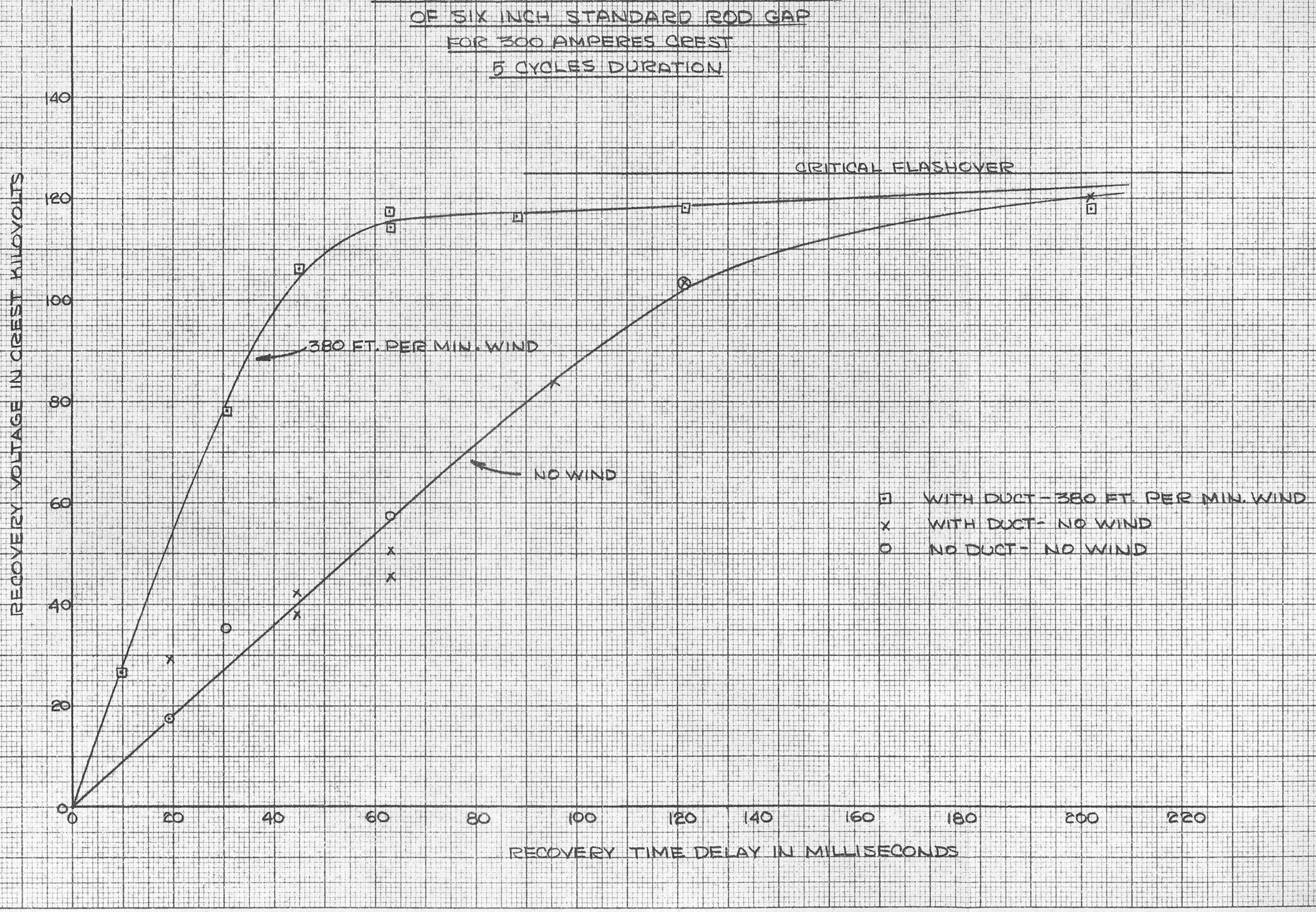

FIG. 28

EFFECT OF PERPENDICULAR WIND ON DIELECTRIC RECOVERY CHARACTERISTICS OF 11 INCH STANDARD ROD GAPS FOR 300 AMPERES - 1/2 CYCLE

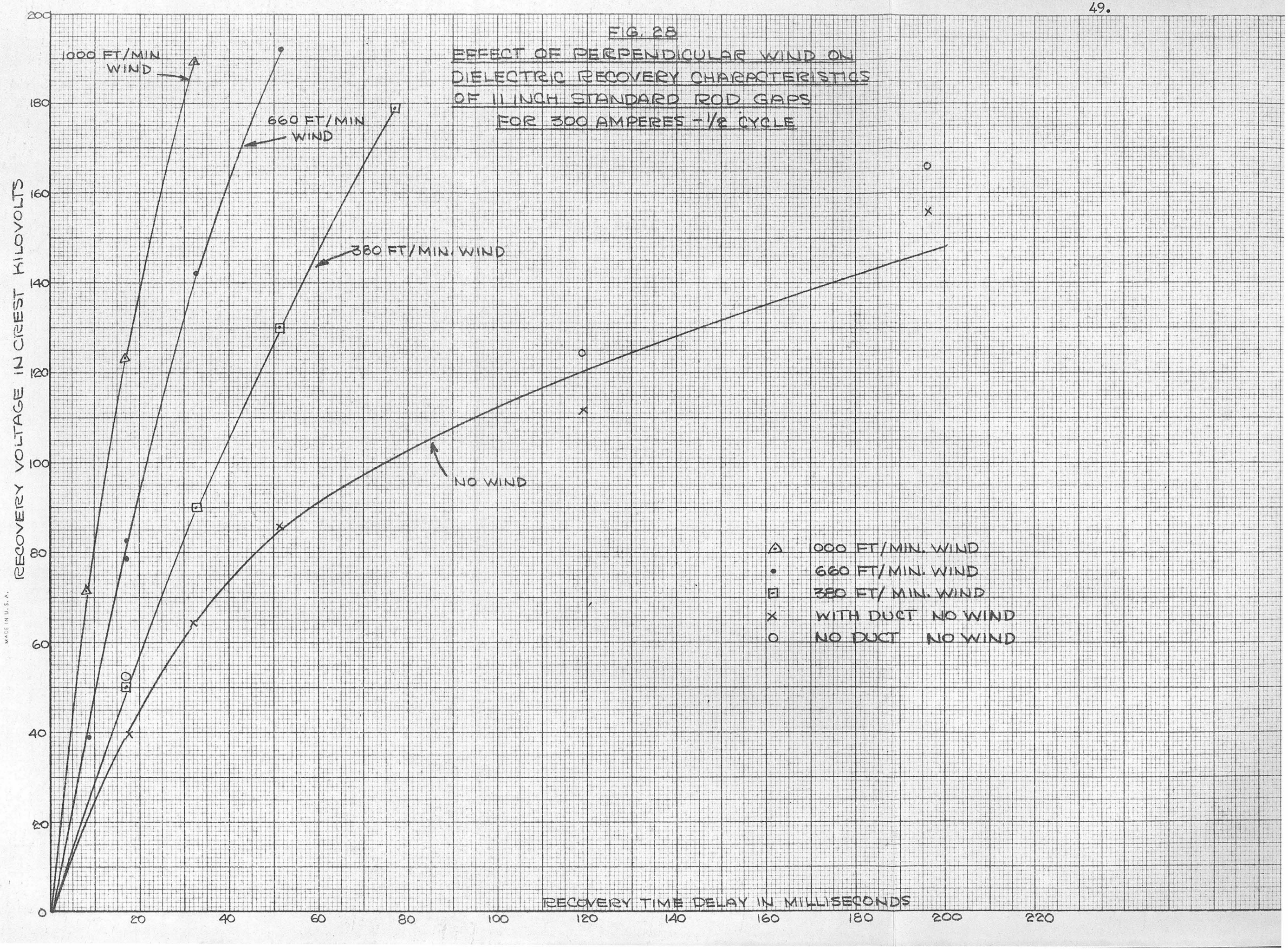

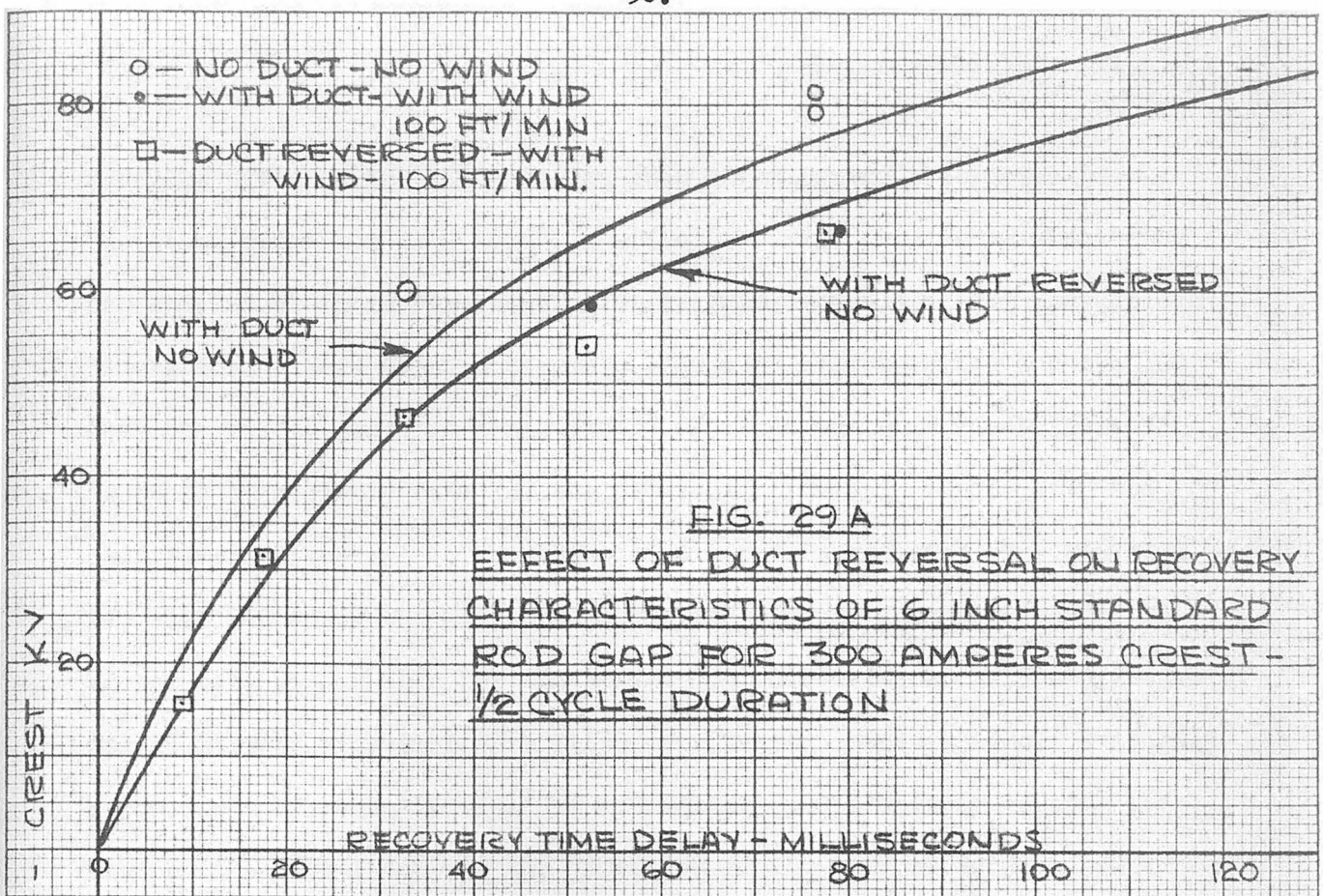

FIG. 29 A

EFFECT OF DUCT REVERSAL ON RECOVERY CHARACTERISTICS OF 6 INCH STANDARD ROD GAP FOR 300 AMPERES CREST - 1/2 CYCLE DURATION

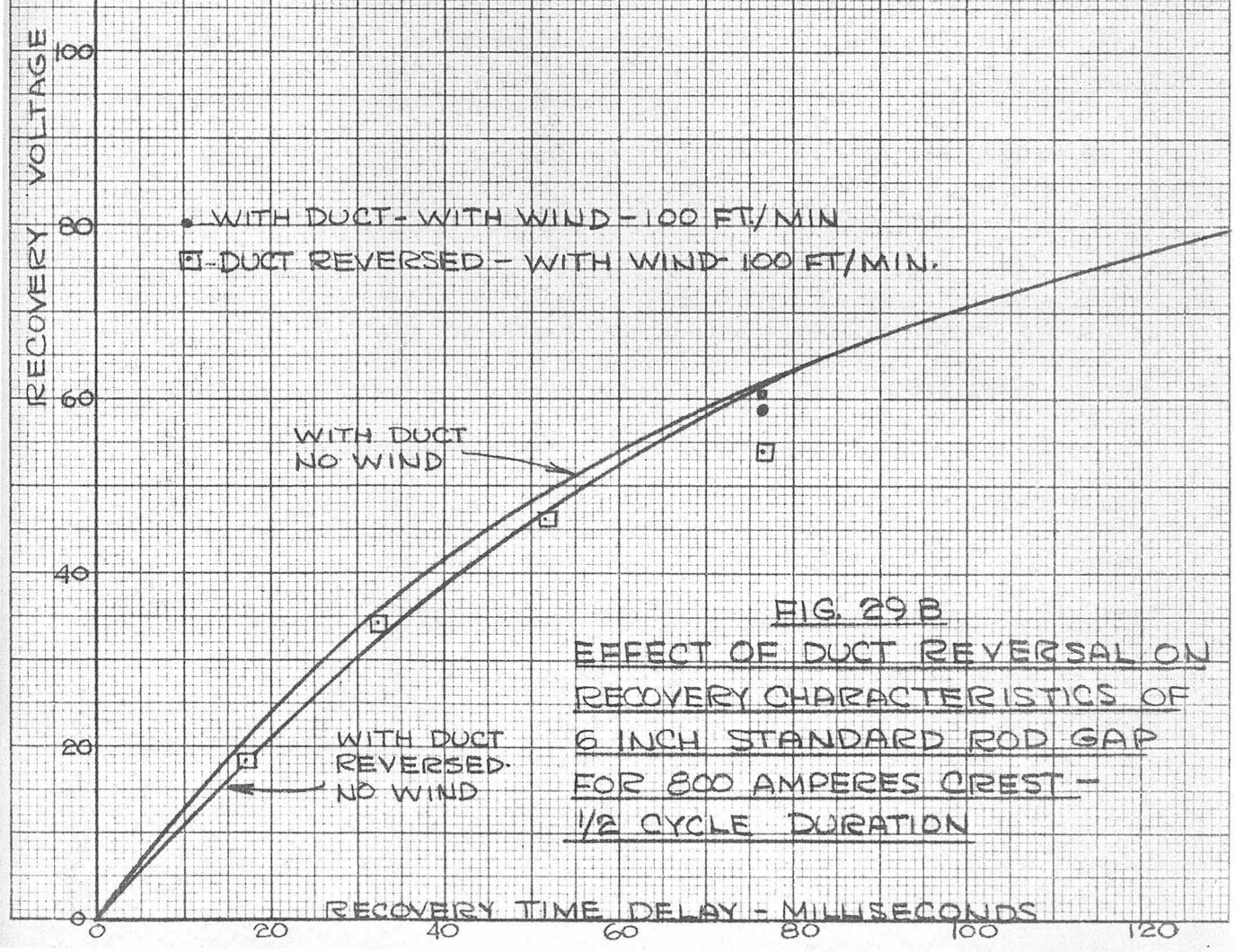

FIG. 29 B

EFFECT OF DUCT REVERSAL ON RECOVERY CHARACTERISTICS OF 6 INCH STANDARD ROD GAP FOR 800 AMPERES CREST - 1/2 CYCLE DURATION

carrying parts of the circuit, has been investigated. To determine if the above condition is a magnetic effect the wind duct is reversed end-for-end, as shown in Fig. 4, without changing the electrical circuit configuration. There is no noticeable change in recovery rate for the 100 feet per minute wind, as shown in Fig. 29, but there is a considerable increase in recovery rate for the 380 feet per minute wind. With the duct reversed the rate of recovery of dielectric strength of a six inch gap with 800 amperes fault current for the 380 feet per minute wind is 22 per cent higher than for the normal duct direction at 17.5 milliseconds, and 15 percent higher at 32.5 milliseconds after current zero. Evidently a component of magnetic field in a direction perpendicular to both the axis of the electrodes and the direction of the wind produces a small displacement of the arc, while fault current flows, in a direction opposite to the normal wind direction. Hence, for a short period of time after current zero, the rate of recovery of dielectric strength is lowered by this magnetic effect for the normal duct configuration, and is raised for the duct reversed.

To study the effect of the wind direction across the test gap the dielectric recovery characteristics have been investigated for the wind directed axially along the electrodes, as shown in Fig. 32. The recovery characteristics of a 6 inch test gap are obtained for this electrode configuration for 300 and 800 amperes crest current of a half cycle duration for 1000 feet per minute wind. The results are shown in Fig. 33.

The effect of turbulence on the dielectric recovery of the ionized gases has been investigated by placing a wire screen at the input

end of the wind duct and measuring the recovery voltage for 1000 feet per minute wind velocity. No charge in the recovery voltage was obtained; hence, introducing turbulence into the laminar flow at wind velocities up to 1000 feet per minute has no effect on the dielectric recovery characteristics of the luminous gases.

III ANALYSIS OF EXPERIMENTAL RESULTS.

The method of establishing the critical recovery voltage for a typical set of data is shown in Fig. 13. The critical is established on the basis of statistical weighting of at least 40 separate tests. One of the main reasons for the spread of data around the critical voltage is because of the variation in path taken by the No. 2 surge generator, as shown in the elevation view for the photographs of the second surge in Fig. 31. The path taken by the No. 1 surge generator can cause a magnetic blow-out effect when the power current flows and cause a considerable shift in the location of the ionized gases when the dielectric strength is tested (see Fig. 41 A.). Another reason for the spread is because of oxide impurities at the cathode which influence the mechanism of arc reignition (32, 33) for low-boiling-point electrodes as described previously under experimental results. The fault current magnitude varies up to 15% for a typical set of data, but the variation in current magnitude is found to be independent of the spread of recovery voltage.

For a short time after current zero the wave shape of the No. 2 surge generator voltage is characterized by a long wave tail representing a

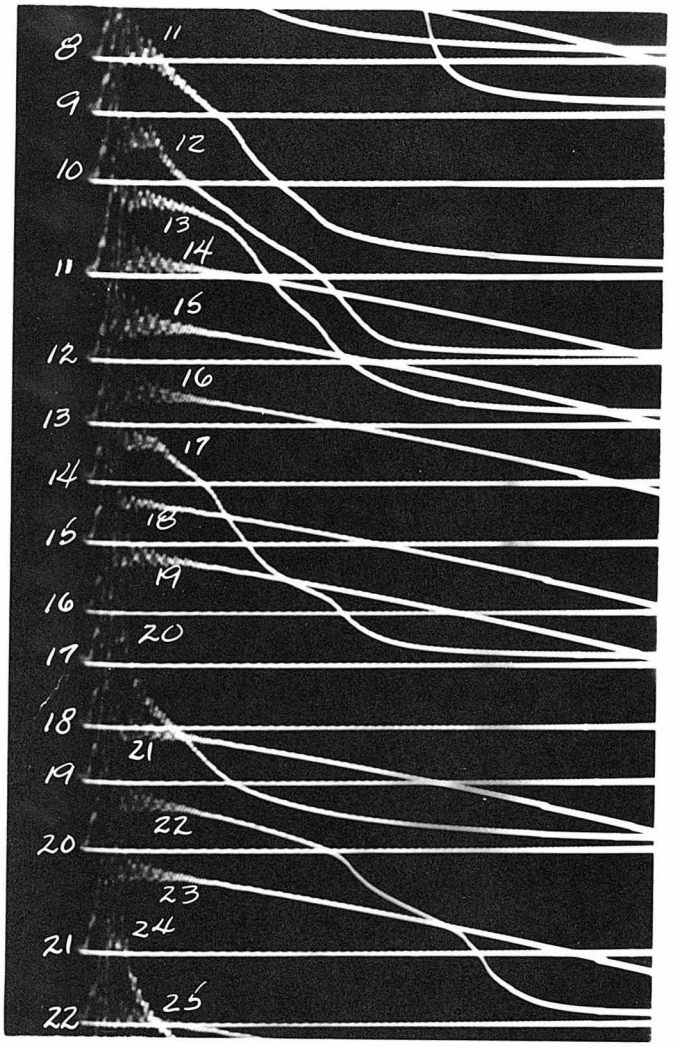

Fig. 30

Illustration of "long tail" flashover of second surge voltage when applied at short time intervals following power current zero. Power current 300 amperes crest for one-half cycle, 6 inch test gap, recovery time delay 8.7 milliseconds, recovery voltage 15 KV crest.

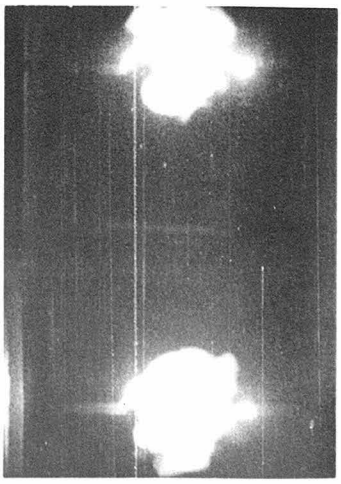

(a)
17.3 millisecs.
800 amperes crest, half cycle
no wind.

(b)
51.9 millisecs.
800 amperes crest, half cycle
380 ft./min. wind perpendicular
to electrodes.

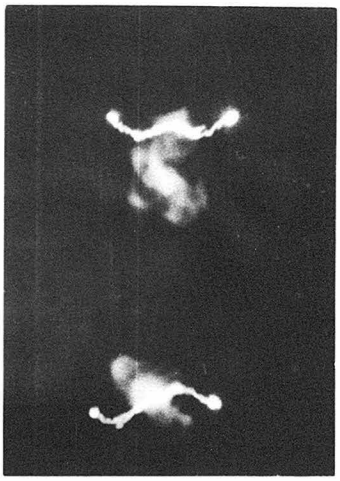

(c)
32.6 millisecs.
300 amperes crest, half cycle
380 ft./min. wind perpendicular
to electrodes.

(d)
51.9 millisecs.
800 amperes crest, half cycle
no wind.

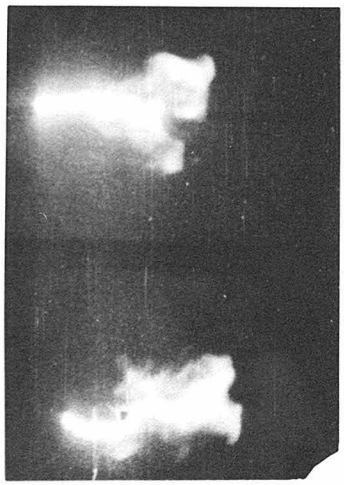

(e)
32.6 millisecs.
800 amperes crest, half cycle
380 ft./min. wind axial
to electrodes.

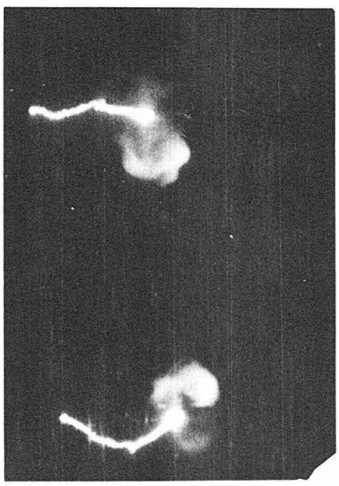

(f)
32.6 millisecs.
300 amperes crest, half cycle
380 ft./min. wind axial
to electrodes.

Fig. 31
Photograph showing variation in path taken
by No. 2 surge generator for various recovery
time delays for 300 and 800 amperes crest.

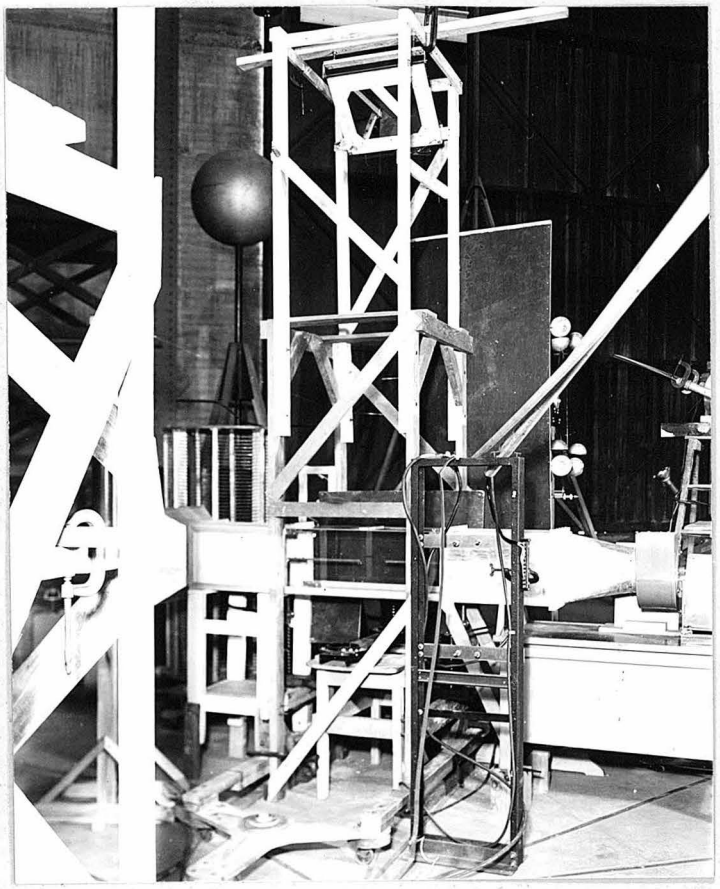

Fig. 32

Photograph Showing Axial Configuration of Electrodes in Wind Duct

FIG. 33

EFFECT OF AXIAL WIND ON DIELECTRIC RECOVERY CHARACTERISTICS OF SIX INCH STANDARD ROD GAP

△ 1000 FT/MIN. AXIAL WIND – 300 AMPS – 1/2 CYCLE
× NO WIND – 300 AMPS – 1/2 CYCLE
⊙ 1000 FT/MIN. AXIAL WIND – 800 AMPS – 1/2 CYCLE
• NO WIND – 800 AMPS – 1/2 CYCLE

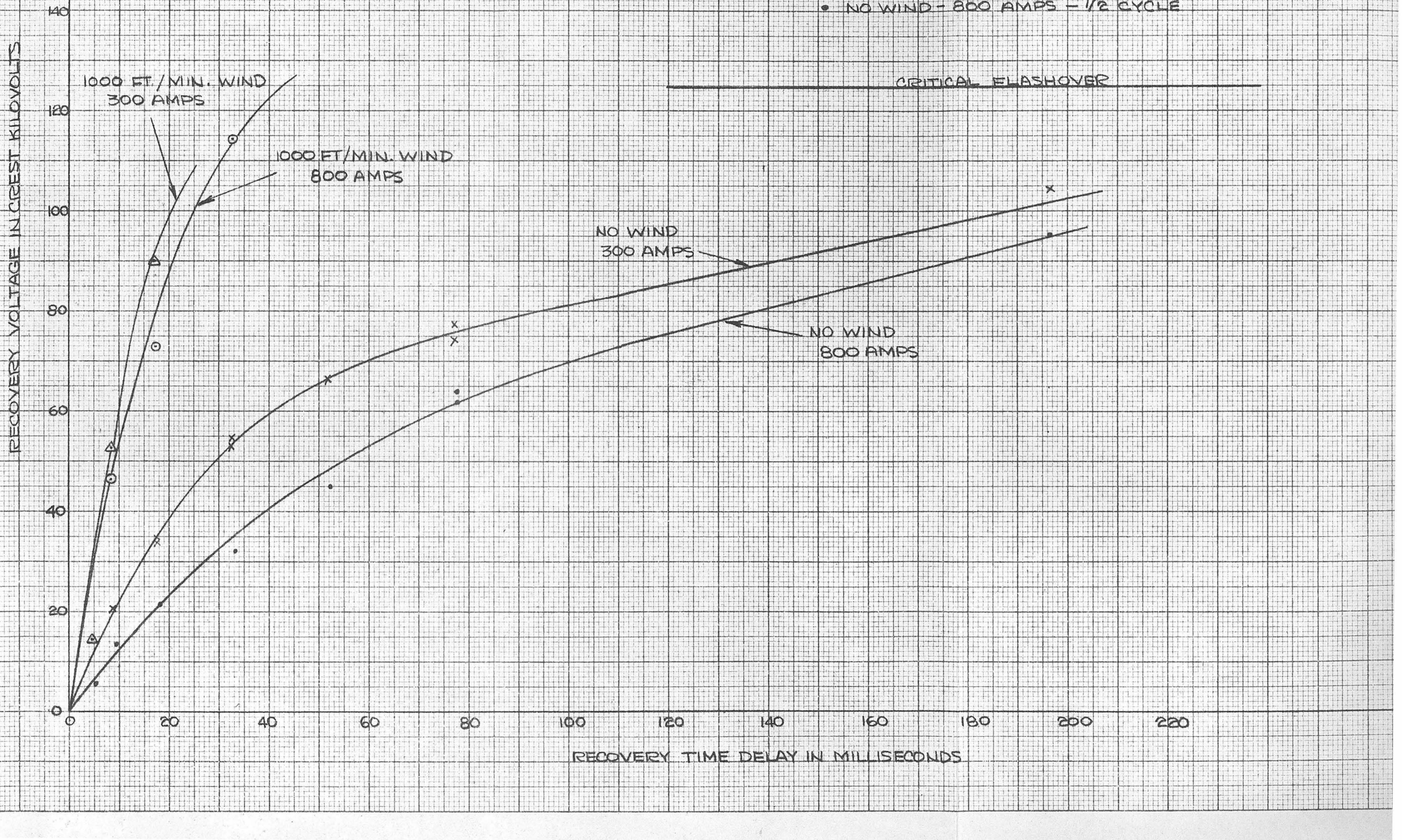

glow discharge type of breakdown. Oscillograms of the long tail breakdowns are shown in Fig. 30. For a 6 inch test gap this breakdown is more pronounced when the critical voltage is less than 20 KV. At this voltage the electric field adjacent to the electrodes is approximately 10 KV per inch and of course is much less than this in the rest of the test gap. Townsend's coeeficient of ionization, α , where α is the number of ionizing collisions per cm. advance in the direction of the field, is negligible at this field strength(41). Hence, the slope of the long tail is directly proportional to the ion density in the arc column, the field strength which determines the mobility of the ions in each part of the column, and inversely proportional to the capacity of the surge generator being used to test the recovery strength.

Fig. 41A. shows the streamer formation of the No. 2 surge generator breakdown in the plan view but not in the elevation view. The shutter of the 3000 frame per second camera is of the rotating prism type and the lower half of the frame (elevation view) is cut off from exposure before the upper half of the frame (plan view). The time during which the upper half of the frame only is exposed is of the order of 20 microseconds which allows ample time for the streamer formation shown in the plan view of the above figure.

The plan views of Fig. 21 and 41 B. have apparent parallel streamers in the No. 2 surge generator breakdown. Parallel breakdown streamers have been observed by Craggs(28) in observations of localized afterglows of long sparks, however, the above parallel streamer formation is too regular and is observed in the plan view only. The less intense streamer

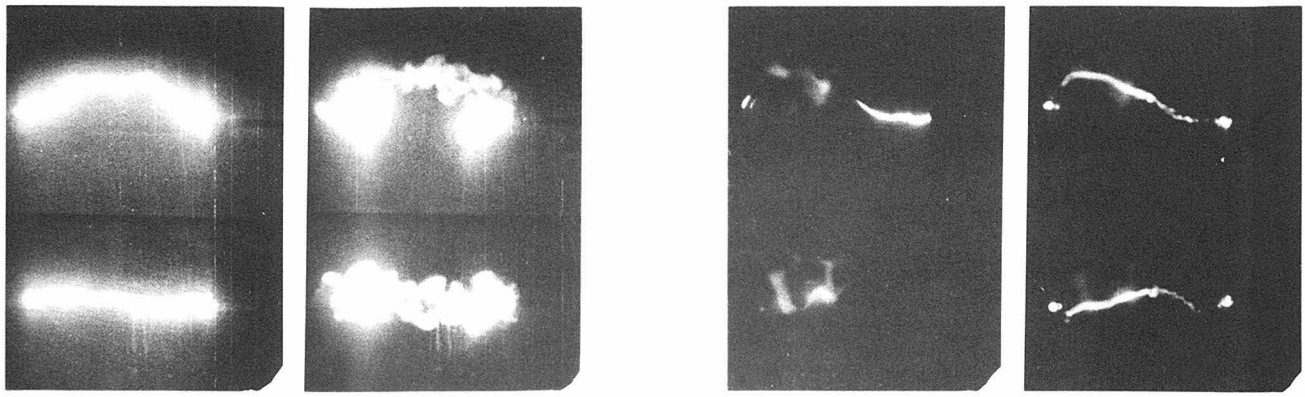

-8.3 msec.
No. 1 Surge Gen.

0 msec.
Current Zero

51.9 msec.
Streamer Formation

52.2 msec.
No. 2 Surge Gen.

Fig. 41 (a)
Photographs of two Surge Generator breakdown of 11-inch axial test gap showing streamer formation in upper view but not in lower.

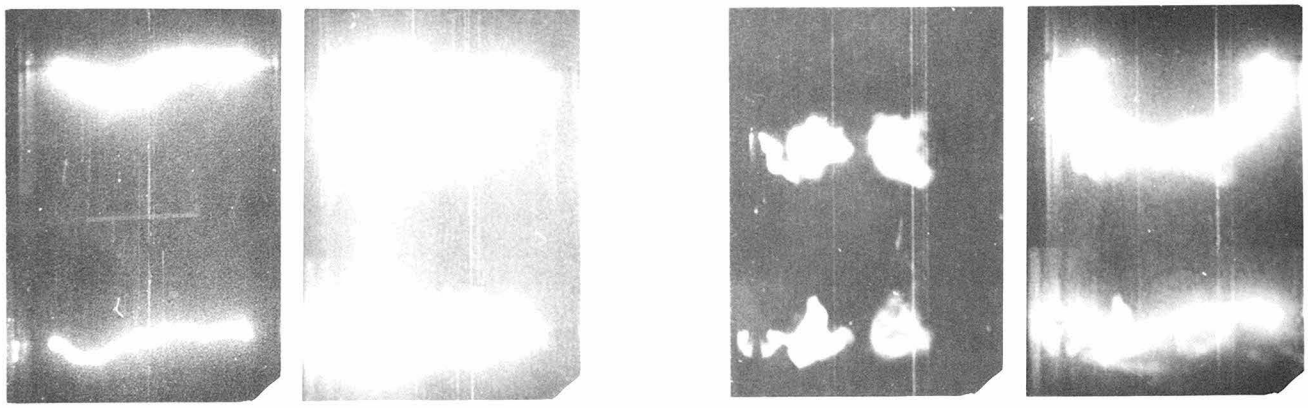

-8.3 msec.
No. 1 Surge Gen.

0 msec.
Current Zero

17.0 msec.

17.3 msec.
No. 2 Surge Gen.

Fig. 41 (b)
Photographs of two Surge Generator breakdown of 11-inch perpendicular test gap for 1000 ft. /min. wind showing parallel breakdown of ionized gases in upper view.

is probably a photographic image of the No. 2 surge generator breakdown, caused by reflection from the mirror holder surfaces which were not blacked out to eliminate reflection.

As stated in the introduction there are two general theories of the dielectric recovery mechanism of arcs under the influence of air blasts. Slepian's diffusion theory states that the rate of recovery of dielectric strength of an arc subjected to an air blast depends upon the rate of diffusion and cooling of the gases, this being greatly enhanced by turbulence produced by the gas blast. Prince's displacement theory states that the rate of recovery is proportional to the velocity of the air blast which is pictured as driving a wedge of unionized air into the ionized gas stream to increase its dielectric recovery strength. No attempt will be made here to prove or disprove either of these theories because both were formulated to explain the extinguishing characteristics of circuit breakers, and, hence, are concerned with arcs of confined cross-sections for blast velocities of the order of sonic speed.

In order to compare directly the effect of gap length, current magnitude and duration for common wind velocities the percentage recovery voltage curves of Fig. 34 A, B, C and D were constructed for wind velocities of 1000, 660, 380 feet per minute and no wind, respectively. For 300 ampere five cycle fault current there is considerable upward thermal convection of the arc column, as shown in Fig. 36, which increases the slope of the five cycle recovery curve above the half cycle curve. (Fig. 34 D.) This is in contrast with the vertical test gap where current duration has no noticeable effect on the recovery characteristics (see Fig. 22).

FIG. 34

CURVES SHOWING PERCENTAGE RECOVERY OF DIELECTRIC STRENGTH FOR 6 AND 11 INCH ROD GAPS

FIG. 34A

PERCENT RECOVERY CURVES FOR 1000 FT/MIN. WIND

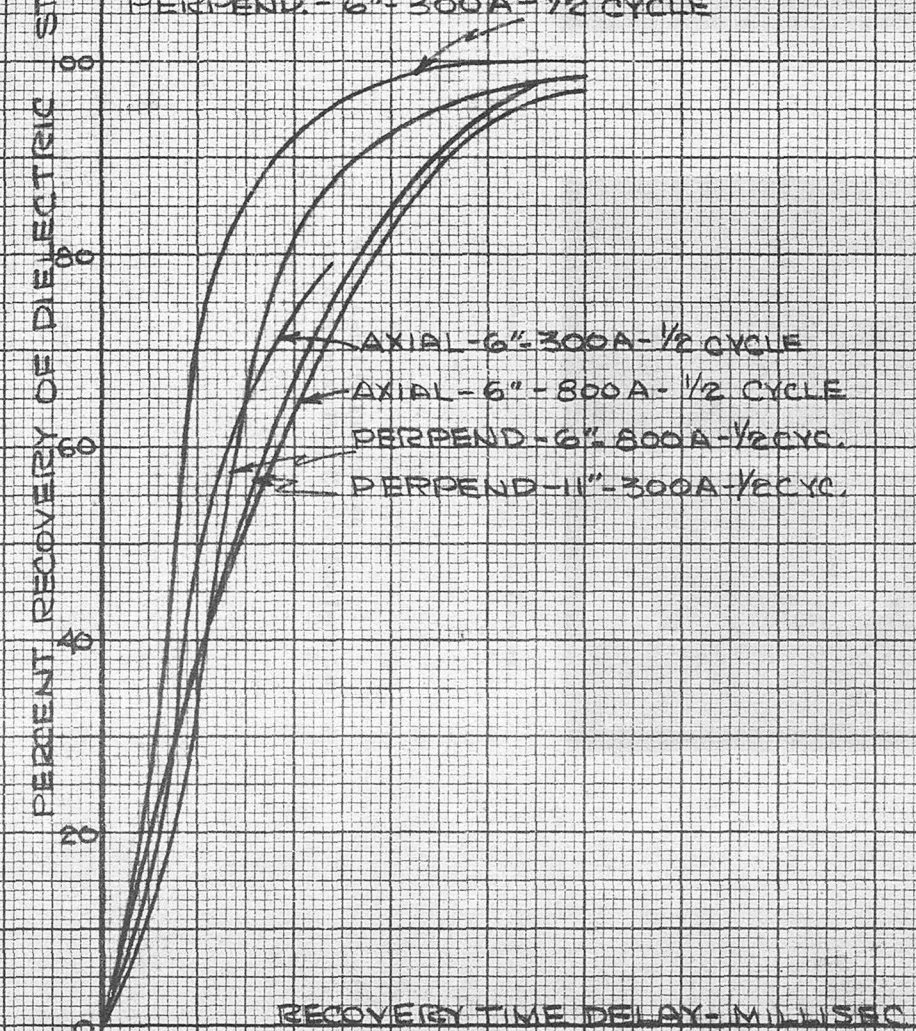

FIG. 34B

PERCENT RECOVERY CURVES FOR 660 FT/MIN WIND

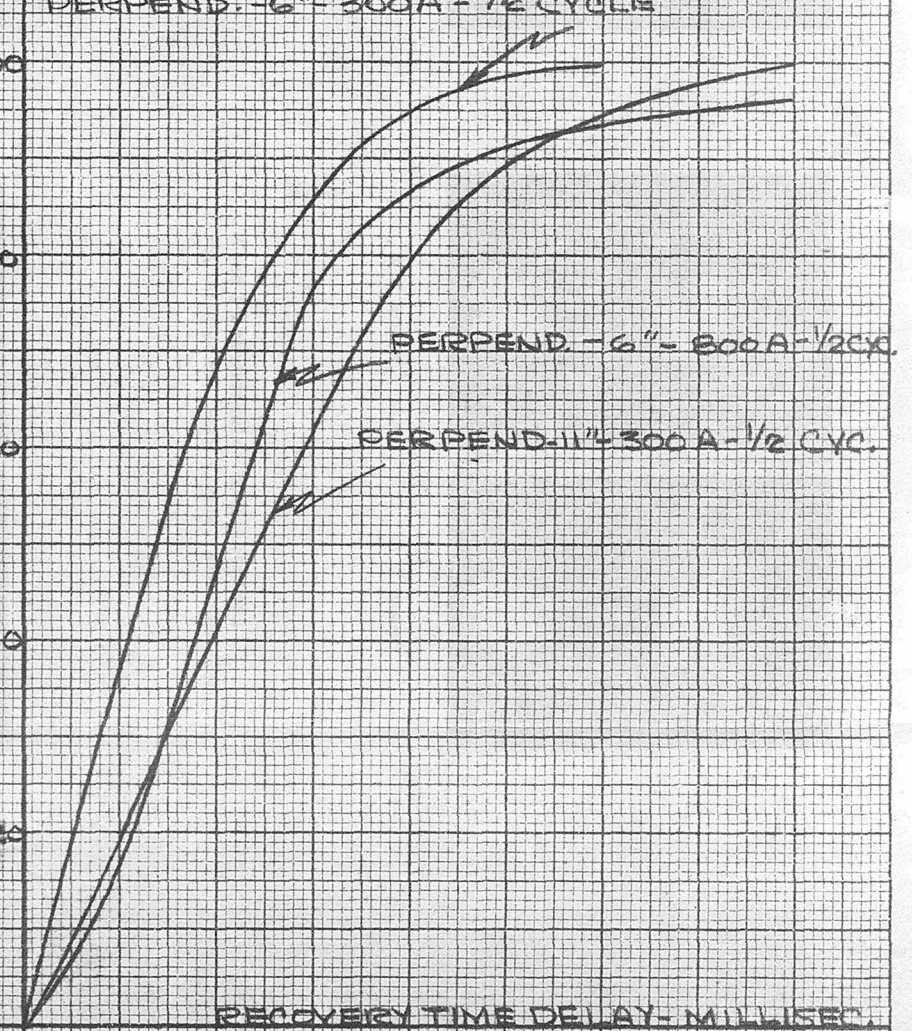

FIG. 34C

PERCENT RECOVERY CURVES FOR 330 FT/MIN. WIND

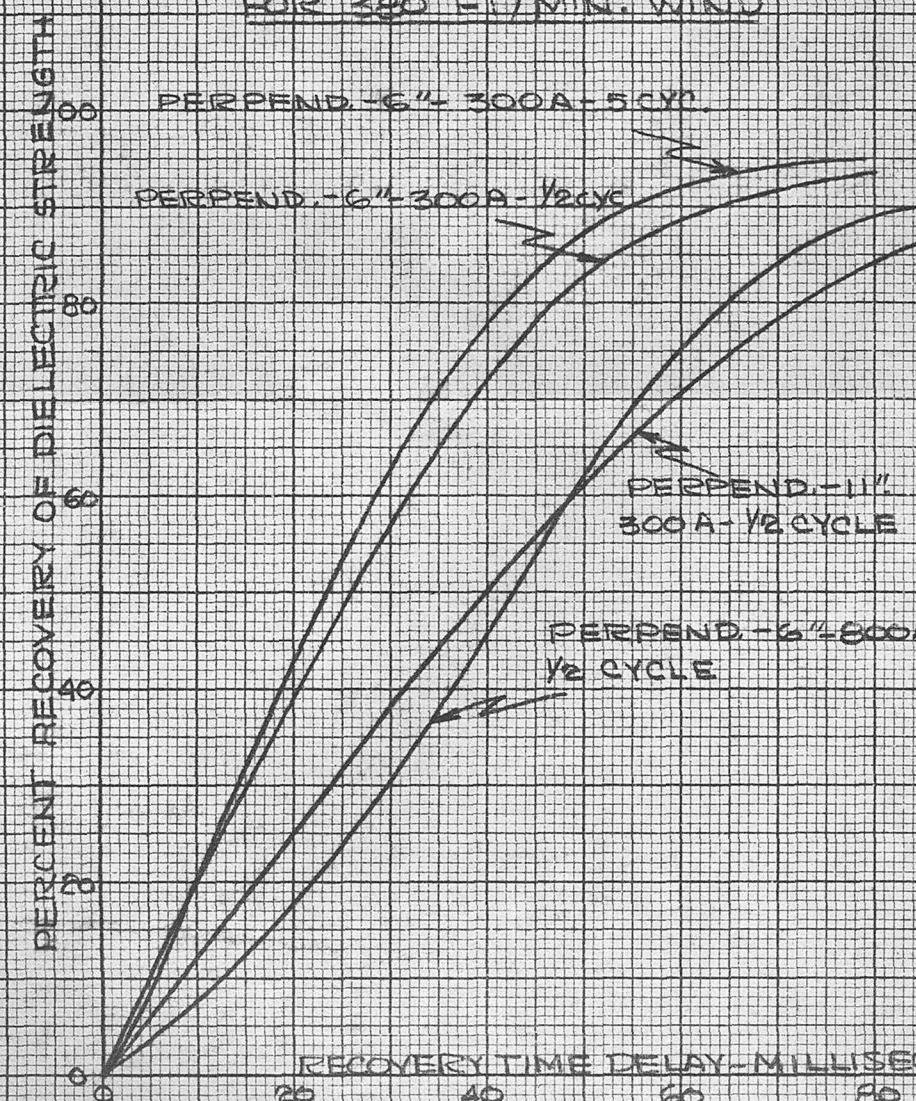

FIG. 34D

PERCENT RECOVERY CURVES FOR NO WIND

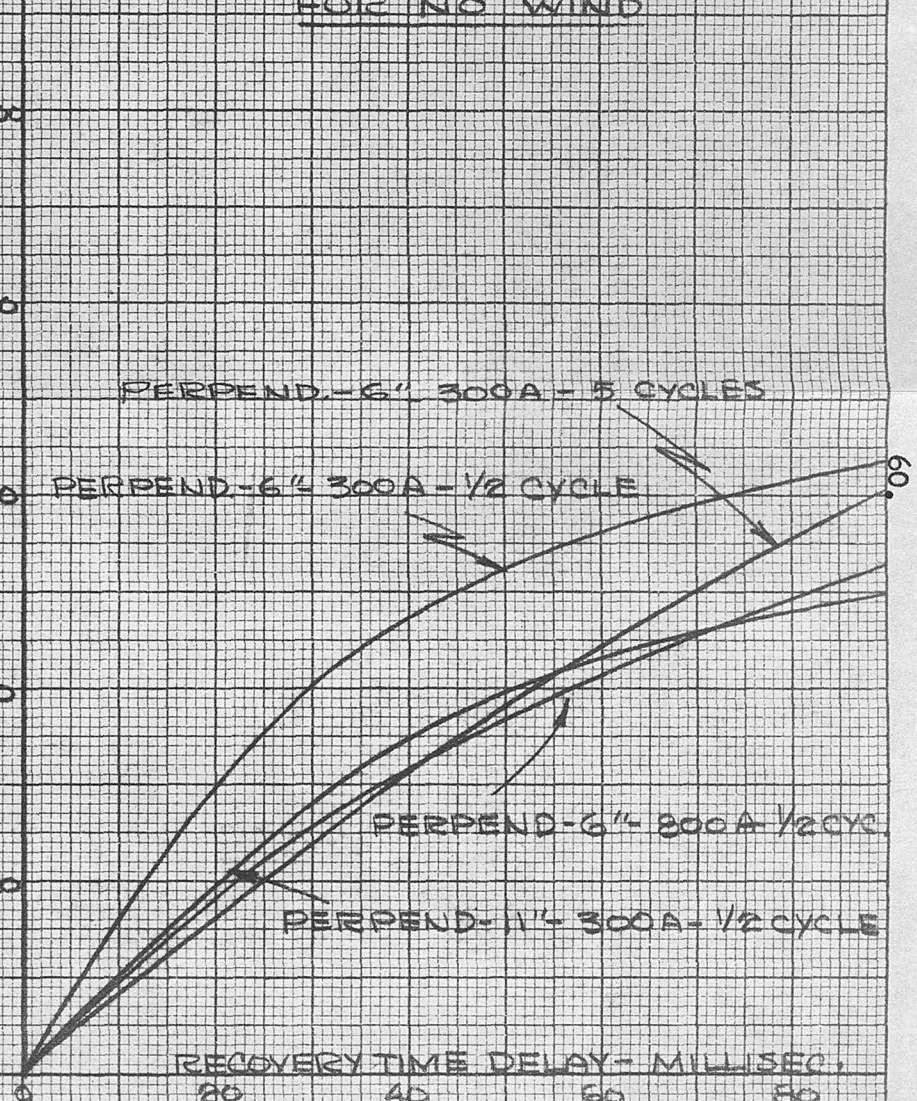

69

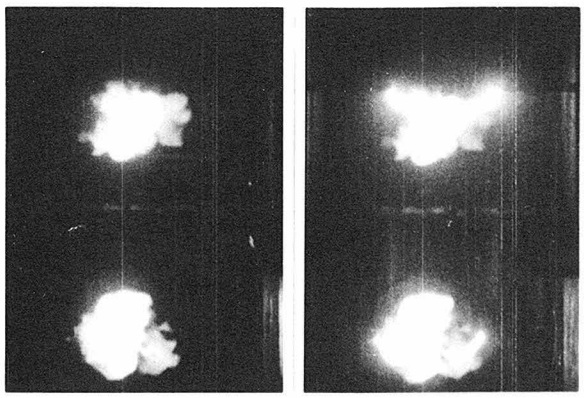

4.2 msec. 4.5 msec

(a)
Wind Perpendicular to Electrodes
300 Amperes, Half Cycle, Six Inch Gap

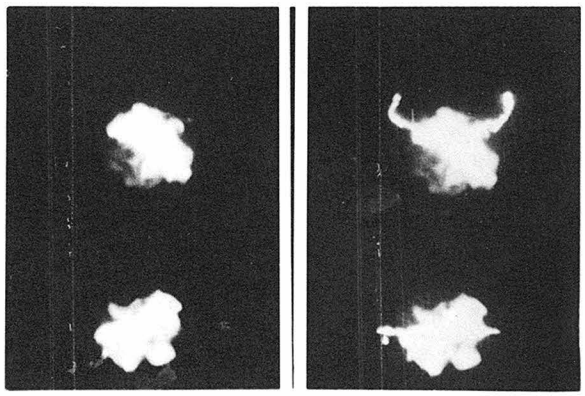

8.4 msec. 8.7 msec.

(b)
Wind Perpendicular to Electrodes
300 Amperes, Half Cycle, Six Inch Gap

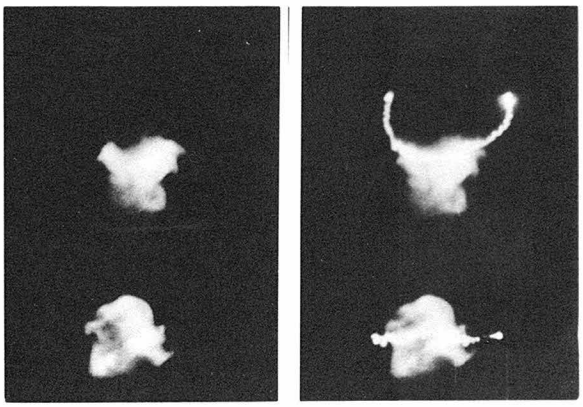

17.0 msec. 17.3 msec

(c)
Wind Perpendicular to Electrodes
300 Amperes, Half Cycle, Six Inch Gap

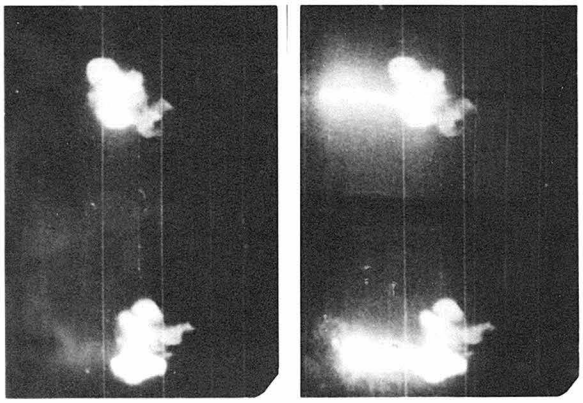

8.4 msec. 8.7 msec.

(d)
Wind Axial to Electrodes
300 Amperes, Half Cycle, Six Inch Gap

Fig. 35

Photographs of arc for 1000 Ft./min. wind showing breakdown path taken by No. 2. Surge Generator through ionized gases for axial and perpendicular electrodes.

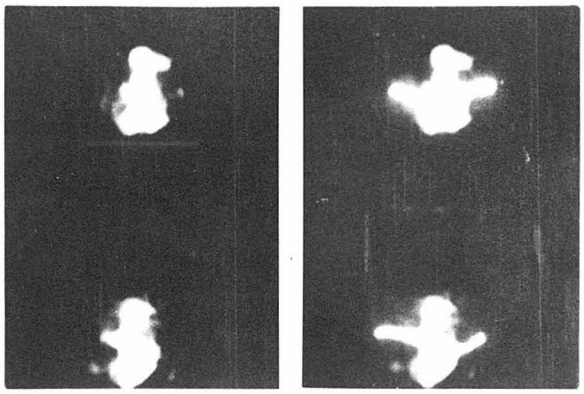

17.0 msec. 17.3 msec.

6 inch test gap
Perpendicular Electrodes
300 amperes crest, half cycle

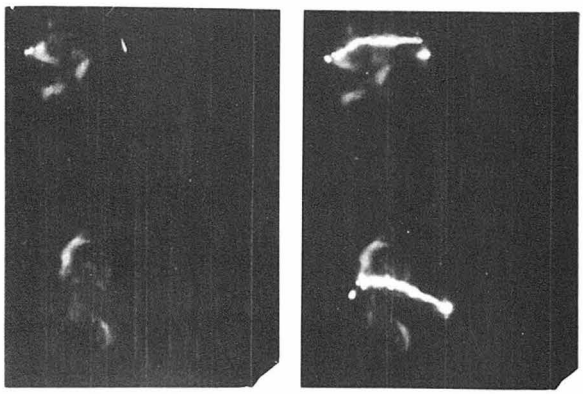

51.6 msec. 51.9 msec.

6 inch test gap
Axial Electrodes
300 amperes crest, half cycle

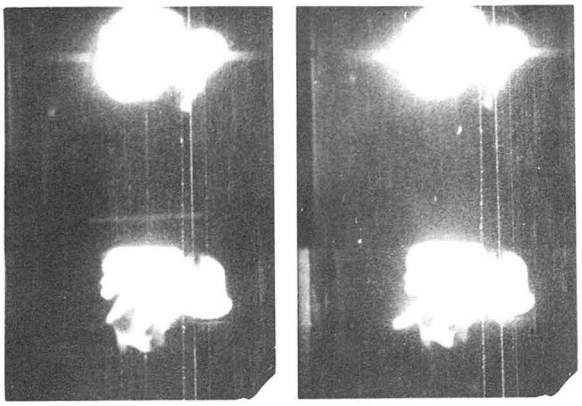

18.8 msec 19.1 msec.

6 inch test gap
Perpendicular Electrodes
300 amperes crest - five cycles

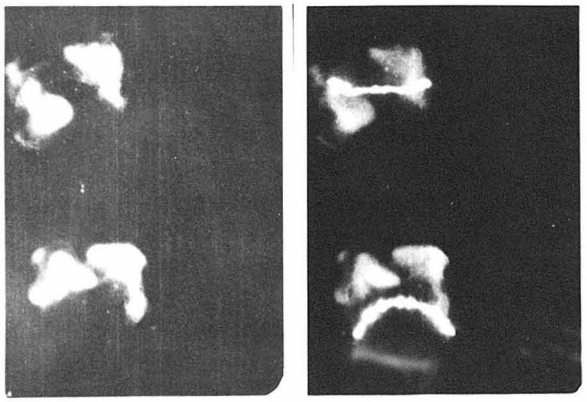

44.3 msec. 44.7 msec.

6 inch test gap
Axial Electrodes
300 amperes crest - five cycles

Fig. 36
Photographic records showing comparitive thermal convection effects of one-half cycle and five cycles of power fault current.

The curves for 1000 feet per minute wind include percentage recovery voltages for both axial and perpendicular direction of the wind across the electrodes. The axial recovery curves are lower than the perpendicular curves because for the perpendicular case the wind displaces the ionized gases from both electrodes, whereas it displaces the gases away from only one electrode in the axial case. This displacement of the ionized gases for axial and perpendicular wind directions is shown clearly in Fig. 35 for 1000 feet per minute wind.

To determine the actual increase in the rate of recovery of dielectric strength produced by the wind it is necessary to plot the difference between the percent recovery voltages with and without wind. Curves showing this difference in percent recovery for various winds and for axial and perpendicular electrodes are shown in Figs. 37 to 40. The dotted lines on these curves represent the calculated increase in recovery strength produced by displacement of the gases at the given wind speed, based on a uniform displacement recovery strength of 20 kilovolts per inch. The ionized gases move away from only one electrode at the wind velocity for the axial configuration so that the displacement lines for the axial case have half the slope of those for electrodes perpendicular to the wind direction. If the percent increase in recovery above the no wind curve followed a displacement curve based on the field strength for the non-uniform rod gap shown in Fig. 42, the initial slope of the recovery would be very much greater than that shown. However, the cool air blowing over the hot electrodes just after current zero becomes heated and the breakdown voltage is lowered accordingly.

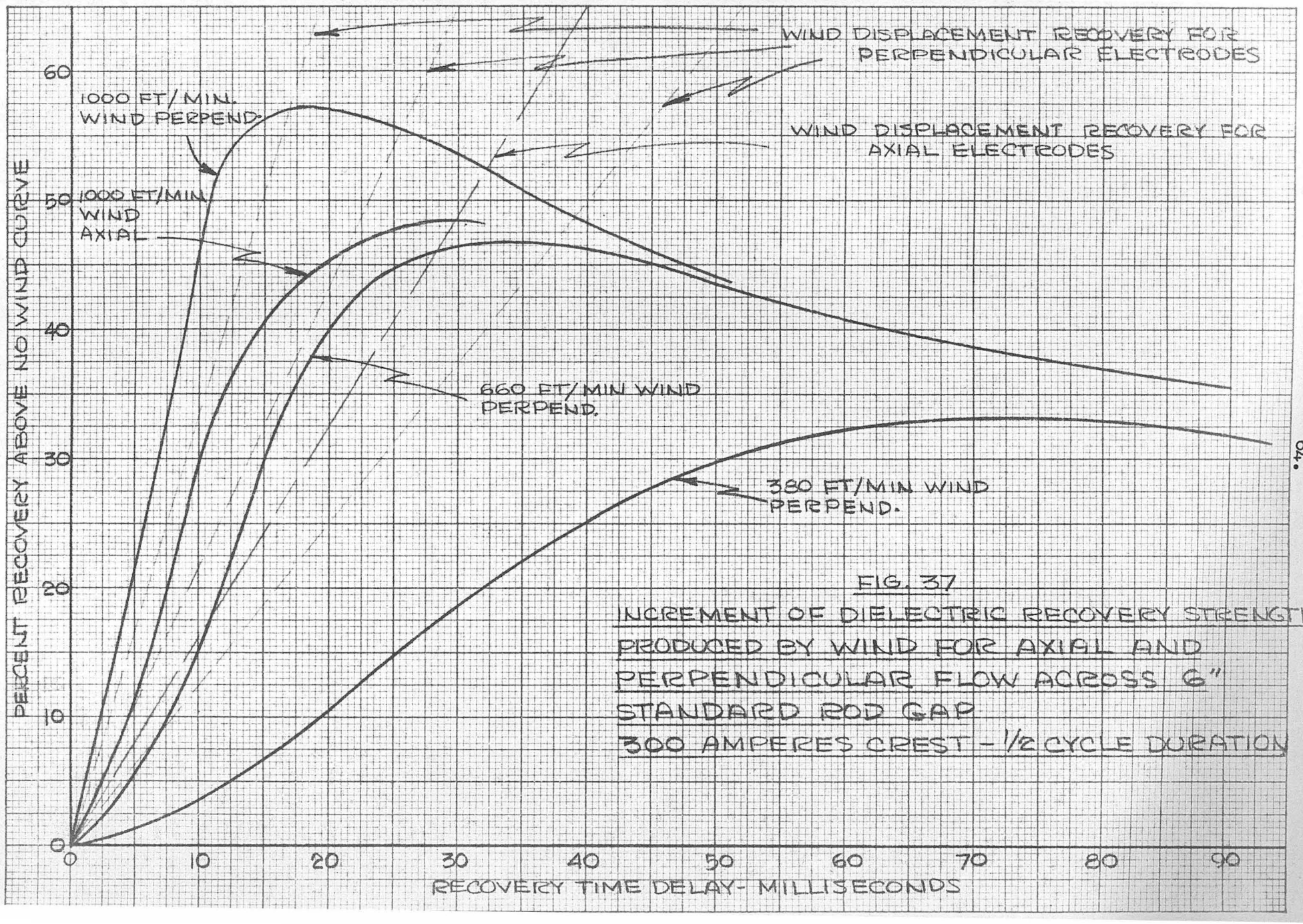

FIG. 37

INCREMENT OF DIELECTRIC RECOVERY STRENGTH PRODUCED BY WIND FOR AXIAL AND PERPENDICULAR FLOW ACROSS 6" STANDARD ROD GAP

300 AMPERES CREST - 1/2 CYCLE DURATION

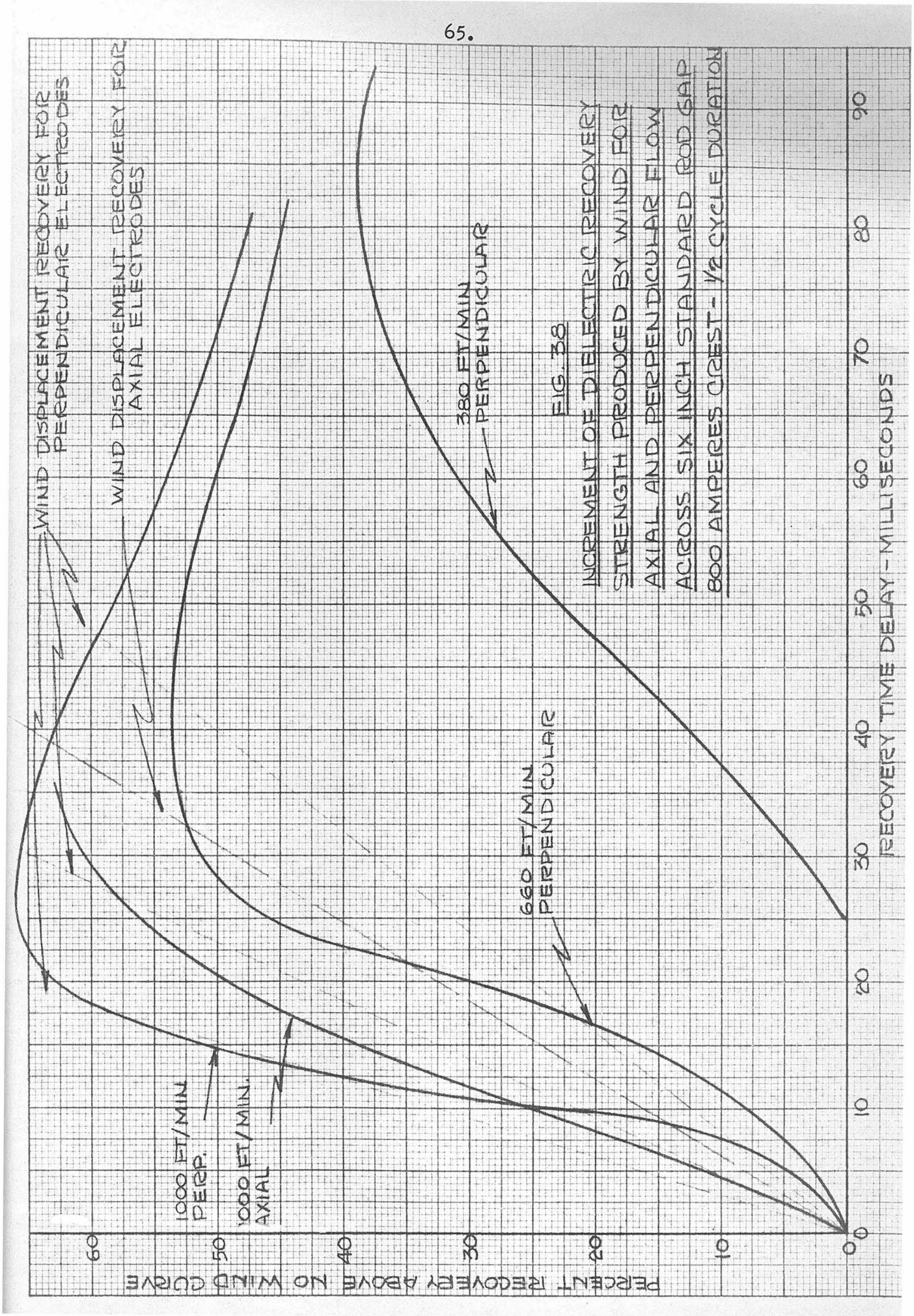

FIG. 38

INCREMENT OF DIELECTRIC RECOVERY STRENGTH PRODUCED BY WIND FOR AXIAL AND PERPENDICULAR FLOW ACROSS SIX INCH STANDARD ROD GAP 800 AMPERES CREST - 1/2 CYCLE DURATION

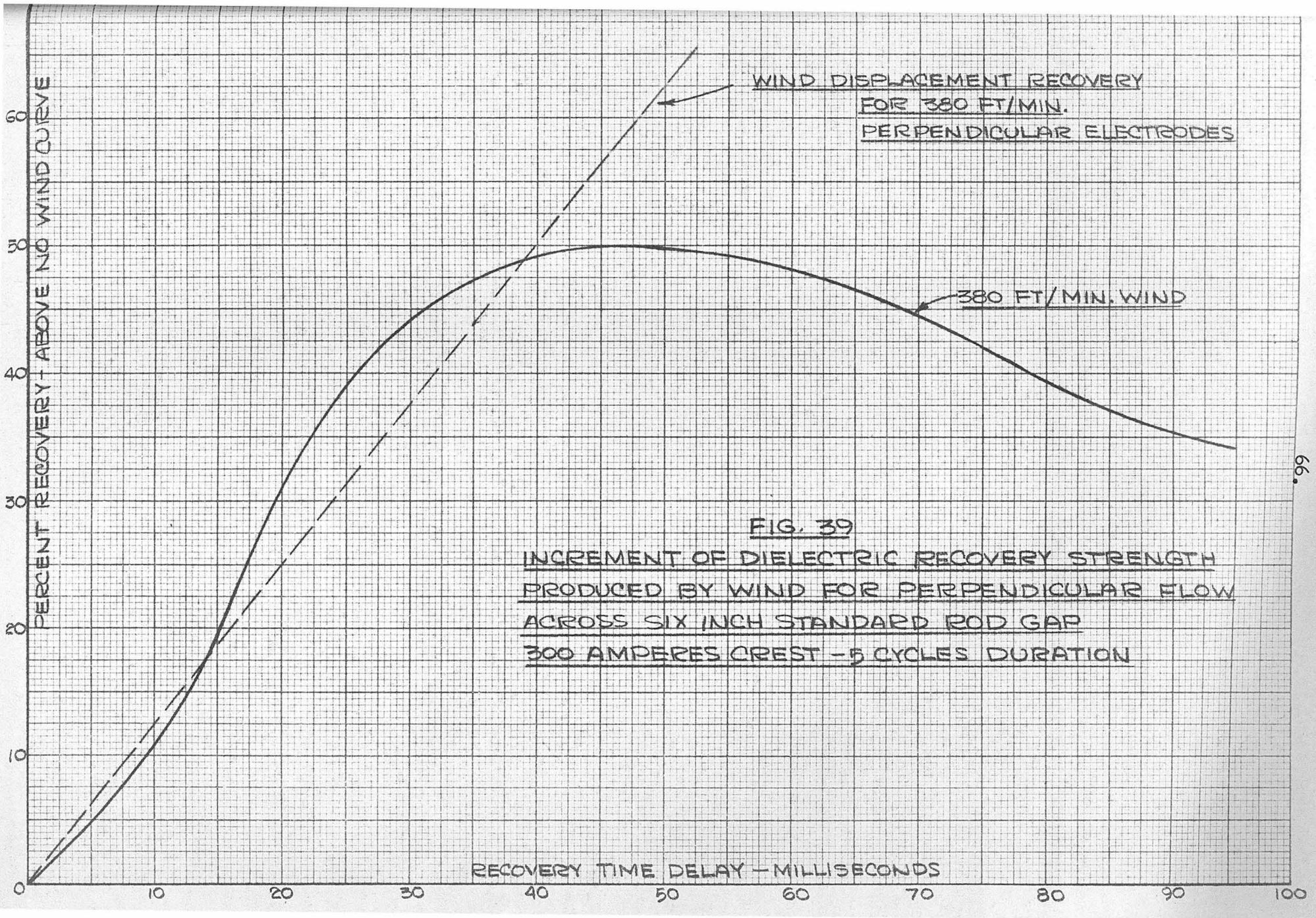

FIG. 39

INCREMENT OF DIELECTRIC RECOVERY STRENGTH PRODUCED BY WIND FOR PERPENDICULAR FLOW ACROSS SIX INCH STANDARD ROD GAP 300 AMPERES CREST - 5 CYCLES DURATION

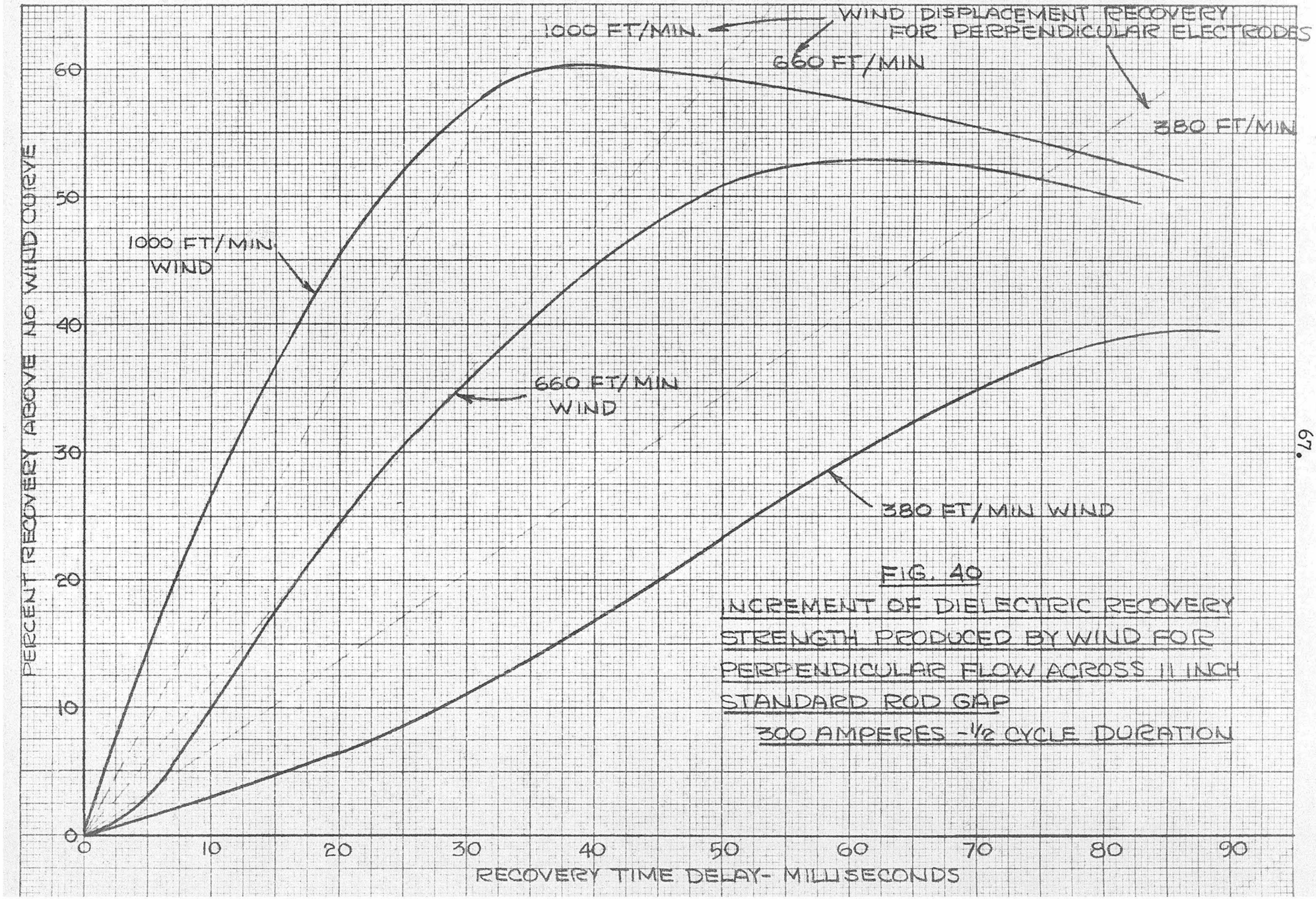

FIG. 40

INCREMENT OF DIELECTRIC RECOVERY STRENGTH PRODUCED BY WIND FOR PERPENDICULAR FLOW ACROSS 1" INCH STANDARD ROD GAP

300 AMPERES - 1/2 CYCLE DURATION

FIG. 42

CURVE OF AVERAGE RELATIVE FIELD STRENGTH ALONG AXIS BETWEEN SIX INCH ELECTRODES FOR 200 VOLTS APPLIED BETWEEN ELECTRODES

USING PROBE IN SALT TRAY

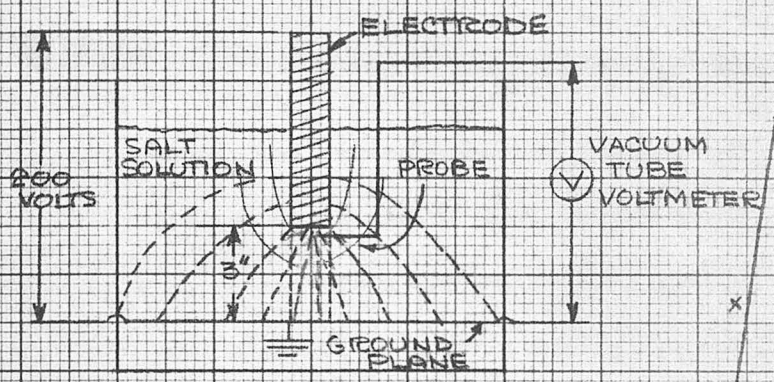

FIELD STRENGTH - VOLTS PER INCH

130
120
110
100
90
80
70
60
50
40
30
20
10

0 1 2 3 4 5 6

DISTANCE FROM LEFT ELECTRODE - INCHES

The increase in actual recovery voltage over the calculated displacement recovery voltage, with increased wind velocity, is due to the greater turbulence at the arc boundary for the higher wind velocities. Suits[34] has applied the analogy of convection-conduction heat loss from solid bodies in fluids to the high-pressure arc column. The arc is considered as a means of energy transfer. Initially electrical energy is used to dissociate and ionize the gas molecules and raise the arc temperature to a high value. The second stage of this energy transfer consists of dissipation of this thermal energy by radiation, conduction and convection. Radiation is considered to be a negligibly small factor.

A correlation of heat transfer from hot cylinders has been made in dimensional units by McAdams[36]. The arc is considered as a hot cylindrical body, but this introduces an error in the analogy because convection currents at the surface of a solid body are zero whereas they are not zero for the arc. However, Suits[37] has found that the heat lost by free convection currents from the arc column is only of the order of 7 percent of the total loss.

The dimensionless heat loss equation given in the Chemical Engineer's Handbook[38] for the case of gases flowing at right angles to single pipes is as follows:

$$\frac{h_m D_o}{k_f} = 0.45 + .33 \left[\frac{D_o G}{f}\right]^{0.56}$$

where

h_m = mean value of h for the apparatus based on the average film temperature, $t_f = \frac{t_o + t_w}{2}$.

It is the local coefficient of heat transfer

$$\frac{\text{B.T.U.}}{\text{hr-sq.ft.-}^{o}\text{F diff.}}$$

D_o = outside diameter of pipe in feet.

k_f = k at the film temperature

It is the thermal conductivity of the fluid in

$$\frac{\text{B.T.U.}}{\text{hr.-sq.ft.-unit temp. grad. in }^{o}\text{F/ft.}}$$

G - mass velocity = $\frac{W}{s}$ in $\frac{\text{lb.}}{\text{hr-sq.ft. of cross section}}$

μ_f = viscosity of the fluid in $\frac{\text{lb.mass}}{\text{hr.-ft.}}$ at the arithmetic mean of the wall and fluid temp

The heat transfer equation for gases flowing outside and parallel to the axis of the pipe[38] is the same as for gases flowing axially inside pipes when the equivalent diameter is taken as four times the ratio of the free cross section to the wetted perimeter. The equation is as follows:

$$\left[\frac{h}{C_p G}\right]\left[\frac{C_p \mu_f}{k}\right]^{2/3} = y$$

where

y = dimensionless constant determined from Reynolds Number in Fig. 8, Curve ABC, p 974 of Chemical Engineer's Handbook[38]

cp = coefficient of specific heat at constant pressure

$$\frac{\text{B.T.U.}}{\text{lb. }^{o}\text{F}}$$

The local coefficient of heat transfer has been calculated in Appendix II for the axial and perpendicular electrode configurations using an arc

diameter of 3.5 inches and an assumed arc temperature of 4000 °F. The local coefficient of heat transfer for 1000 feet per minute wind velocity perpendicular to the arc is 8.4 $\frac{\text{B.T.U.}}{\text{hr.ft.}^2\ ^\circ\text{F}}$ whereas for no wind the heat transfer coefficient is only 0.06. Similarly for 1000 feet per minute wind velocity axial to the arc the local coefficient of heat transfer is 1.4. From the above, it appears that the 1000 feet per minute perpendicular wind condition should recover more than twice as fast as for the axial wind. Because the cross section of the arc with the axial wind is smaller than for the perpendicular wind, (see Fig. 41 C.) the energy loss by convection is much greater for the axial than for the perpendicular wind. Hence, the increase in recovery for the axial wind is greater than half that of the perpendicular wind as shown in Figs. 37 and 38.

It is of interest to extrapolate linearly the increment of recovery strength over wind from 1000 feet per minute to 30,000 feet per minute (500 feet per second) for wind directed perpendicular to a six inch standard rod gap with a half cycle of 300 ampere fault current. The slope of the dielectric recovery produced is 33 times the 4.8 volts per microsecond obtained for 1000 feet per minute, or 165 volts per microsecond. For the extinction of an arc in an air blast circuit breaker, assuming six inch spacing and that the arc gap is to recover one quarter of its dielectric strength in 10 microseconds, it must have a rate of increase of dielectric strength of the order of 3000 volts per microsecond. Thus the recovery rate of the confined arc in the circuit breaker must be enhanced at least 18 times the extrapolated value obtained for the unconfined arc. The local coefficient of heat transfer for this higher wind velocity perpendicular to

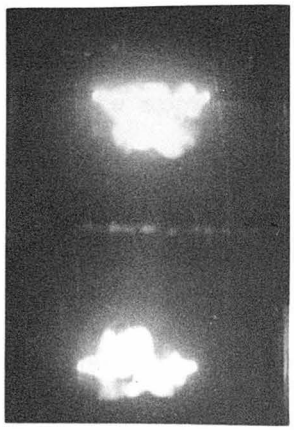

Current Zero

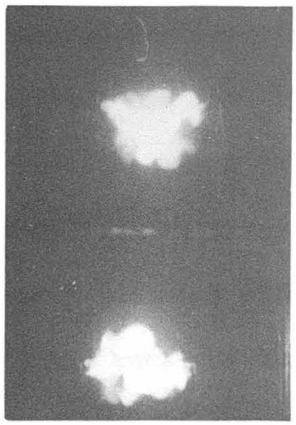

1. 7 msec.

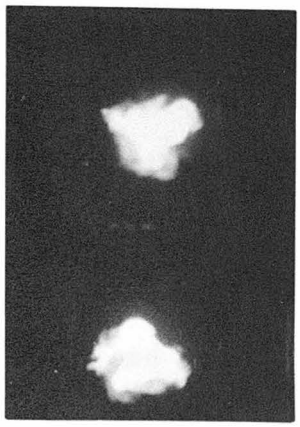

5. 0 msec.

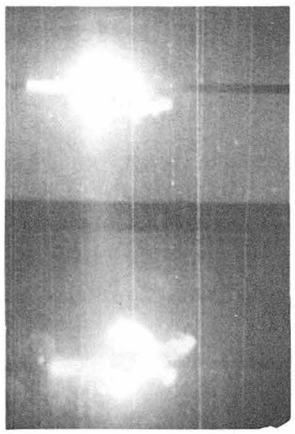

Current Zero

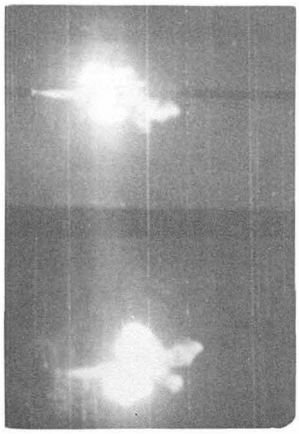

1. 7 msec.

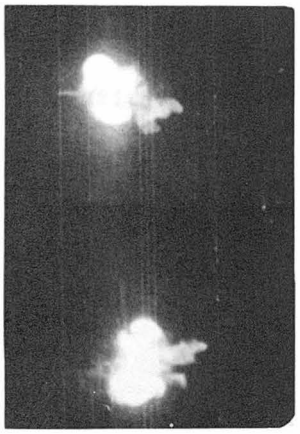

5. 0 msec.

Fig. 41 (c)
Photograph comparing the corss-section of the luminous gases, near current zero, for axial and perpendicular winds in a six inch test gap for a 300 ampere current of half cycle duration.
Upper series - for perpendicular wind
Lower series - for axial wind

the electrodes has been calculated in Appendix II. It is found to be 56, which is approximately seven times the heat transfer coefficient for the 1000 feet per minute case. Thus the extra rate of recovery in the confined arc, which is approximately three times that for the unconfined arc, must be due to the cooling and deionizing effect of the confining walls, the increase in pressure[39], and enhanced turbulence in the arc itself. It is interesting to note that the heat transfer coefficient for the 30,000 feet per minute axial blast is 23 times the heat transfer for 1000 feet per minute axial wind, but it is only one half of the coefficient for 30,000 feet per minute perpendicular wind. However, the loss of heat by convection from the boundary has been neglected in this analogy and with the reduced arc cross section for the axial wind, its convection heat loss will be much greater than for the perpendicular configuration.

According to Slepian's theory of the extinction of the long arc, the critical breakdown gradient for reignition of the arc is determined approximately by the following equation:

$$X_c = \frac{D}{(a\ n)^{\frac{1}{2}}}$$

In his development Slepian equates the rate at which energy is supplied to the arc column by the electric field, ($W_2 = kX^2 e n \pi \frac{a^2}{4}$), to the rate at which energy is lost by the unionized column of gas, ($W_o = C_2 \pi a$), at the temperature, T_o, at which profuse ionization of the gases is assumed to begin. The rate at which ions (and therefore energy) continue to be lost by the arc column through diffusion to the boundary at the temperature, T_o, is also dependent on the perimeter of the arc section. This energy loss

can also be included in the term W_o which represents the rate of energy loss of the arc column per unit length of the arc. Energy loss represented by recombination of ions and dissociated molecules represents only the loss of energy from the arc column by radiation, which is considered by Suits (34) to be a small factor in the energy dissipated of the arc. Hence, the application of the above equation to obtain the critical gradient is based on the assumption that below the critical temperature, T_o, there is very little ionization and above it the ionization increases very rapidly.

Appendix III contains calculations of the recovery voltage for 6 and 11 inch test gaps based on the approximate equation for the breakdown gradient,

$$X_c = D \frac{a^{\frac{1}{2}}}{(a^2n)^{\frac{1}{2}}}$$

where

a = average diameter of the arc section from the two views of the arc.

(a^2n) = integrated density of the arc section obtained directly from the micro-densitometer reading.

D = a constant for the gas.

A comparison of the calculated and the experimental recovery voltages is shown in Fig. 44. The calculated values for the 800 ampere half cycle, 6 inch gap and the 300 ampere half cycle, 11 inch gap are higher than the experimental values. This variation is probably due to differences in sensitivity of the 16 mm. film and changes in the background density of the film due to variations in development. The determination of the density of

FIG. 43 A

PLOT OF TOTAL DENSITY OF LUMINOUS CLOUD ACROSS SIX-INCH TEST GAP 300 AMPERES- 1/2 CYCLE

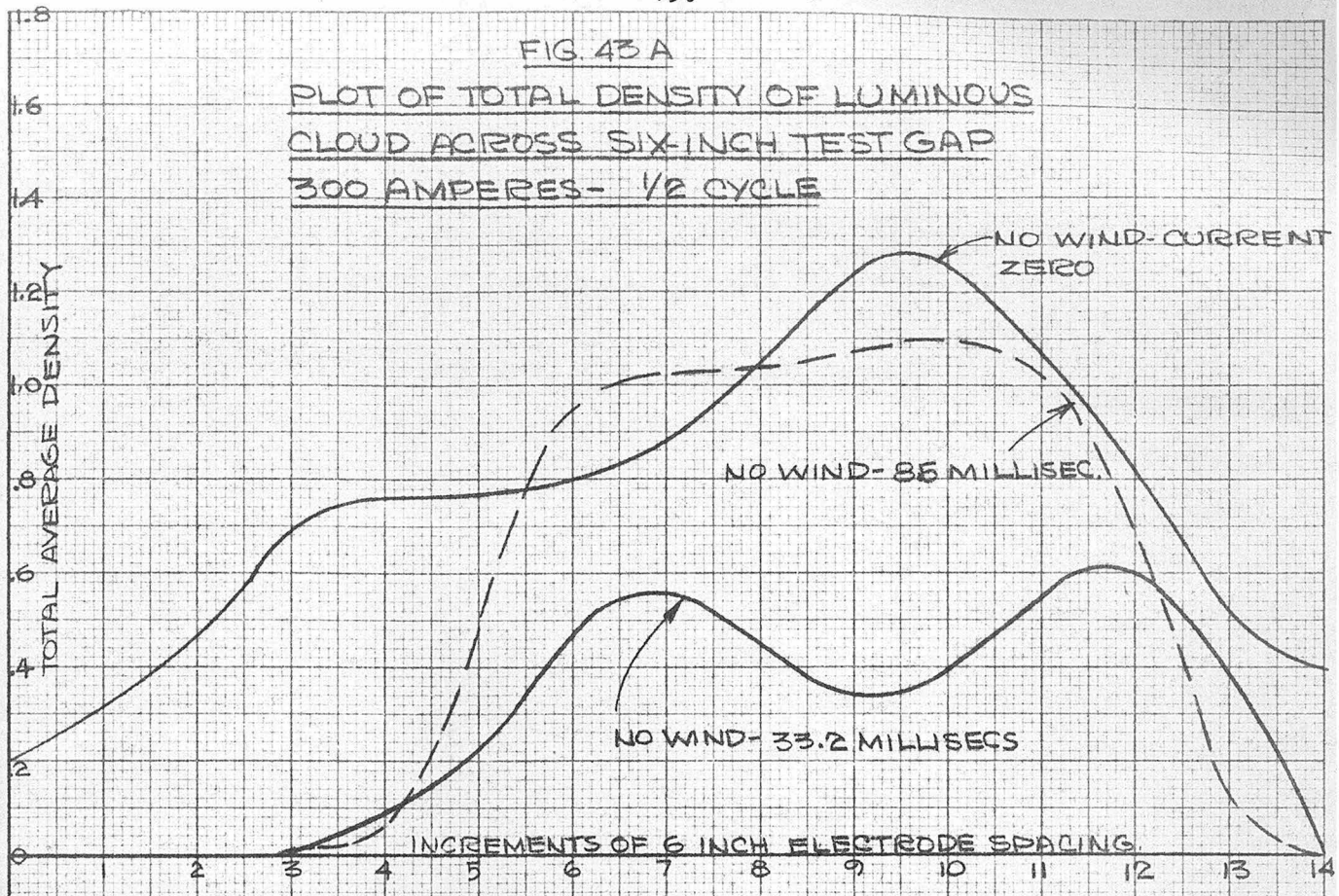

FIG. 43 B

PLOT OF TOTAL DENSITY OF LUMINOUS CLOUD ACROSS 11- INCH TEST GAP 300 AMPERES - 1/2 CYCLE

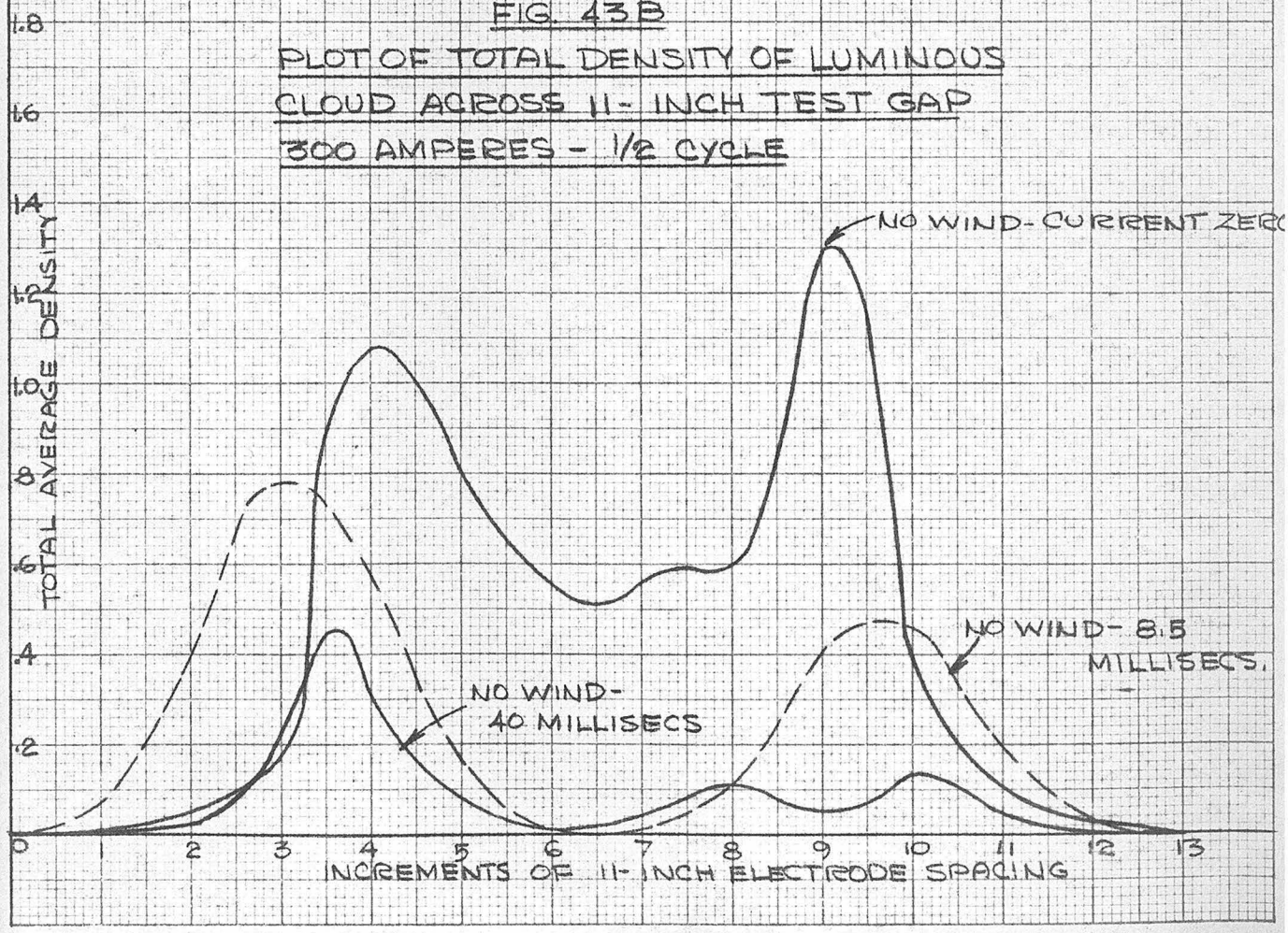

APPENDIX III

FIG. 44

COMPARISON OF EXPERIMENTAL RECOVERY CURVES AND CALCULATED VALUES OF RECOVERY VOLTAGE USING SLEPIAN'S APPROXIMATE EQUATION

$$X_c = D \frac{a^{1/2}}{(a^2 n)^{1/2}}$$

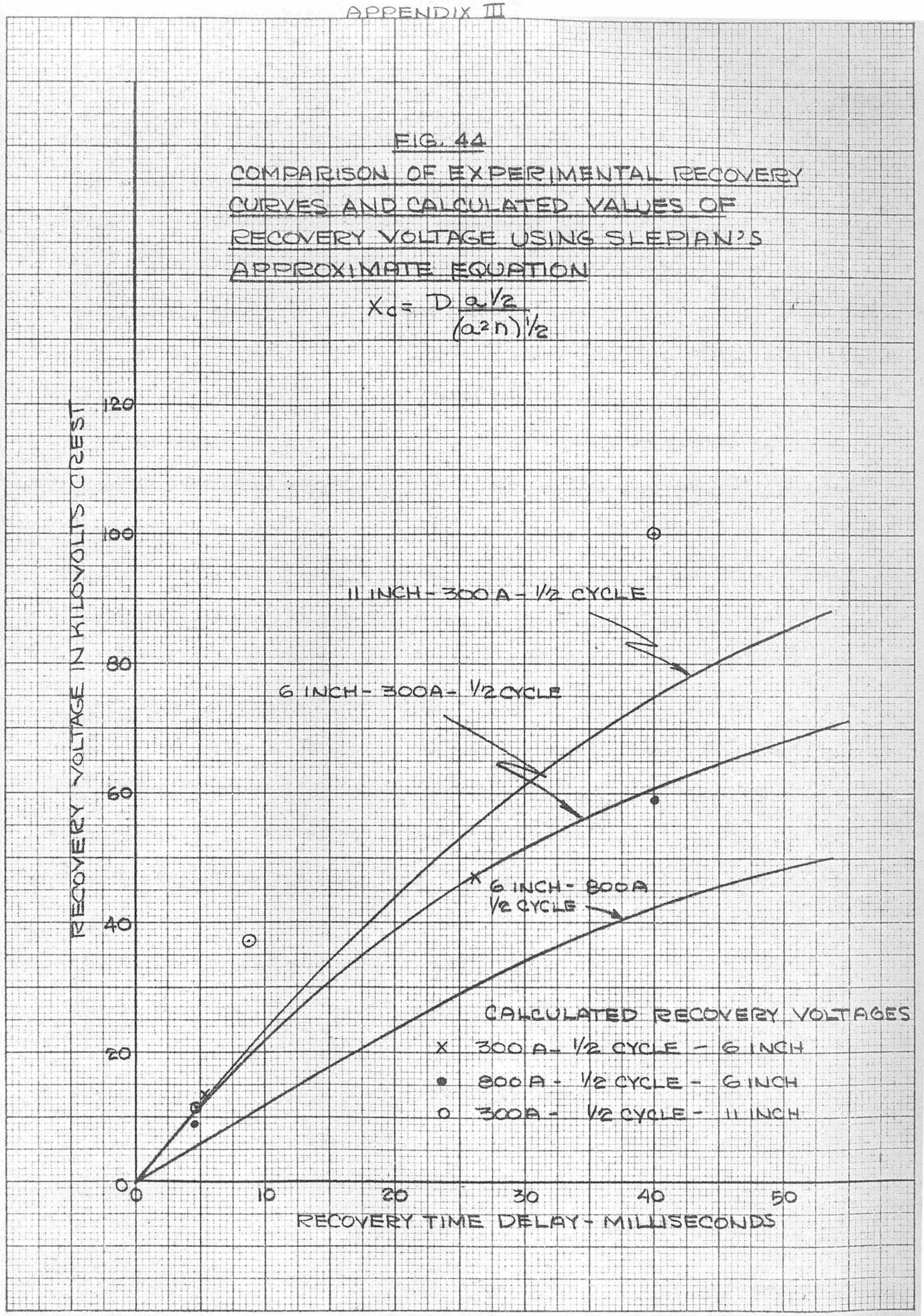

ionization is also in error because the film was not sensitive to infra-red radiation and because the ultra-violet radiation was eliminated by the glass lens system of the camera. Because of the approximations upon which this analysis is based and the random mechanism of the discharge, these calculations show only that the calculated recovery voltages are in general qualitative agreement with the experimental results. To obtain more definite results as to the recovery mechanism a more extensive study will be necessary.

The effect of wind on the per unit density of the ionized gases is shown in Fig. 45 as a function of the increment of the test gap. The 1000 feet per minute wind density, at 8.5 milliseconds time delay, is lower than the no wind density, indicating that wind does increase the heat transfer coefficient of the arc. A comparison of the arc cross-section in plan and elevation view for 300 and 800 amperes half cycle is shown in Fig. 46. The 800 ampere arc, which has a larger diameter than the 300 ampere arc, has a lower ratio of surface to volume; hence, the rate of deionization by diffusion and cooling is lower for the 800 ampere arc than the 300 ampere arc(40). This effect is reflected in the lower recovery rate for the 800 ampere current even though the initial average ionization density for the 800 ampere appears to be lower than for the 300 ampere section (see Fig. 47). However, this is partly due to over-exposure of the film near current zero, for the 800 ampere arc, with the resulting saturation of the film (the f-8 operature was used for both 300 and 800 ampere fault currents)and low reading on the microdensitometer.

If it is assumed that deionization is chiefly produced by diffusion of the ions to the boundary of the luminous gases, for a short time after

FIG. 45

EFFECT OF WIND ON PER UNIT VOLUME DENSITY OF LUMINOUS GASES ACROSS SIX INCH TEST GAP, 800 AMPERES, 1/2 CYCLE

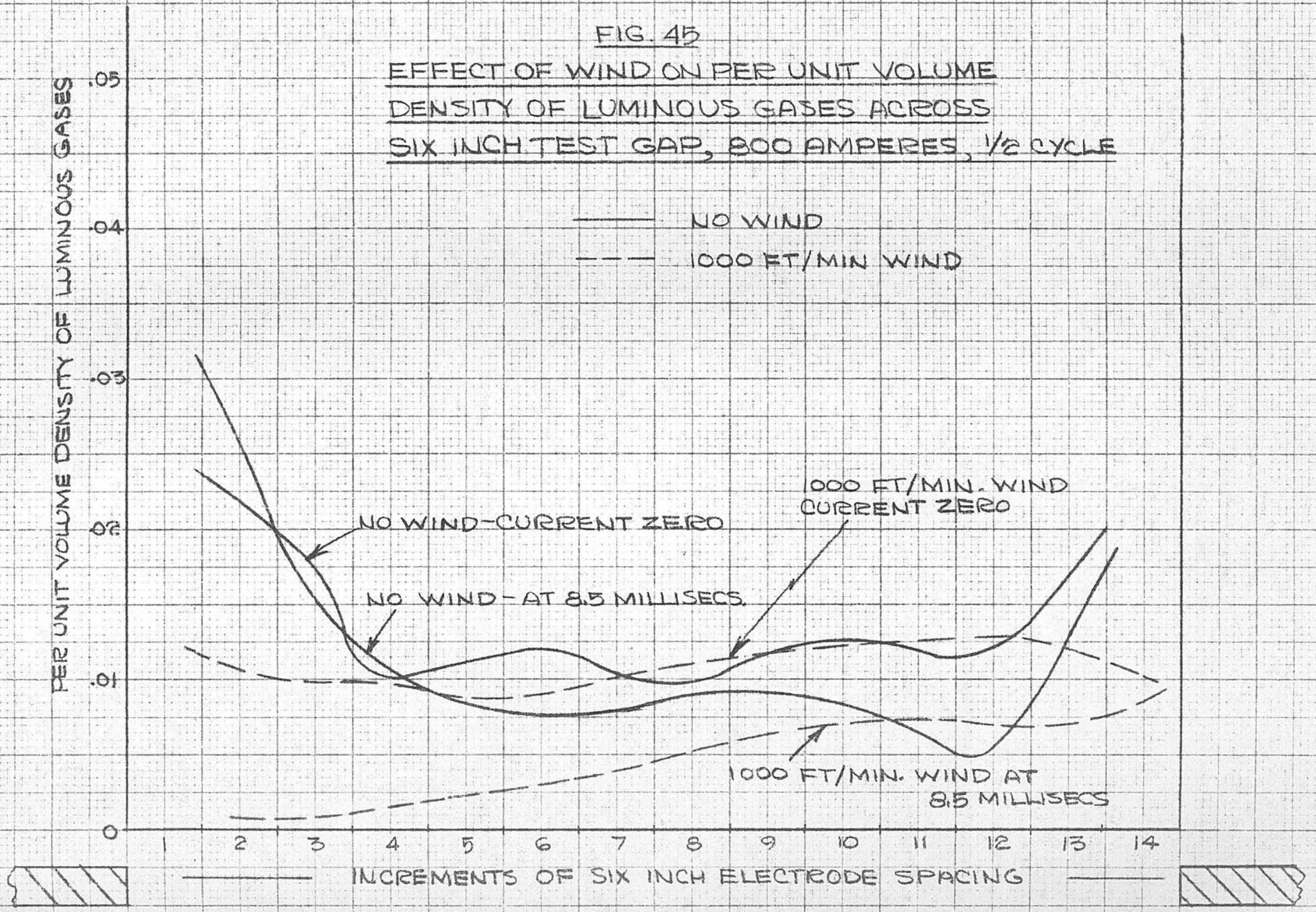

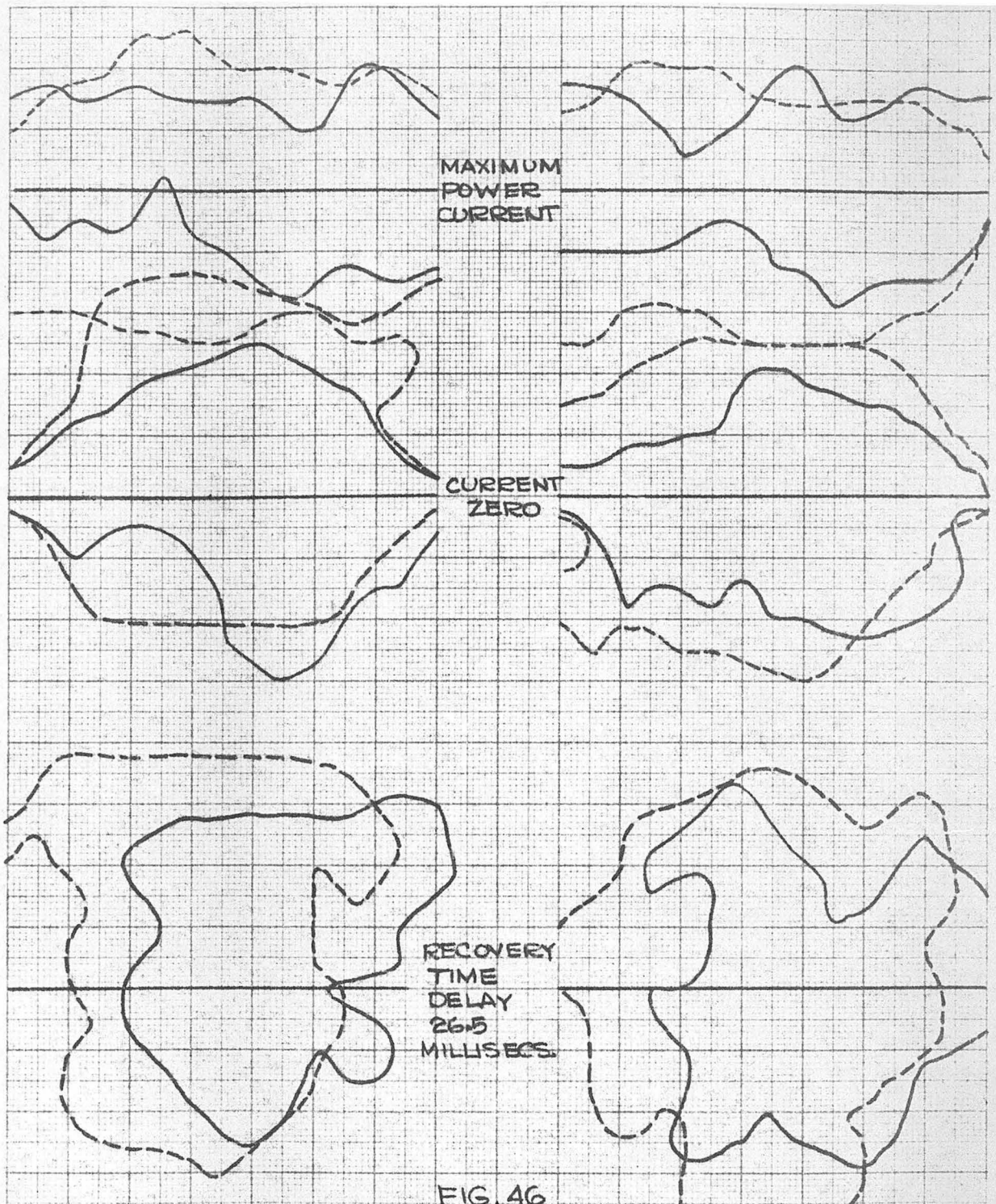

FIG. 46
COMPARISON OF CROSS-SECTIONS OF 300 AND 800 AMPERE 6 INCH ARC
LEFT- PLAN VIEW OF ARC SECTION
RIGHT- ELEVATION VIEW OF ARC SECTION
——— 300 AMPERES - HALF CYCLE
- - - - 800 AMPERES - HALF CYCLE

FIG. 47

VARIATION OF AVERAGE DENSITY OF LUMINOUS GASES FOR 300 AND 800 AMPERES WITH RECOVERY TIME DELAY.

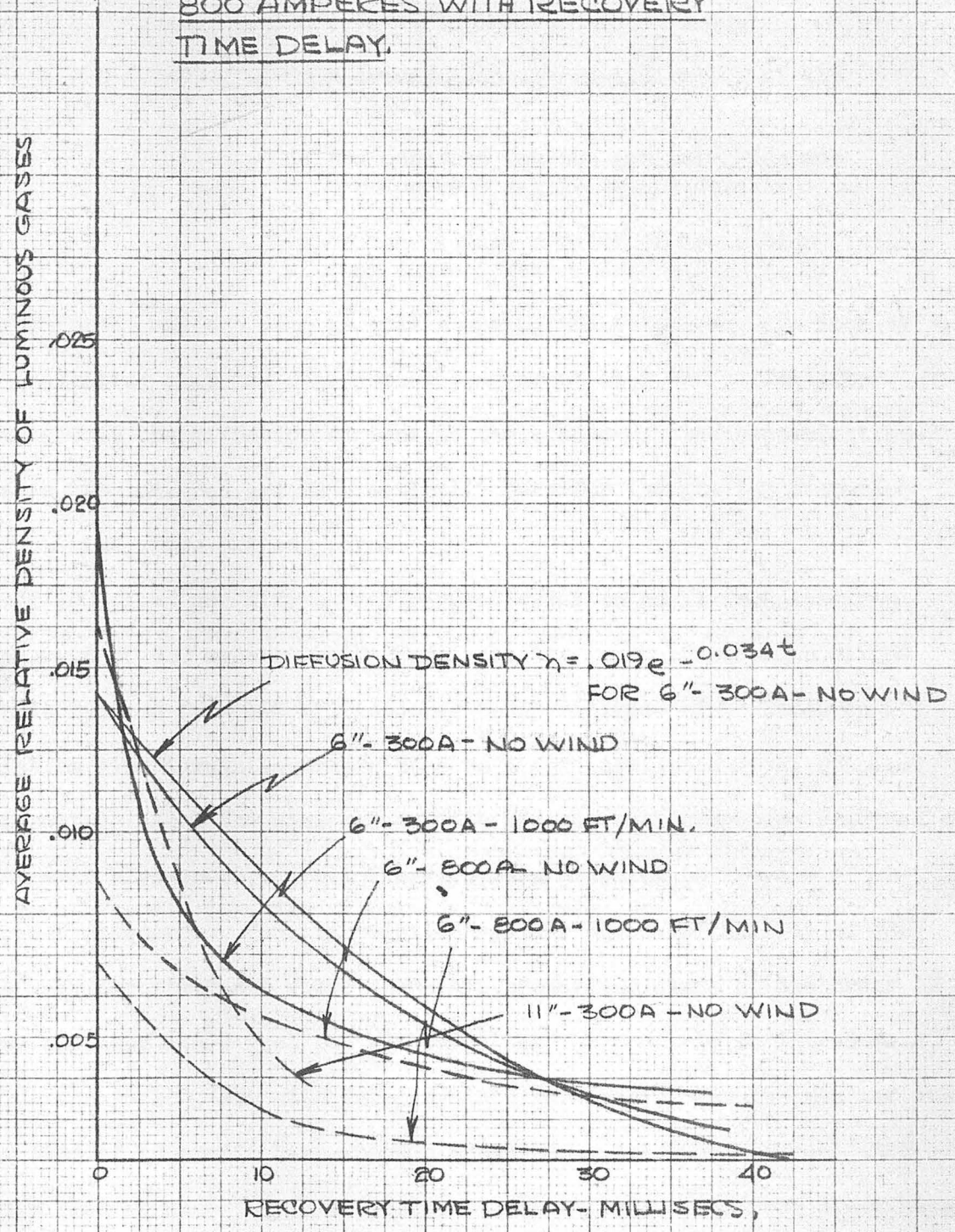

current zero, an exponential density variation is obtained (see Fig. 47), where

$$n = N_o e^{-At}$$

n = average density of ionization at the time, t.

A = a constant for the gas which depends on current magnitude and duration.

N_o = the average density of ionization at current zero.

This exponential has the same general shape as the actual average density curves indicating that the chief deionizing agent at a short time after current zero is the diffusion of ions to the boundary. The recombinations of ions in the luminous gas is practically zero for the gas temperatures at a short time after current zero.(40)

With 1000 feet per minute wind perpendicular to an 11 inch test gap and a current of 300 amperes half cycle, the time to half strength of the air gap is reduced from 100 milliseconds to 15 milliseconds. Based on a transmission line insulation ratio of 4 to 1 for insulation level compared with circuit voltage, the wind reduces the minimum reclosing time required for automatic high-speed circuit breakers from 6 cycles to 1 cycle of 60-cycle power frequency. For transmission systems where reliability of service is very important and where there are prevailing winds of the order of 15 miles per hour (1000 feet per minute) it may be possible to introduce a variable representing the wind velocity into the control for the minimum reclosing time of automatic high-speed circuit breakers. Shorter reclosing times can then be used for fault isolation where there are strong prevailing winds with a corresponding increase in reliability of service.

IV CONCLUSIONS AND SUGGESTIONS FOR FUTURE RESEARCH.

1. Up to the present time very little research has been done on the mechanism of dielectric recovery of large air gaps because of the difficulties involved in obtaining a satisfactory test technique. The technique presented here is very satisfactory for determining the recovery characteristics of various insulations. It is possible to obtain data for the critical recovery voltages of insulation materials at the rate of one record every minute. The results contained in this thesis represent a total of more than 13,000 separate records.

2. The duration of the fault current has little affect on the recovery characteristics of the vertical air gap. The initial recovery rate of a horizontal air gap for five cycles of power current is lower than for a half cycle because of the greater ionization present at current zero with the longer current duration. However, the displacement of the ionized gases by thermal convection increases the slope of the recovery for the five cycle current above that for the half cycle at later recovery times.

3. The increase in rate of dielectric recovery produced by wind velocities up to 1000 feet per minute is mainly due to displacement of the ionized gases from the test gap. There is a noticeable increase in heat transfer from the ionized gases at the higher wind speeds which decreases the density of ionization and enhances the recovery rate for the higher wind speeds. In comparing the recovery voltages for wind directed axially along the test gap with that for wind directed perpendicular to the test gap, the perpendicular wind produces nearly twice as large a

recovery rate as the axial wind for wind velocities up to 1000 feet per minute. The high speed photographs show clearly that the breakdown occurs in the weakest path through the ionized gas even when this path is 2 or 3 times as long as the distance between the electrodes.

4. At short times after current zero, the breakdown is a glow discharge because the low field strength at the breakdown voltage, produces negligible ionization by collision in the test gap.

5. The electrode material affects the dielectric recovery characteristics of the 6 and 11 inch test gaps. The lower the boiling point and the lower the ionization potential of the electrode material, the lower the rate of dielectric recovery.

6. Turbulence in the wind stream does not affect the recovery characteristics of the air gap for wind velocities up to 1000 feet per minute.

7. Wind velocities of 100 feet per minute do not affect the recovery characteristics. According to Suits[37] the free convection velocities in the arc are of the order of one meter per second or (200 feet per minute) so that in the time required for recovery the effect of a superimposed wind of 100 feet per minute is small.

8. If the effect of a 1000 feet per minute wind is considered in obtaining the minimum reclosing times for high-speed automatic-reclosing circuit breakers the minimum reclosing time can be reduced from 6 to 1 cycle power frequency.

9. The cross-section of the arc is greater for 800 amperes of fault current of a half cycle duration than for 300 amperes. For a short time

after current zero, the deionizing agent in the luminous gases is mainly diffusion.

10. All of the dielectric recovery characteristics included in this thesis are for unconfined air gaps. As most of the arc paths for transmission line faults are across porcelain insulator surfaces, an extensive investigation of the dionizing time for long arcs across insulators would be directly applicable to improving insulation coordination on transmission and distribution systems. Fatigue tests of porcelain insulators subjected to power fault currents could be combined with such a study.

11. An attempt has been made to calculate the recovery voltages for ionized gases in long air gaps. Because of the large number of variables involved in this calculation and the approximations made, the results are not accurate but they do show general qualitative agreement with the experimental results.

12. In order to determine more completely the mechanism of dielectric recovery the temperature of the luminous gases as a function of time is required. One of the methods by which this temperature can be determined is by a time-resolved spectrographic analysis of the arc. The temperature can be obtained from Saha's equation when the electron density is determined from the width of the spectal lines[42]. Another method of determining the temperature is by assuming the spectral energy distribution of the arc is a black body radiation.[43] By measuring the response of two phototubes, having maximum response characteristics at opposite ends of the visible spectrum, the change in response of the phototubes can be recorded

on oscilloscopes and the temperature determined from the known black body radiation distribution as a function of temperature.

13. In order to apply de-ion tubes effectively and economically a study of the behaviour of arcs in parallel for various circuit constants and configurations would be of value.

14. A study of the influence of magnetic and electric fields on the dielectric recovery characteristics of long air gaps would increase the fundamental knowledge of the recovery mechanism. Yadoff[31] has investigated the effect of a radial electrostatic field on arc extinction and found that the luminosity of the arc decreases, with increased radial electrostatic field, until final arc extinction.

AIEE
ical Paper
50-96

mber 1949
ho in USA

DIELECTRIC-RECOVERY CHARACTERISTICS OF POWER ARCS IN LARGE AIR GAPS

G. D. McCann
Member AIEE

J. E. Conner
Nonmember AIEE

H. M. Ellis
Student Member AIEE

All of:
California Institute of Technology
Pasadena, Calif.

A paper recommended by the AIEE Committee on Transmission and Distribution and approved by the AIEE Technical Program Committee for presentation at the AIEE Winter General Meeting, New York, N. Y., January 30-February 3, 1950. Manuscript submitted November 2, 1949; made available for printing December 2, 1949.

PRICE: 30¢ To Members
60¢ To Nonmembers

DIELECTRIC-RECOVERY CHARACTERISTICS OF POWER ARCS IN LARGE AIR GAPS

by

G. D. McCann,[1] J. E. Conner and H. M. Ellis

Summary

A satisfactory test technique has been developed for studying the rates of dielectric recovery of large air gaps and other types of power system insulation. This permits the accurate control of the fault conditions so that all practical types of fault currents can be studied. These are (1) very high magnitude-short duration surges typical of lightning currents (2) currents of power system frequencies and (3) intermediate duration currents such as those which might result from high frequency current zeros produced by natural system oscillations.

Results are presented showing the rate of dielectric recovery of three, six and eleven inch standard rod gaps for power frequency fault currents up to 700 amperes. Electrode cooling effects were found important at three inch gap spacings but not at six inches or above. The eleven inch gap data are proportionately higher than the six inch data indicating that the results can be extrapolated. The data show that for arcs of a few cycles, actual duration has little effect on rate of recovery. A range of current magnitudes from 50 to 700 amperes causes only about a two to one variation in rate of recovery. For the normal ratios of transmission line insulation level to operating voltage (about four to one) minimum delay times of from 0.025 seconds (for 100 ampere faults) to 0.05 seconds (for 700 ampere faults) are required before the recovery voltage reaches the magnitude of the normal applied voltage. Time intervals of 0.05 to 0.08 seconds are required before the voltage strength has built up to twice this level or one half the initial gap strength. This is contrasted with a corresponding time interval of only two to three thousand microseconds for very short duration lightning surge currents.

High speed camera studies of the arcs show that for power frequency faults of one half to one cycle duration, visible luminous gases are present in the gap space for times after current zero up to 0.07 or 0.08 seconds. The photographs and voltage breakdown curves show that subsequent breakdowns will occur through the region of brightest photographic luminescence if such still exists in the gap space. Under these conditions breakdown is started by initial streamers from each electrode which, however, propagate at much slower velocities than for breakdown of air under normal conditions. Time intervals as high as 30 or 40 microseconds are required for a low impedance path to be established.

This research program is being extended to other insulating media and fault conditions and fundamental studies are being made of the dielectric recovery mechanism.

[1] All of California Institute of Technology, Pasadena, California.

Introduction

Knowledge of the dielectric recovery characteristics of power system insulation following flashover or breakdown is of fundamental importance in determining and improving power system performance. However, relatively little fundamental data have been obtained because of the complexity of the phenomena and the difficulty of performing significant tests on representative insulation media. The bulk of the data that have been gathered apply only to the circuit breaker art or to small gaps where electrode effects dominate.

Studies of the primary insulations are important in determining probabilities of insulation failure resulting in sustained faults, permissible reclosing times for circuit breakers and the performance of disconnect switches. A study of the performance of simultaneous arcs through similar and dissimilar insulating media and at various distances apart on systems is required for better coordination of such protective devices as "De-ion" protector tubes. Dielectric recovery studies are also of great importance in determining the characteristics of system transients during such faults as arcing grounds. The conditions under which arc extinction and reignition occur determine the characteristics and magnitudes of the resulting system transient voltages. Of particular importance in this connection are the conditions under which "current zeros" can be forced in arc extinction with the resulting high voltages.

Recognizing this to be a general field of considerable importance at the present time, a cooperative research program on dielectric recovery has been instigated at the High Voltage Laboratory of the California Institute of Technology. This program is being sponsored by the Dept. of Water and Power of the City of Los Angeles, the Kelman Electric and Manufacturing Co., and the Southern California Edison Co. The first phase of this program, discussed in this paper, deals with air insulation at normal atmospheric conditions. This medium was chosen first since it is the most fundamental one of the practical insulations and is subject to the least number of controlling factors. A limited amount of data had been obtained elsewhere on large air gaps[3,4] * by artificially producing faults and determining system conditions under which reignition did or did not occur. Also safe circuit reclosing times have been determined from staged tests under a limited range of conditions[1,2]. Such techniques, however, permit a very limited variation in the important parameters and require so long that either insufficient data are obtained or important variations have occurred in the conditions during the period of the test. Also many such staged tests are performed by closing in on an artificially produced or fused fault. Accurate timing of the start of the fault current is thus not obtained, and vaporized metal may be produced in the gap by the fused element.

A testing technique has been developed which overcomes these difficulties and is an extension of work performed earlier on lightning current faults[5]. The insulation medium is first broken down by a surge generator, the fault current allowed to flow a specified time and then shut off; after which the dielectric strength of the insulating medium is tested over a wide range of time delays with a second surge generator. By this means data for complete dielectric recovery curves can be obtained for a wide range of fault current magnitudes and durations.

* See list at end of paper for all numbered references.

Because of the very flat breakdown characteristics of air insulation, particularly while still under the influence of a predischarge, such data are applicable to all practical types of system over-voltages. This technique permits the accumulation of a large mass of data so that effects of the various important parameters can be studied and quantitative correlations made with theoretical approaches to the problem.

Test Circuits and Techniques

The main test and auxiliary control circuits are of interest not only because they represent a new technique for studying dielectric recovery phenomena, but also because of certain new control methods that are being applied to surge generator testing. A general schematic diagram of the test circuit is shown in Fig. 1 and a photograph of the main power circuit in Fig. 2. This part of the test circuit is shown by heavy lines in Fig. 1. Sixty cycle power is supplied from a 17 KV bus through a single phase induction regulator. This energizes a bank of four 150 KVA; 8.6 to 2.4 KV transformers which supply the actual test circuit. By various combinations of series or parallel connections a range of power currents and voltages can be supplied to the test gap. A further fine control of the fault current is obtained with the current limiting inductor which can be varied in approximately one ohm steps up to 60 ohms. Fault currents up to approximately 3000 amperes can be obtained. The Ignitron circuit shown in Fig. 1 is used to control the fault current duration if the self extinguishing characteristics of the circuit are not to be studied directly.

To start a fault condition, the test gap is first broken down by the surge generator designated as No. 1. Its firing time is accurately synchronized with the main 60 cycle power source by means of the "phase-shifting selsyn, peaking transformer" trip circuit shown in Fig. 3. Thus fractions or multiples of half cycles of fault current can be accurately duplicated. As shown in Fig. 3, radar pulse transformers, rated 8 to 30 KV, have been used with excellent results for tripping the surge generators.

The facilities of the Cal Tech High Voltage Laboratory include two 100 KV surge generator charging circuits and two separate 10 bank, 1000 KV surge generators that can be used as two separate generators or as one two-million volt generator. In this test the two separate units comprised generators Nos. 1 and 2.

When the main 60 cycle power circuit of Fig. 1 is energized, the test gap shunt resistors are isolated by means of a small air gap to reduce their required power rating. For breaking down the test gap, surge generator No. 1 is adjusted to cause gap flashover on the wave front and thus produce a very short duration voltage pulse which (due to its high effective frequency) can be kept out of the main power circuit by means of the filter circuit shown in Fig. 1. The inductor and capacitors of this circuit are shown in Fig. 2 together with the test gap and power transformers. At high frequencies this circuit is a high impedance as viewed from the test gap and thus permits sufficient voltage from surge generator No. 1 for gap breakdown in short times but allows very little voltage to reach the transformer terminals.

With the use of only the one surge generator and by blocking cut-off of the Ignitron circuit, it is possible to study directly the reignition

characteristics of the test gap over a limited range of system recovery voltages and frequencies, as indicated by the range of variation of voltage and filter circuit constants shown in Fig. 1. Natural system frequencies from 300 to 7000 c.p.s. can be obtained.

The No. 2 surge generator is used for the second type of dielectric recovery study in which the insulation strength of the test medium is tested at various time intervals following the end of a controlled fault current. The No. 2 surge generator and Ignitron circuit are both timed by a pulse taken from the No. 1 generator as shown schematically in Fig. 1. The Ignitron bias control and timing control circuits are shown in Fig. 4. The pulse from the No. 1 generator is applied to a single shot multivibrator circuit whose time delay in sending out a pulse can be controlled by the variable capacitor shown. This pulse is applied to the grid of a 2050 thyratron whose plate circuit supplies current to high speed relays in the bias control circuits of the F6105 Ignitron control thyratrons (see Fig. 4). These relays have a delay time of only five milliseconds so that the Ignitron circuit can cut off the fault current at any desired current zero. For fractions of a half cycle it was found readily possible to trip the F6105 grid bias circuit by an induced pulse from the No. 1 generator. Thus the Ignitrons are immediately conditioned to block off at the first current zero. The duration of fault current is then varied by the initial trip time of the No. 1 generator.

Ten Stage Scale of Two Counting Circuit. It is of course desired to accurately control the time of firing of the No. 2 surge generator to study the dielectric recovery properties of the test medium over a wide range of times after the end of the fault current. For this purpose a binary or scale of two "flip-flop" circuit[6] was developed which counts pulses from a variable frequency square wave generator. This circuit is shown in Fig. 5 with its schematic diagram in Fig. 6.

Each stage of the counting circuit consists of two tubes which have two stable states and can be changed from one to the other by the appropriate trigger pulse; the two stable states being distinguished by which tube is conducting. The terminal "Out" of one scale of two is connected directly to the terminal "In" of the next scale of two and so on for 10 stages. When T-2 (Fig. 6) of the preceding stage becomes conducting a negative signal is applied to the plate of the "Off" tube and through the RC cross coupling to the grid of the "On" tube, which causes the flip-flop to pass to its other stable state. When T-2 of the preceding state becomes non-conducting the resulting positive pulse has no effect on the following scale of two. Each scale of two produces one negative pulse for each two that are applied to it from the preceding stage so that for 10 stages a total of 2^{10} or 1024 pulses input to the first stage are required to produce a complete operation of the counting circuit. Thus by varying the frequency applied to the counting circuit a varying time delay can be obtained. The oscillator driving the square wave generator will apply frequencies up to 80 kilocycles and thus for 10 stages, time delays from over one minute and down to about 13,000 microseconds can be obtained. Less stages are used for shorter delays. Values less than 100 microseconds can be reproduced.

The counting circuit is triggered by a pulse from the firing of the first surge generator which changes the stable state of the 6SN7 gate control tube thus putting a positive bias on the 6SJ7 amplifier tube and allowing this tube to supply square waves to the first scale of two. The stable state of the gate control tube is returned again to its cut-off state by a negative pulse from the

counting circuit at the end of its operation which in turn negatively biases the 6SJ7 to cut-off and resets the counting circuit for its next operation. The control pulse out of the counter is fed to the No. 2 surge generator trip pulse circuit shown in Fig. 3.

Automatic Fuse Changer. Although the LC-filter of the main power circuit (Fig. 1) presents sufficient impedance for the short duration pulse of the No. 1 generator, it is not very practical to have a filter of sufficient impedance to allow a conventional surge generator to produce a full wave with a tail of 40 microseconds or more. It was however found quite easy to use a series fused gap so coordinated as to allow the fault current to flow but to insulate against the discharge of the No. 2 generator. An automatic fuse changer was developed to allow continuous operation without shutting off the main power circuit between test shots. This is shown in Fig. 7. The device pulls a small diameter copper wire from a spool around and between gap terminals at the top. The fuse holder is driven through an insulated shaft by a limit switch position controlled motor that accurately positions each quarter turn of the fuse holder rotor.

Recording Equipment. The complete circuit is suitable for testing insulating media with initial insulation levels up to about 300 or 400 KV. As shown in Fig. 1, shunts are used for measuring the gap current and voltage. Low frequency records are obtained with a magnetic oscillograph and high speed records with a Westinghouse-Cold Cathode-ray oscillograph with both electrostatic sweep control and a high speed drum type film holder. The C R O can be tripped from the No. 1 or No. 2 generator as desired. In addition photographic studies of the arc path can be made with two cameras; a high speed (3000 frame per second) Eastman prism shutter type 16 mm movie camera and a high speed rotating camera with film mounted on a rotating 3600 rpm 12 inch drum which rotates past a fixed lens.

Tests Using Actual System Recovery Voltage

Standard rod gaps were used in all studies reported here. The test circuit insulation levels are adequate for studying gap spacings up to about 15 inches. Previous data on lightning surge currents[5] had been obtained at gap spacings of six and eleven inches. Most of the data discussed here were obtained at the same spacings to correlate with those tests. In addition three inch gaps were studied.

When using the actual system recovery voltage of the circuit supplying the fault current the logical procedure is to vary one of several possible parameters until critical reignition is reached. A point on a dielectric recovery curve can then be obtained by the crest magnitude and time to crest of the system recovery voltage when the arc just fails to restrike. The parameters which can be varied are the time constant of the circuit to control the rate of rise of the system recovery voltage, the applied circuit voltage to control the magnitude of the recovery voltage, the magnitude of the fault current, and the gap spacing. Unfortunately, it is difficult to vary any one of the above parameters without causing appreciable changes in one or more of the others. Variation of circuit voltage or system natural frequency at a fixed fault current produces a very slow test procedure since it requires an accurate readjustment of the current limiting reactor. The best test procedure found was to set the circuit voltage, natural system frequency and limiting reactor and then vary the gap spacing until the critical reignition condition is reached.

With gaps of the order of three to six inches it was found that the circuit voltage had to be reduced to the order of 1000 volts rms (or less) before arc extinction would occur naturally with fault currents of practical magnitudes. This was true with system natural frequencies as low as 300 cps. Even then the currents were below 50 amperes. This phase of the study was necessarily confined therefore to currents of this magnitude or less. Under these conditions the arc drop was appreciable and as is to be expected accurate reproduction of test conditions was difficult. It was found in all cases that if the arc extinguished itself naturally it did so within the first half cycle or at the first current zero. However, for any two faults with identical settings of the controllable parameters the magnitude and duration of fault current from its start to the first current zero varied considerably. This erratic characteristic therefore requires so many tests to get a mean critical condition that enough points for even a portion of a dielectric recovery curve can not be obtained in a short enough time that the effects of variations in atmospheric conditions can be eliminated or studied.

Table I lists 77 sets of critical reignition test runs that were made. In the tabulation are given the applied voltage crest fault current, percent of one half cycle of the fault current, crest magnitude and time to crest of the system recovery voltage. The current data apply to the actual oscillograms from which the recovery voltage point was scaled at the test shot on which the circuit just recovered. A typical oscillogram from which these data were obtained is shown in Fig. 8. As shown in Table I, the crest current ranges from seven to 52 amperes and the time to current zero from 18 per cent to 100 per cent of a half cycle. Various analyses of the data were attempted such as segregating into groups of limited current variation, but the spread in the points as plotted on dielectric recovery curves completely masks any effects of variation in the fault current. The only logical segregation found is with regard to gap spacing. In Fig. 9 are plotted all records segregated into two groups of gap spacings. These data will be discussed in more detail later.

Tests Using Two Surge Generators

With the Ignitron circuit and sufficiently high circuit voltages that arc drop is not a factor, accurate control of the magnitude and duration of the fault current is obtained. Individual tests can be made at the charging rate of the surge generator or one minute intervals. Thus the study of the effects of the controlling factors becomes practicable since the circuit test conditions can be accurately duplicated and many test points obtained during essentially constant atmospheric conditions.

The method of testing the gap, at a given time interval following the end of the fault current, is to raise the voltage applied by the No. 2 generator until breakdowns occur. Then oscillograms are obtained over a sufficient voltage range to produce a volt-time or time-lag curve. It is not considered necessary to use a standard 1-1/2 x 40 microsecond wave. The volt-time curves under the conditions of a predischarge are much flatter than with no predischarge and unaffected by large variations in the tail of the test waves. This had been observed previously for the lightning surge studies[5]. Typical volt-time curves both with and without a predischarge are shown in Fig. 10. Two things of interest are illustrated by this figure. One is the more random nature of the data when the medium is recovering from a fault. The other is the fact that although the volt-time curves

plotted through points obtained in this way have less turn up than for gaps without a pre-discharge, the breakdown can occur at much longer time lags. Further it was found that for a region of time intervals (that increases with magnitude of the fault current) breakdown can occur at a relatively slow rate. This is illustrated by the oscillograms of Fig. 11. This same phenomena had been observed when studying gaps recovering from high current short duration surge currents[5]. There, however, it was found only for time intervals less than about 100 or 200 microseconds or when the gap is still carrying small currents. In the case of one or two half cycles of power frequency fault current this region extends to about 40,000 microseconds for 100 ampere faults and to about 70,000 microseconds for currents as high as 700 amperes. The percentage of such slow breakdown records decreases at the longer intervals. However, even though all breakdowns are at this slow rate there still exists a definite critical voltage below which breakdown will not occur. Because of this type of breakdown and the possibility of the media not supporting voltages below the apparent critical it was considered desirable to use as long tail test waves as practicable. Surges with a time to half value of about 80 microseconds were used for the data in all of the dielectric recovery curves except the highest point on the 11 inch gap curve (Fig. 14b). As shown by Fig. 11, partial breakdowns were also recorded at the shorter time delays after current zero.

High Speed Camera Studies. Much valuable information has been obtained from the high speed photographic studies, particularly from the records obtained with the 3000 frame per second movie camera. Portions of one of the more interesting of these records is shown in Fig. 12. The first group of frames shows the first 2300 microseconds of the fault current arc. The second group shows the luminous gases present in the arc 0.013 seconds after the start of the fault or 0.0043 seconds after the end of current flow. The third group shows the luminous gas in the arc just prior to the flashover produced by the No. 2 surge generator 0.041 seconds after the start of the fault or 0.0322 seconds after the end of the fault current flow. In all cases photographed the luminous gases either moved out of the center of the gap toward the electrodes or the gases near the electrode remained luminous longer. As shown in the third group of records in Fig. 12 there still remains a faint path of luminosity in the gap through which the second discharge occurred. In all recorded cases the period in which visible luminous gas remains in the central region of the gap corresponds to the maximum delay for which slow voltage breakdown is observed. The fourth group shows the second discharge and the fifth the luminosity which still persisted at one terminal after 0.12 seconds. Faint traces of luminous gas are visible in such a record as long as 0.15 to 0.17 seconds after the end of the fault current even though no second discharge is applied.

Detailed examination of such records shows that extensive motion in the arc path occurs even during the half cycle of fault current. The arc developes, then expands radially (in of course a tortuous corkscrew path) with visible diameters of two or three inches. The luminous area shown in the frames reaches its maximum at the crest of the fault current and diminishes only slightly by the time the fault current reaches zero. For half cycle faults it is quite intense for three or four more half cycles. However, it does not drift out or away from the general region of the gap in the period that it is photographically visible.

The record in Fig. 12 is of particular interest since it shows that a large time interval was required for the second discharge to build up to maximum intensity. This corresponds to the show rate of breakdown mentioned previously.

The first frame of the fourth set shows initial streamers propagating from each electrode through the trail of luminous gas. The next frame shows the intense "return streamer" that completes the discharge. Of these two initial streamers the one passing through the gas of greatest luminosity is more intense itself. The time interval between these two frames is about 400 microseconds, but of course about 300 microseconds of time is lost by the shutter action and the first faint trace may have started just before the shutter closed. Thus the actual time of build up can not be determined from such a record. Actually the longest times for breakdown to develop as recorded with the oscillograph were of the order of 30 or 40 microseconds. This was true even for very short time intervals between the end of the fault current and the application of the test voltage.

The photographic records showed that for time intervals above 70 or 80 thousand microseconds, the second discharge departs greatly from the path of visual luminosity. By this time the hot gases have disappeared in the central region of the gap and the second discharge takes a straight path between the electrodes.

Effect of Atmospheric Conditions. The tests reported here were performed with air under natural conditions and subject to normal variations. As significant changes occurred in the weather, test runs were repeated to determine the effect. In such cases the variations between mean critical breakdown values were of the same order of magnitude as the standard correction factors to be applied to air without a predischarge. Typical data of this type is shown in Fig. 13. The principal results of the grouping of the three runs is the correspondingly greater spread in the points. The application of the standard correction factor for varying atmospheric conditions to the test data brought the grouping closer together. In most of the data presented here, such correction factors amount to only three or four per cent at the most. Under these conditions they were applied to the data but probably have no significance. Only the two points shown in Fig. 14b had larger correction factors.

Dielectric Recovery Curves. Thirty-five or forty test points appear to be adequate for establishing a critical point on a dielectric recovery curve. However, two to four such runs were made at each time interval in an attempt to accurately establish the dielectric recovery curves presented here. Thus each point is the result of 70 to 150 actual tests. The data obtained for longer time intervals is plotted in Fig. 14 for three, six and eleven inch horizontal rod gaps. As shown, the bulk of the data has so far been obtained for one half cycle of power current. Shorter duration arcs have not yet been studied in detail. It has been found that the rate of recovery is relatively insensitive to longer durations. Points obtained with one or two cycles of fault current are not appreciably different than those for one half cycle.

Comparison of the three inch and six inch gap data in Fig. 14 shows that not only is the strength of the three inch gap proportionately higher at any time interval but its relative rate of recovery is more rapid. Examination of critical breakdown curves for rod gaps without a predischarge shows that the relative strength of a three inch gap is greater than a six inch gap whereas the curve becomes a straight line above six inches. This is due to the gap configuration and probably also explains the first of the above comparisons for the cases with predischarges. The second effect is probably due to electrode cooling. The greater conductivity of the electrodes can have an appreciable effect in cooling air

adjacent to each electrode. For gaps of six inches or more this effect should not be appreciable as shown by the comparison between the eleven inch and six inch gap curves. These show quite similar rates of recovery and the eleven inch data has the same proportionality factor at all points. It thus appears evident that data obtained from gaps of these lengths can be extrapolated to larger gap spacings. These same considerations apply to data of Fig. 9 for tests obtained using natural system recovery. Here gaps in the region of three inches have about twice the proportionate rate of recovery as six inch gaps. This is somewhat higher than the proportionate ratio observed in Fig. 14.

The six and eleven inch gap data of Fig. 14 show that for fault currents of 100 to 700 amperes, time intervals of 0.02 to 0.04 seconds are required for the insulation to recover to one fourth of its original strength and 0.05 to 0.08 seconds to recover to one half its original strength. This region corresponds to the normal range of ratios of original transmission line insulation strength to normal applied voltage showing the time intervals required after the interruption of the fault before it is safe to reclose the breakers.

Fig. 15 shows the correlation (in the region of shorter time delays) between the two types of tests described here and data previously obtained[7] with high magnitude-short duration fault currents representative of lightning surges. The very rapid recovery to lightning surge currents is contrasted with the much slower recovery, even to power frequency currents as low as 20 to 50 amperes. The relatively slow rates of recovery for 60 cycle fault currents make it appear unlikely that normal power line insulation would recover after an appreciable fraction of a half cycle of fault current flows unless after such long times that the arc has extended itself greatly by rising out of the central region of the gap. Assuming an average of 0.25 for the ratio of normal system voltage to normal insulation strength one finds from the dielectric recovery curves that even if the system transient or recovery voltage did not exceed normal voltage, its frequency would have to be less than 60 cycles to prevent its crossing the dielectric recovery curve. For a system natural frequency of 1000 c.p.s. and assuming an overvoltage of 1.5 times normal the ratio of normal applied voltage to normal insulation level would have to be of the order of 0.01 or less. However, as shown by the dielectric recovery curves for short duration surges a good probability exists for recovery at a high frequency current zero. This has been discussed in Reference 5.

Future Tests. Unfortunately this is a very complex subject and many more tests are required before some of the important conclusions can be reached on this subject. Data have to be obtained for fault current durations between the range of the short duration lightning surges and appreciable fractions of one half cycle of power frequency. The effects of appreciable air velocities and of gap positions must be studied and similar data obtained for other media such as insulator strings and wood insulation. This, together with a fundamental study of the mechanism of recovery and breakdown during the second discharge through the weakened arc path constitute the second phase of this project that is now in progress.

Acknowledgements

The authors wish to acknowledge the valuable assistance rendered by B. N. Locanthi in the development of the electronic equipment, Sol Matt and L. H. Tejada in helping to obtain the test data and A. T. Puder who helped with equipment construction.

List of References

1. Keeping the Line in Service by Rapid Reclosing
by S. B. Griscom and J. J. Torok, Electric Journal, May 1933, p 201

2. Systematic Tests with Automatic High Speed Reclosing in the Goesgen and Laufenburg Power System
by W. Wanger, Brown Boveri Review, Dec. 1945

3. Deionization Time of High Voltage Fault-Arc Paths
by E. J. Harrington and E. C. Starr, AIEE Tech. Paper No. 49-205

4. Insulation Flashover Deionization Times as a Factor in Applying High Speed Reclosing Breakers
by A. C. Boisseau, B. W. Wyman and W. F. Keats, AIEE Tech. Paper No. 49-221

5. Dielectric-Recovery Characteristics of Large Air Gaps
by G. D. McCann and J. J. Clark, AIEE Trans. Jan. 1943, Vol. 22, p 45

6. The Model 200 Pulse Counter
by W. A. Higinbothom, James Gallagher and Matthew Sands, Review of Scientific Instruments, Oct. 1947, Vol. 18, No. 10, p 706

TABLE I

SUMMARY OF ACTUAL SYSTEM RECOVERY TESTS

Osc. No.	Test Gap (in.)	Gap Crest Amperes	Per cent Half Cycle	Crest Transf. Volts	Crest Gap Volts	Recovery Time Microseconds
75	6.0	18.8	50	1750	2700	1160
78	6.0	7.2	50	1530	2100	895
80	6.5	7.7	50	1585	1660	1010
85	6.5	8.4	50	1590	2475	1230
87	6.5	11.3	72	1560	2060	1305
116	6.5	21.7	90	1565	3140	1285
119	6.75	24.0	86	1580	2920	1640
138	6.75	11.4	27	608	426	343
139	4.0	10.4	36	609	372	286
141	3.0	23.0	59	630	255	248
142	2.5	19.6	59	637	240	145
149	3.5	12.6	32	601	195	200
150	3.5	21.8	59	627	487	343
151	3.0	24.1	63	640	568	457
153	2.75	38.7	71	640	675	420
154	2.63	27.6	64	625	375	410
155	2.56	41.4	73	625	765	571
167	6.75	21.8	86	1740	3080	1605
176	6.75	13.4	77	1600	2680	1016
184	6.75	15.1	86	1310	2145	1218
187	6.75	22.1	55	1310	1237	670
193	6.75	25.0	82	906	1065	650
195	6.75	17.3	68	896	740	608
199	6.0	20.7	68	875	940	781
200	6.0	19.6	55	947	880	694
202	6.0	27.6	77	947	1206	770
241	6.75	23.0	73	1040	1085	710
253	3.5	20.2	50	806	260	257
254	3.5	12.1	18	806	279	262
255	3.5	19.4	50	806	316	171
257	3.5	16.1	50	867	224	286
258	3.5	10.3	36	867	405	344
263	3.75	11.4	23	806	281	294
265	3.75	16.1	45	947	300	417
271	3.69	29.9	64	952	794	455
279	3.94	17.2	36	940	152	214
283	3.94	27.6	68	804	386	305
290	4.25	34.4	59	934	837	498
297	5.0	36.3	50	793	105	286
298	5.0	56.5	50	793	216	271
299	5.25	56.5	50	806	291	381
301	5.25	19.4	27	778	71	105
302	5.25	44.4	45	804	185	328

TABLE I (Cont'd.)

SUMMARY OF ACTUAL SYSTEM RECOVERY TESTS

Osc. No.	Test Gap (in.)	Gap Crest Amperes	Per cent Half Cycle	Crest Transf. Volts	Crest Gap Volts	Recovery Time Microseconds
306	5.25	48.4	50	804	306	617
307	6.0	52.3	50	764	435	509
309	6.0	48.4	50	793	425	530
396	2.56	32.2	90+	700	404	496
438	5.75	21.8	90+	1032	486	621
441	5.88	27.6	90+	1032	649	785
444	5.63	22.3	90+	1025	738	814
449	6.88	27.6	90+	985	760	864
452	6.38	25.3	90+	962	680	553
454	6.0	20.7	90+	962	513	456
456	5.94	33.9	90+	962	868	585
462	5.38	34.6	90+	962	870	829
471	4.50	33.8	90+	962	924	644
506	5.63	30.2	90+	1202	813	595
513	6.75	36.8	90+	1147	876	657
527	6.75	28.7	90+	1019	726	540
528	6.75	28.7	90+	1019	789	723
539	6.75	27.2	90+	941	671	585
544	6.75	29.9	90+	941	664	520
545	6.75	24.8	90+	941	535	460
551	6.75	25.3	90+	941	638	572
559	6.75	17.9	90+	941	388	463
561	6.75	23.0	90+	941	513	458
563	6.75	23.2	90+	941	583	660
565	6.75	25.3	90+	835	398	530
566	6.75	34.5	90+	835	518	534
567	6.75	18.4	90+	835	168	303
568	6.75	39.1	90+	835	513	440
571	6.75	30.3	90+	835	403	430
572	6.75	36.8	90+	835	525	473
573	6.75	32.2	90+	835	495	469
575	6.75	32.2	90+	835	488	520
576	6.75	26.4	90+	835	358	475

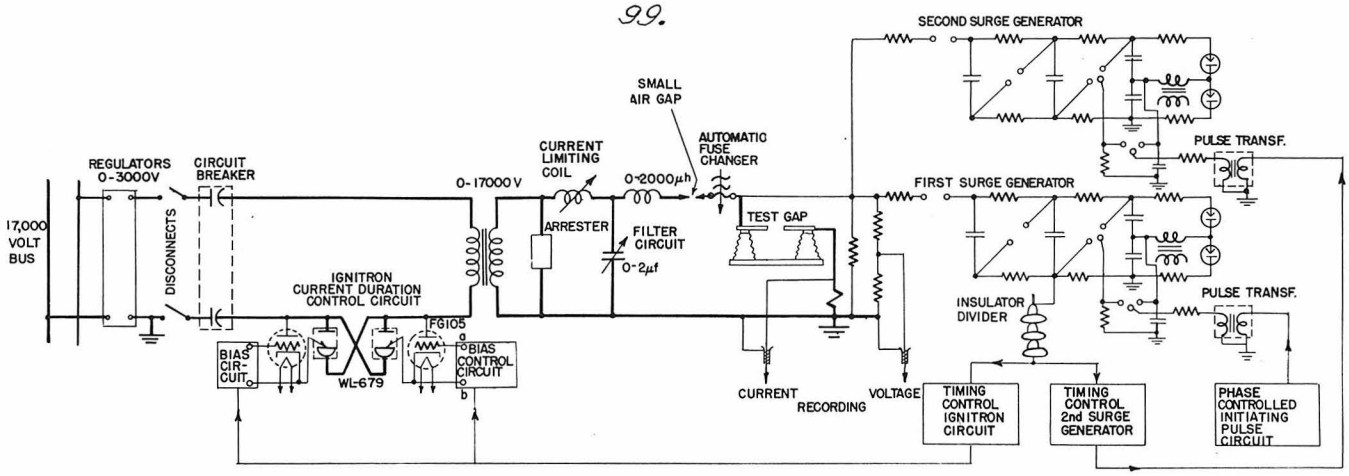

Fig. 1 Schematic diagram of dielectric recovery test circuit.

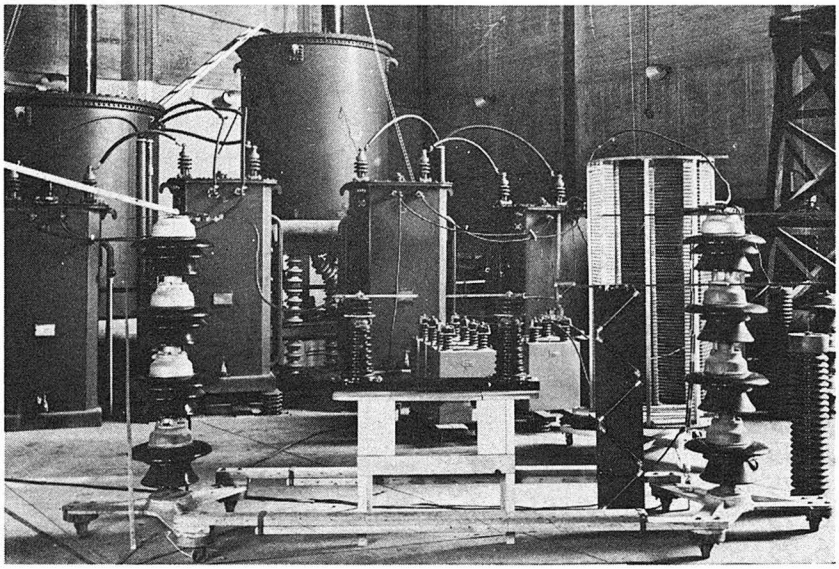

Fig. 2 View of main power circuit showing test gap in foreground and power transformers in background. Capacitors and inductor of filter circuit are on right side.

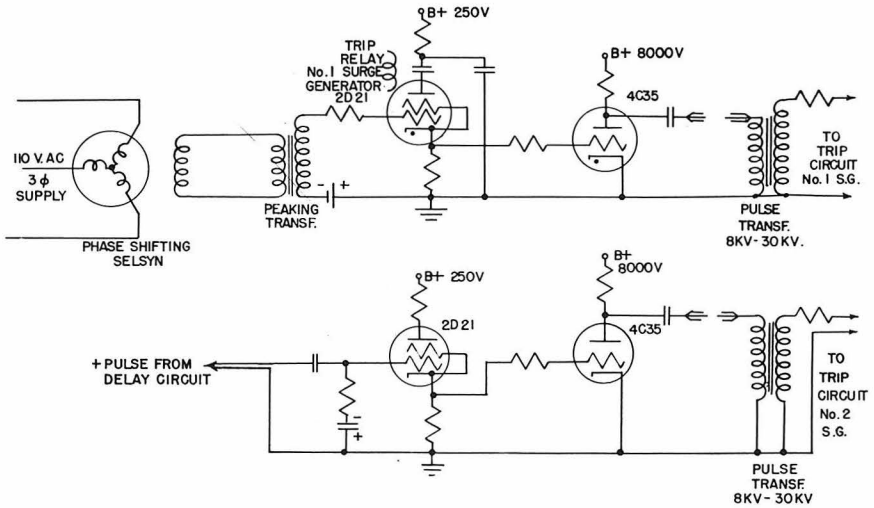

Fig. 3 Control pulse circuits for timing surge generator trip circuits.

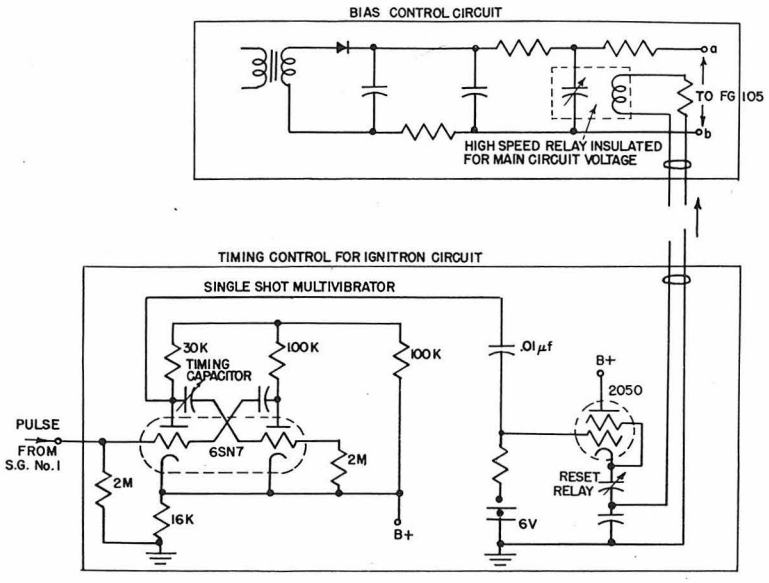

Fig. 4 Timing and bias control circuits for main Ignitron fault duration control circuit.

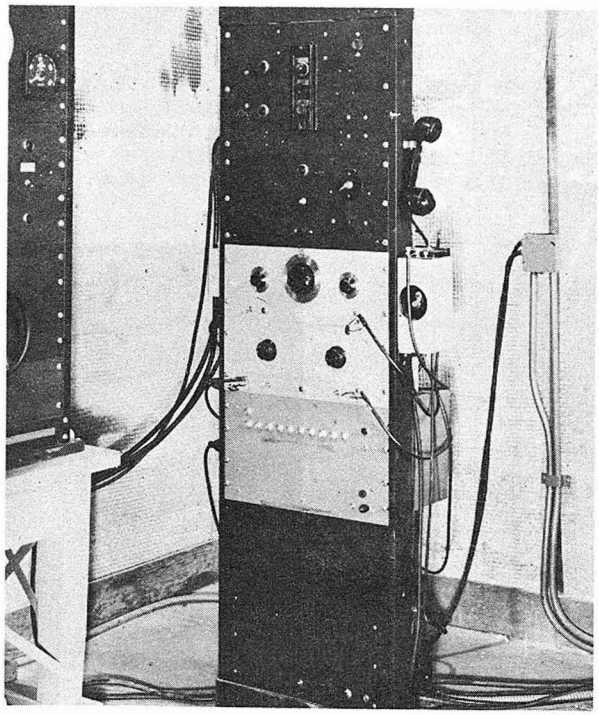

Fig. 5 View of timing control circuit for the No. 2 surge generator:
(1) oscillator (2) square wave generator
(3) binary counting or delay circuit.

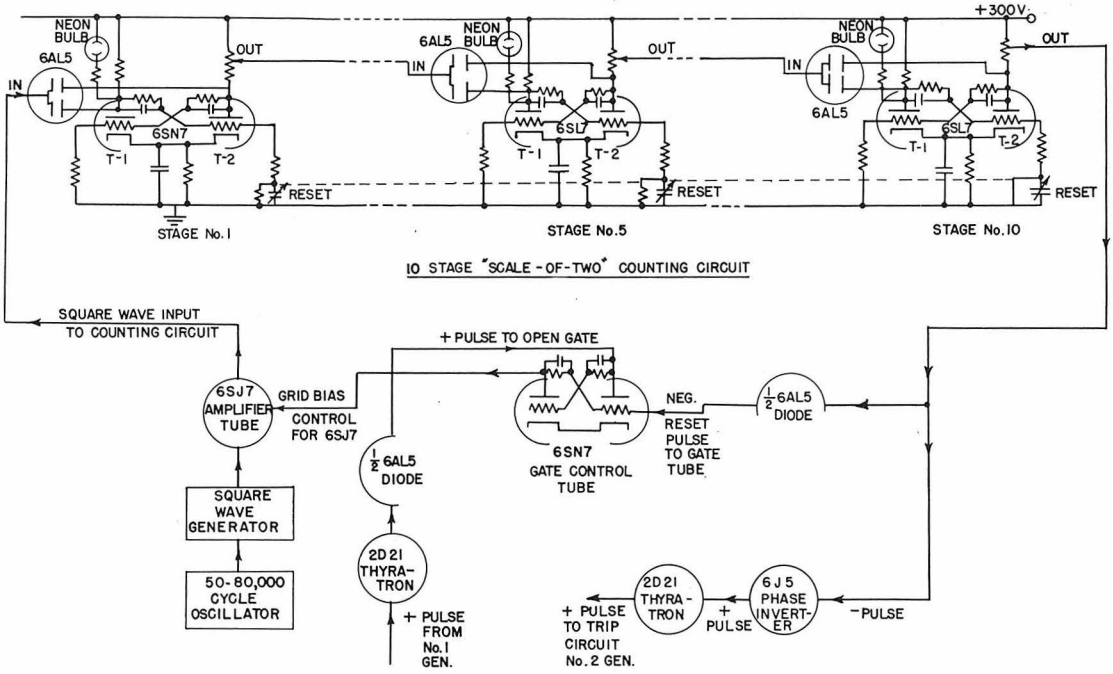

Fig. 6 Schematic diagram of timing control circuit for No. 2 generator.

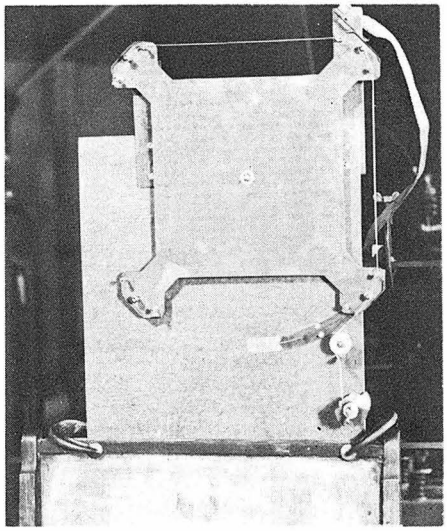

Fig. 7 Automatic fuse changer for series gap in main power circuit.

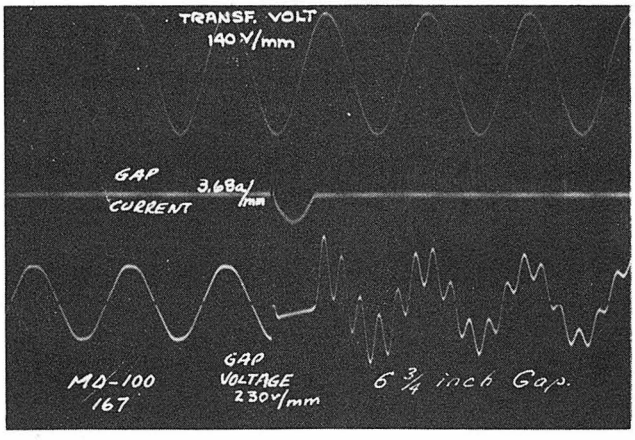

Fig. 8 Typical fault current-recovery voltage oscillogram for tests using natural system recovery voltage. (Test 167 of Table I)

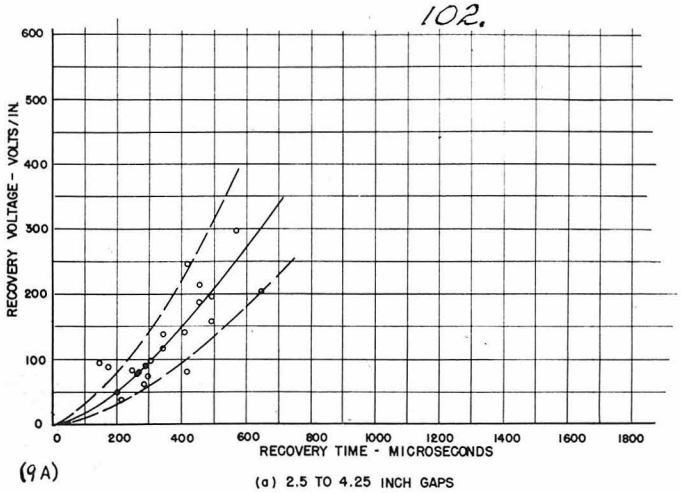

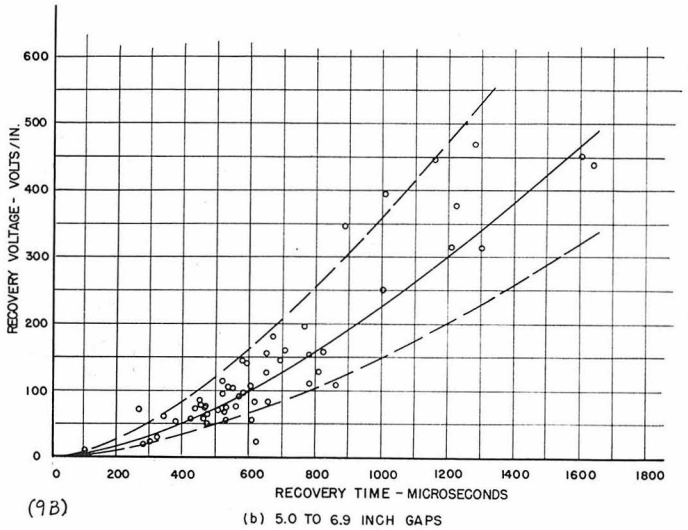

Fig. 9 Data on dielectric recovery of standard rod gaps using natural system recovery voltages. (See Table III)
(a) Gap spacings from 2.5 to 4.25 inches
(b) Gap spacings from 5.0 to 6.9 inches

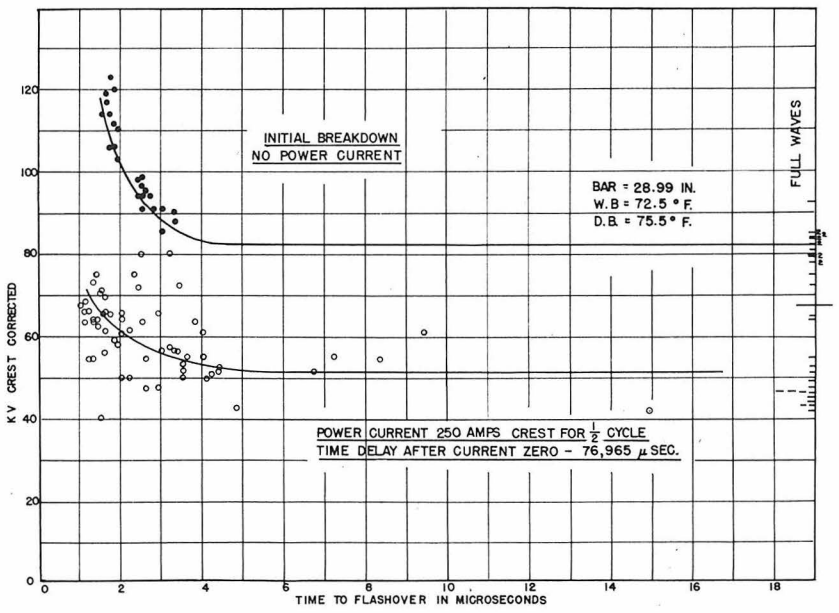

Fig. 10 Comparison of time-lag or volt-time curves (obtained by two generator tests) for three inch rod gap with no predischarge and predischarge of one half cycle 250 ampere crest.

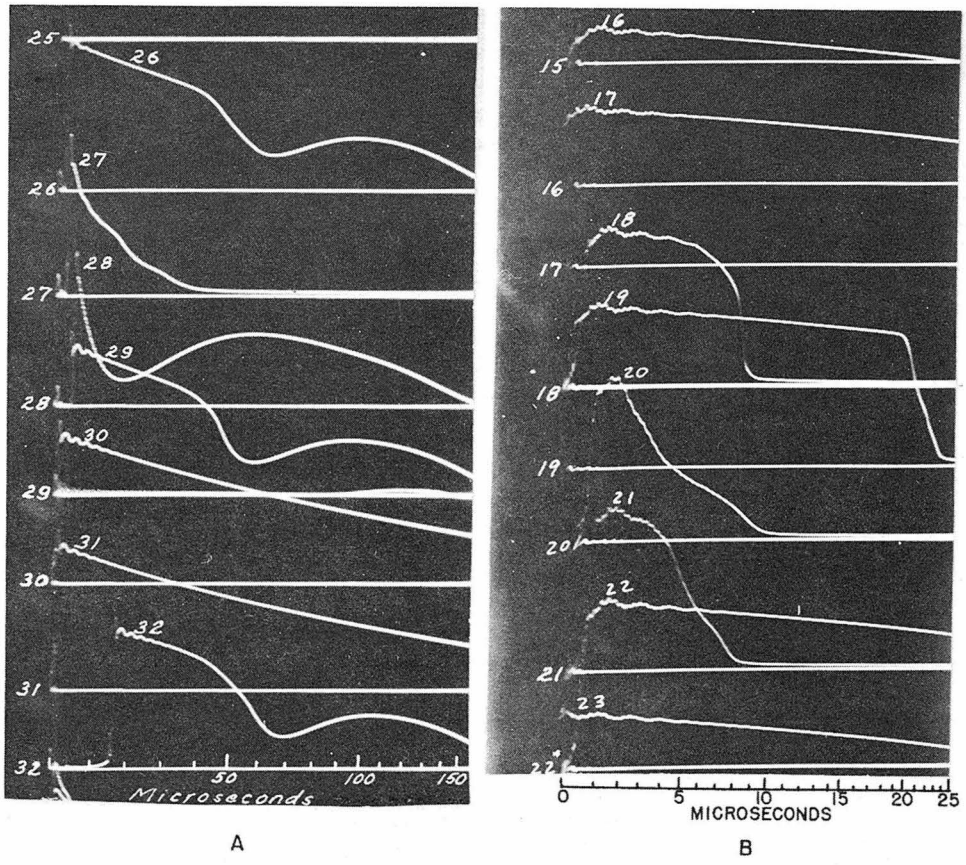

Fig. 11 Typical oscillograms showing slow breakdown characteristics obtained when No. 2 generator voltage is applied at short time intervals.

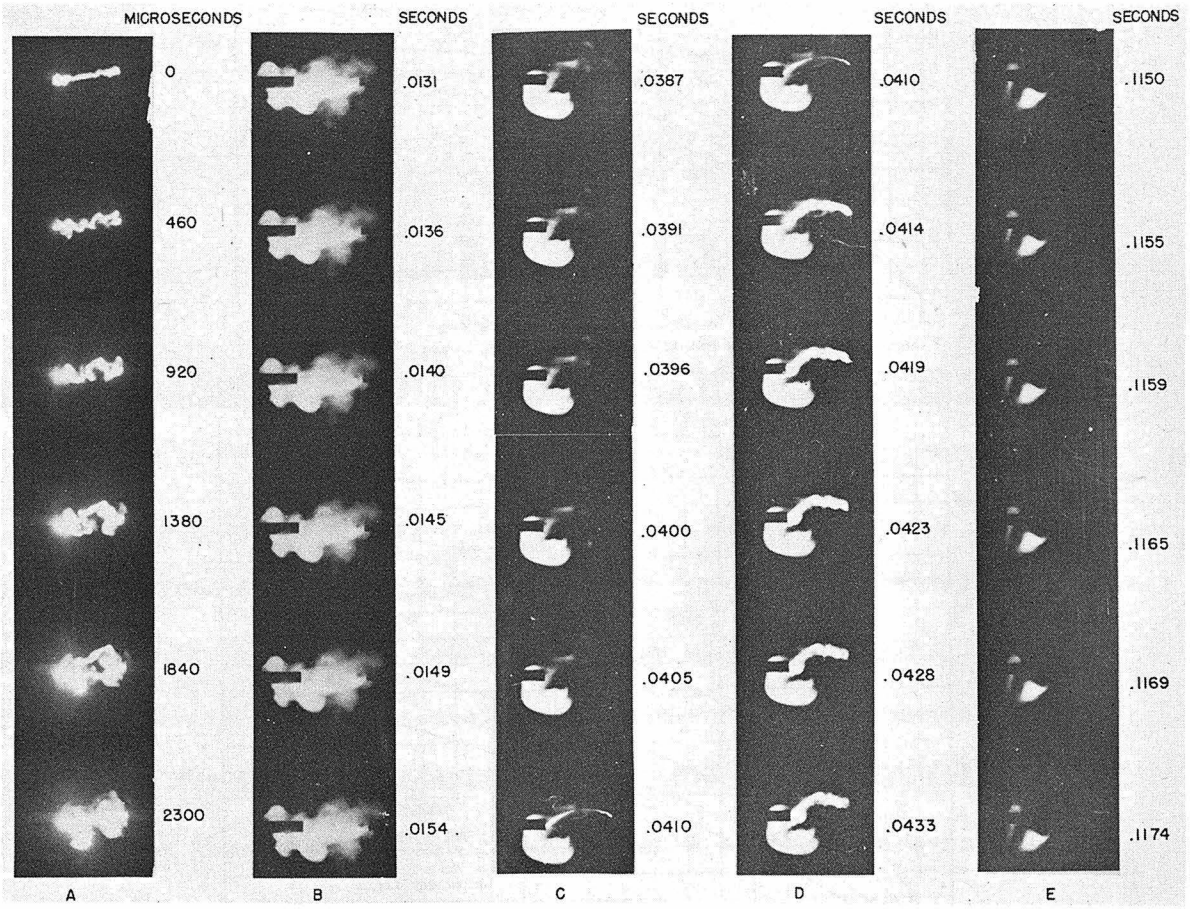

Fig. 12 High speed movie camera record of 3 inch gap discharge. Initial fault current one half cycle of 100 ampere crest
(a) Start of fault current
(b) During second half cycle of time from start of arc
(c) Period just prior to second discharge
(d) Period just after second discharge
(e) Period toward end of visual luminescence showing ionized gas in region of one terminal only

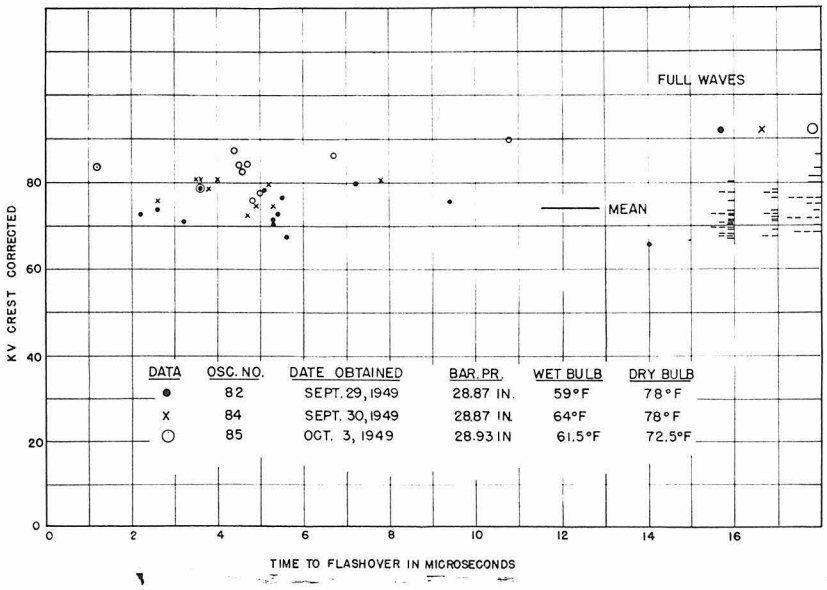

Fig. 13 Volt-time data for three separate runs showing effect of varying atmospheric conditions. 6 in. rod gap, 1/2 cycle-10 ampere crest fault current. Time delay after current zero 77,000 microsec.

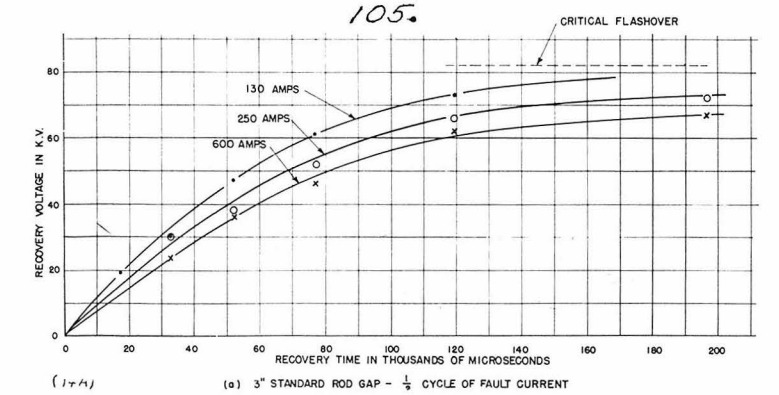

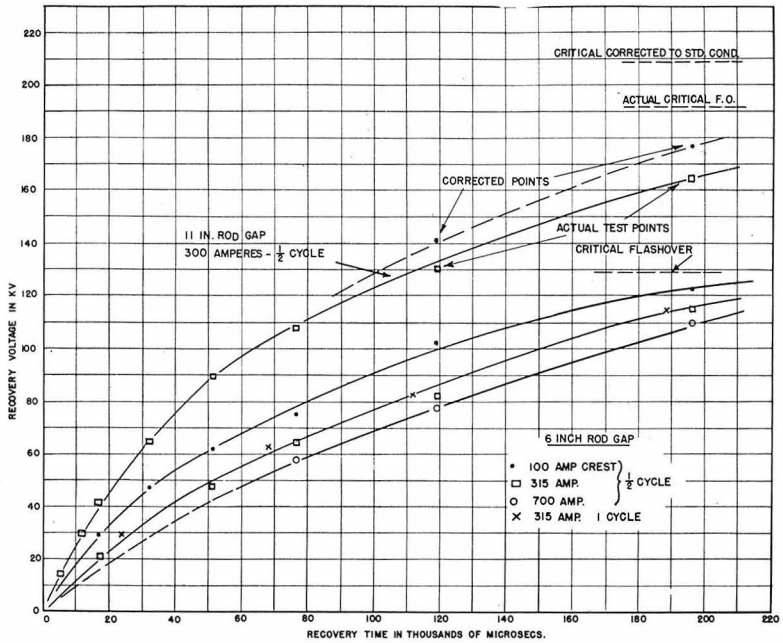

Fig. 14 Dielectric recovery curves obtained with two generator tests.
(a) Three inch standard rod gaps
(b) Six and eleven inch gaps

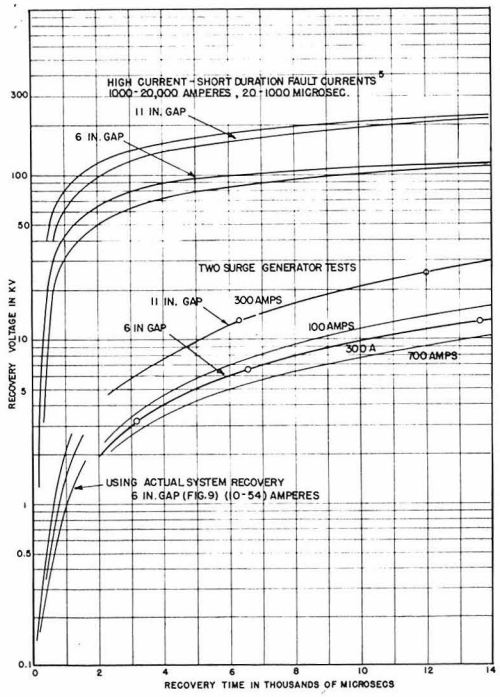

Fig. 15 Comparison of dielectric recovery characteristics of standard rod gap for different types of predischarge.

APPENDIX II

CALCULATION OF HEAT TRANSFER COEFFICIENT FOR HIGH PRESSURE ARC COLUMN

I CALCULATION OF THE FILM HEAT TRANSFER COEFFICIENT FOR 1000 FEET PER MINUTE WIND

A comparison of the film heat transfer coefficients for a 3.5 inch arc cross section will be calculated for wind both axial and perpendicular to the test electrodes. The wind velocity is 1000 feet per minute and the assumed arc temperature is 4000 degrees F. The values for the other constants, some of which are extrapolated from values given in the Chemical Engineer's Handbook,[45] are as follows:

U - wind velocity of 1000 ft./min.

ρ_{70} - density of air at 70° F = 0.08 lb./ft.^{3}

μ_{2000} - viscosity of the fluid at the film temperature = 0.052 centipoises.

t_o - bulk temperature 70° F.

t_f - film temperature 2000° F.

k_{2000} - thermal conductivity 0.04 $\frac{\text{B.T.U. ft.}}{\text{hr.-ft.}^2\text{-°F.}}$

k_{70} - 0.015 $\frac{\text{B.T.U. ft.}}{\text{hr.-ft.}^2\text{-°F.}}$

$C_{p_{70}}$ - specific heat at constant pressure 0.238 $\frac{\text{B.T.U.}}{\text{lb. °F.}}$

$$G = U\rho_{70} = 4800 \frac{\text{lb}}{\text{hr-ft}^2}$$

$$\text{Re - Reynolds' No.} = \frac{DG}{\mu} = \frac{D\,U\rho}{\mu}.$$

For the case of the wind perpendicular to the arc

$$Re = \frac{3.5}{12} \times \frac{1000}{60} \times \frac{.08}{.052 \times 6.74 \times 10^{-4}} = 1.11 \times 10^4$$

$$\frac{hmDo}{k_f} = 0.45 + .33\left[\frac{DoG}{\mu}\right]^{.56}$$

$$\therefore \frac{h_m \times \overset{3.5}{12}}{.04} = .45 + .33\ (1.11 \times 10^4)^{.56}$$

$$h_m = 8.4 \ \frac{B.T.U.}{hr.ft.^2\ {}^oF.}$$

For no wind $\frac{hmDo}{k_f} = 0.45$, therefore $h_m = .45\left(\frac{.04}{3.5}\right)(12) = .06$

For the case of the wind axial to the arc

$$Do^1 = \frac{(14)^2 - \pi/4(3.5)^2}{\times\ 3.5} = 68".$$

$$\therefore Re_{axial} = 1.11 \times \frac{68}{3.5} = 21.6 \times 10^4 .$$

From Fig. 8, Curve ABC, page 974 of Chemical Engineers' Handbook,[45]

$y = .002$, therefore

$$\left[\frac{h}{C_p G}\right]\left[\frac{C_p \mu_f}{k}\right]^{2/3} = .002$$

$$\left[\frac{h}{.238 \times 4800}\right]\left[\frac{.238 \times .052 \times 6.74 \times 10^{-4} \times 3600}{.015}\right]^{2/3} = .002$$

$$h = 1.43 \ \frac{B.T.U.}{hr.\text{-}ft.^2\text{-}{}^oF}$$

II CALCULATION OF THE FILM HEAT TRANSFER COEFFICIENTS FOR 30,000 FEET PER MINUTE WIND

For the case of the wind perpendicular to the electrodes, Reynolds' Number

$$Re = \frac{DG}{\mu} = \frac{3.5}{12} \times \frac{30,000}{60} \times \frac{.08}{.052 \times 6.74 \times 10^{-4}}$$

$$= 3.33 \times 10^5$$

and

$$\frac{hm \frac{3.5}{12}}{.04} = .45 + .33 (3.33 \times 10^5)^{.56}$$

$$hm = 56.$$

For the wind axial to the electrodes,

$$Re = 3.33 \times 10^5 \times \frac{68}{3.5} = 6.48 \times 10^6$$

therefore

$$\left[\frac{h}{C_p G}\right]\left[\frac{C_p \mu f}{k}\right]^{2/3} = 0.0015$$

and

$$h = 32.1$$

APPENDIX III

CALCULATION OF DIELECTRIC RECOVERY VOLTAGE

According to Slepian's theory of the extinction of the long a.c. arc[17], which is briefly summarized in the introduction to this thesis, the critical breakdown gradient for reignition of the arc is determined approximately by the following equation,

$$X_c = \frac{D}{a^{\frac{1}{2}} n^{\frac{1}{2}}}$$

where

D = constant

a = diameter of the arc

n = volume density of ions of one sign in arc column.

To obtain data on the variation of the density, n, and the diameter of the arc, a, with time a high speed photographic study of the arc was made. Two mutually perpendicular views of the arc were obtained as described previously. Because of the irregular shape of the arc section and the non-linear field distribution for the rod gap, the arc section was divided into 13-14 equal lengths and the critical breakdown gradient for each section was determined independently. The diameter of each section was determined by averaging the diameters of the two mutually-perpendicular views of the arc. These dimensions of the arc were obtained from 5 x 7 inch enlargements of the 16 mm. film. By making masks of the electrodes from views where they could be located and superimposing these masks on later frames where the electrodes were not visible, the

luminous gases were located with reference to the test gap. The density of the luminous gases was obtained by the use of a microphotometer. A long narrow slit in the microphotometer made it possible to obtain a density reading of the integrated intensity for that increment of the arc section. By moving this slit across the arc section, a response curve of density was obtained, similar to the curves shown in Figs. 43 A and B. By comparing the position of the luminous cloud in the 5 x 7 enlargement of a frame for a particular time after current zero with the density curve corresponding to that particular frame it was possible to position the density curve with reference to the test gap electrodes. By rearranging the equation for the critical breakdown gradient to

$$X_c = \frac{D(a)^{\frac{1}{2}}}{(a^2n)^{\frac{1}{2}}}$$

where

(a^2n) = for a particular incremental section of the arc is directly proportional to the integrated density for that section as determined from the microphotometer reading, d, as shown in Fig. 43 A and B.

therefore

$$X_c = C \left(\frac{a}{d}\right)^{\frac{1}{2}}.$$

Calculations for the apparent value of X_c are shown in Tables I-III.

In order to obtain the axial voltage gradient in a 6 inch standard rod gap, the voltage distribution between an electrode and a ground plan spaced three inches from the electrode was obtained by a voltage probe in a salt tray. A plot of the field strength across the 6 inch gap for

200 volts applied across the gap is shown in Fig. 42. Assuming there is no space charge in the long arc column[35] the above voltage gradients are then directly applicable to the ionized arc. The field strength ratio was determined from the plot of field strength, and by comparing the apparent field strength with this ratio the lowest breakdown of the arc, in the four sections closest to the electrodes, was determined and the breakdown voltages for the other sections determined on the basis of the field strength ratio. It should also be mentioned that the zero level of the apparent field strength was determined by calculating X_c at current zero and all values of the apparent X_c determined after this were obtained by subtracting this zero reading from the calculated X_c. The breakdown voltage was then obtained by adding all of the incremental effective values of X_c and multiplying by a constant. This constant was determined at 300 amperes, half cycle for a 6 inch test gap at 26.5 milliseconds after current zero by comparing the sum of the effective field strengths with the experimentally determined breakdown gradient of 47 kilovolts as shown in Table I. The calculated recovery voltages for other conditions are all based on the constant determined above and the results of the calculations are shown in Fig. 44. The calculated recovery voltages for 11 inches, 300 amperes, half cycle and 6 inches, 800 amperes, half cycle are higher than the experimentally determined values. Difficulty was experienced in obtaining optimum exposure conditions over the range of intensities so that it was necessary to over-expose the film close to current zero in order to have correct exposure of the film later in the sequence.

TABLE I

CALCULATION OF RECOVERY VOLTAGE FOR 300 AMPERES, $\frac{1}{2}$ CYCLE, 6 INCH TEST GAP

Recovery Time Delay	Value Calculated	INCREMENTAL SECTION OF ARC													
		1	2	3	4	5	6	7	8	9	10	11	12	13	14
0	d	.27	.45	.55	.75	.77	.77	.79	.93	1.15	1.25	1.10	0.90	.65	.43
	a	2	3.0	4.0	4.0	5.0	5.5	8.0	9.0	9.5	9.0	8.0	6.5	4.0	2.0
	$a/d^{\frac{1}{2}}$	2.72	2.58	2.69	2.31	2.54	2.67	3.18	3.10	2.87	2.68	2.69	2.69	2.48	2.15
	AVERAGE VALUE OF $a/d^{\frac{1}{2}}$ FOR ZERO STRENGTH = 2.67														
26.3 Milliseconds	d	-	-	-	-	.28	.55	.75	.75	.60	.57	.68	.53	.35	.13
	a	-	-	-	-	7.0	10.0	9.0	9.0	8.5	8.0	8.5	7.5	6.0	4.5
	$a/d^{\frac{1}{2}}$					5.0	4.26	3.46	3.46	3.76	3.74	3.53	3.76	4.13	5.88
	Apparent Xc					2.33	1.59	0.79	0.79	1.09	1.07	.86	1.09	1.46	3.21
	Field Str. Ratio	1.0	.54	.22	.15	.13	.12	.12	.12	.12	.13	.15	.22	.54	1.0
	Effective Xc	3.21	1.73	0.71	0.49	0.42	0.38	0.38	0.38	0.38	0.42	0.49	0.71	1.46	3.21
	CRITICAL VOLTAGE = C(EFFECTIVE Xc) = C(14.37) FROM EXPERIMENTAL RECOVERY CURVE Vc = 47 KV. $\therefore C = \frac{47}{14.37} = 3.27$.														

TABLE I (Cont.)

Recovery Time Delay	Value Calculated	INCREMENTAL SECTION OF ARC													
		1	2	3	4	5	6	7	8	9	10	11	12	13	14
5.5 Milliseconds	d	-	-	.20	.42	.60	.59	.85	1.15	1.30	1.40	1.20	.85	.40	-
	a	-	-	3.0	4.5	5.5	6.5	8.5	10.0	10.0	10.5	10.0	8.0	4.0	-
	$a/d^{\frac{1}{2}}$	-	-	3.87	3.26	3.03	3.32	3.16	2.95	2.77	2.74	2.88	3.07	3.16	-
	Apparent Xc.	-	-	1.20	0.59	0.36	0.65	0.49	0.28	0.10	0.07	0.21	0.40	0.49	-
	Field Str. Ratio	1.0	.54	.22	.15	.13	.12	.12	.12	.12	.13	.15	.22	.54	1.0
	Effective Xc	0.91	0.49	0.20	0.14	0.12	0.10	0.10	0.10	0.10	0.07	.14	.20	.49	.91
		Total Voltage = 4.07 (3.27) = 13.3 KV													

TABLE II

CALCULATION OF RECOVERY VOLTAGE FOR 800 AMPERES, ½ CYCLE, 6 INCH TEST GAP

Recovery Time Delay	Value Calculated	INCREMENTAL SECTION OF ARC													
		1	2	3	4	5	6	7	8	9	10	11	12	13	14
0	d	.58	.80	.92	1.05	1.15	1.20	1.25	1.15	1.15	1.12	.85	.65	.49	.41
	a	4.0	6.5	8.0	10.0	10.5	11.0	11.0	10.5	10.5	9.5	8.5	7.5	4.0	2.0
	$a/d^{\frac{1}{2}}$	2.62	2.85	2.95	3.08	3.02	3.02	2.96	3.02	3.02	2.91	3.16	3.40	2.86	2.21
		AVERAGE VALUE OF $a/d^{\frac{1}{2}}$ FOR ZERO STRENGTH = 2.93													
5.5 Milliseconds	d	-	.50	.95	1.10	1.20	1.25	1.30	1.25	1.15	1.05	.85	.60	.35	-
	a		5.5	8.0	9.5	11.0	11.0	11.5	11.0	10.5	9.5	9.0	7.0	4.0	
	$a/d^{\frac{1}{2}}$		3.31	2.90	2.94	3.02	2.96	2.97	2.96	3.02	3.01	3.26	3.41	3.37	-
	Apparent Xc	-	.38	0	.01	.09	.03	.04	.03	.09	.08	.33	.48	.44	-
	Field Str. Ratio	1.0	.54	.22	.15	.13	.12	.12	.12	.12	.13	.15	.22	.54	1.0
	Effective Xc	.70	.38	0	.01	.09	.03	.04	.03	.08	.08	.11	.15	.38	.70
		TOTAL VOLTAGE = 2.78 x 3.27 = 9.1 KV													
40.0 Milliseconds	d	-	.30	.55	.60	.58	.57	.59	.50	.36	.27	.49	.22	-	-
	a		7.5	8.0	10.0	12.0	12.0	10.5	9.5	6.0	4.5	6.0	5.0		
	$a/d^{\frac{1}{2}}$		5.0	3.81	4.08	4.55	4.59	4.22	4.35	4.07	4.07	3.50	4.76		
	Apparent Xc		2.07	0.88	1.15	1.62	1.66	1.29	1.42	1.14	1.14	0.57	1.83		
	Field Str. Ratio	1.0	.54	.22	.15	.13	.12	.12	.12	.12	.13	.15	.22	.54	1.0
	Effective Xc	4.0	2.07	.88	.61	.52	.47	.47	.47	.47	.52	.57	.88	2.16	4.0
		Total Voltage = 18.09 x 3.27 = 59.1 KV.													

TABLE III

CALCULATION OF RECOVERY VOLTAGE FOR 300 AMPS, $\frac{1}{2}$ CYCLE, 11 INCH TEST GAP

Recovery Time Delay	Value Calculated	INCREMENTAL SECTION OF ARC												
		1	2	3	4	5	6	7	8	9	10	11	12	13
0	d	.65	1.18	1.0	.70	.64	.50	.49	.55	.58	1.0	1.30	1.20	.73
	a	6.0	7.5	6.0	6.0	5.0	4.0	5.5	5.25	5.0	6.75	8.5	7.5	6.0
	$a/d^{\frac{1}{2}}$	3.03	2.52	2.45	2.92	2.79	2.83	3.34	3.06	2.94	2.60	2.56	2.50	2.87
		AVERAGE VALUE OF $a/d^{\frac{1}{2}}$ FOR ZERO STRENGTH = 2.80												
5.5	d	.18	.57	.78	.60	.37	.17	.10	.09	.17	.55	.80	.56	.23
	a	3.5	6.5	7.5	5.0	4.0	4.0	4.0	3.0	3.0	6.25	8.75	6.5	3.0
	$a/d^{\frac{1}{2}}$	4.40	3.38	3.10	2.88	3.28	4.84	6.34	5.76	4.20	3.37	3.31	3.40	3.61
	Apparent Xc	1.60	0.58	0.30	0.08	0.48	1.04	3.54	2.96	1.40	.57	.51	.60	.81
	Field Str. Ratio	1.0	.54	.21	.15	.13	.12	.12	.12	.13	.15	.21	.54	1.0
	Effective Xc	.81	.44	.17	.08	.11	.09	.09	.09	.11	.12	.17	.44	.81
		TOTAL VOLTAGE = 3.53 x 3.27 = 11.5 KV.												
8.5 Milliseconds	d	-	.23	.58	.68	.34	.07	-	-	.25	.41	.33	.08	-
	a		6.0	7.5	7.0	3.5	3.0			6.0	8.25	7.0	2.5	
	$a/d^{\frac{1}{2}}$		5.10	3.60	3.20	3.20	6.54			4.90	4.49	4.60	5.58	
	Apparent Xc		2.30	.80	.40	.40	3.74			2.10	1.69	1.80	2.78	
	Field Str. Ratio	1.0	.54	.21	.15	.13	.12	.12	.12	.13	.15	.21	.54	1.0
	Effective Xc	2.66	1.44	.56	.40	.35	.32	.32	.32	.35	.40	.56	1.44	2.66
		TOTAL VOLTAGE = 11.83 x 3.27 = 38.5 KV.												

TABLE III (Cont.)

Recovery Time Delay	Value Calculated	INCREMENTAL SECTION OF ARC												
		1	2	3	4	5	6	7	8	9	10	11	12	13
40.0 Milliseconds	d	-	-	.22	.30	-	-	-	.10	-	.13			
	a			4.0	5.5				2.0		3.0			
	$a/d^{\frac{1}{2}}$			4.26	4.27				4.47		4.80			
	Apparent Xc			1.46	1.47				1.67		2.00			
	Field Str. Ratio	1.0	.54	.21	.15	.13	.12	.12	.12	.13	.15	.21	.54	1.0
	Effective Xc	6.95	3.75	1.46	1.04	.90	.84	.84	.84	.90	1.04	1.46	3.75	6.95
		Total Voltage = 30.72 x 3.27 = 100KV												

BIBLIOGRAPHY

1. Evans, R. D., A. C. Monteith and R. L. Witzke, Power System Transients Caused by Switching and Faults, A.I.E.E. Trans. (1939) Vol. 58, pp. 386-94.

2. McCann, G. D., Impulse Characteristics of Oil Gaps from the Standpoint of Insulation Coordination, Ph.D. Thesis, Calif. Institute of Technology, 1939.

3. Wagner, C. F., G. D. McCann, and G. L. MacLane, Jr., Shielding of Transmission Lines, A.I.E.E. Trans. (1941) Vol. 60, p. 313.

4. Bellaschi, P. L., Lightning and 60-Cycle Power Tests on Wood-Pole Line Insulation, A.I.E.E. Trans. (1947) Vol. 66, pp. 838-50.

5. McCann, G. D. and Edward Beck, Field Research on Lightning Arrester Discharges, A.I.E.E. Trans. (1947) Vol. 66.

6. Rorden, Harold A., Lightning Arresters as a Criterion for Insulation Levels, A.I.E.E. Tech. Paper No. 50 - 14. Presented in January 1950 at Winter Convention of A.I.E.E.

7. Witzke, R. L. and T. J. Bliss, Coordination of Arrester Location with Transformer Insulation Level, A.I.E.E. Tech. Paper No. 50-153. Presented in June 1950 at Summer Convention of A.I.E.E.

8. Monteith, A. C. and W. G. Roman, Application of Station Type Lightning Arresters, Electric Journal, March 1938.

9. Evans, R. D. and A. C. Monteith, Recovery Voltage Characteristics of Typical Transmission Systems and Relation to Protector-Tube Applications, A.I.E.E. Trans., August 1938, Vol. 57, pp. 432-40.

10. Peterson, H. A., W. J. Rudge, Jr., A. C. Monteith and L. R. Ludwig, Protector Tubes for Power Systems, A.I.E.E. Trans., May 1940, Vol 59.

11. Evans, R. D. and W. A. Lewis, Selecting Breaker Speeds for Stable Operation, Electrical World, Feb. 15, 1930, pp. 336-40.

12. Grescom, S. B. and J. J. Torok, Keeping the Line in Service by Rapid Reclosure, Electrical Journal, May 1933, p. 201.

13. Sporn, P. and D. C. Prince, Ultra High-Speed Reclosing of High Voltage Transmission Lines, A.I.E.E. Trans., 1937, pp. 81-90.

14. Boisseau, A. C.,B. W. Wyman and W. F. Skeats, Insulator Flashover Deionization Times as a Factor in Applying High-Speed Reclosing Breakers, A.I.E.E. Trans., 1949, Vol. 68 Pt. II, pp. 1058-67.

15. Maury, E., Arc Extinction in the Ultra-Rapid Single-Phase Reclosure of 220 KV Lines, Rev. Gen. Elect., May 1944, Vol. 53, 79-90.

16. Slepian, J., Extinction of an A. C. Arc, A.I.E.E. Trans., Oct. 1928, Vol. 47.

17. Slepian, J., Extinction of a Long A. C. Arc, A.I.E.E. Trans., April 1930., Vol. 49.

18. Compton, K. T., Thermal Ionization Theory of Positive Column of Arc, Phys. Rev., 1923, Vol. 21, p. 286.

19. Saha, M. M., Ionization in Solar Chromosphere, Phil. Mag., 1920, Vol. 40, p. 472.

20. Slepian, J., Displacement and Diffusion in Fluid Flow Arc Extinction, A.I.E.E. Trans., 1941, p. 162.

21. Browne, T. E., Jr., Extinction of A. C. Arcs in Turbulent Gases, A.I.E.E. Trans., March 1932, Vol. 51

22. Browne, T. E., Jr., Dielectric Recovery by an A. C. Arc in an Air Blast, A.I.E.E. Trans., 1946, p. 169-175.

23. Prince, D. C., Theory of Oil Blast Circuit Breakers, A.I.E.E. Trans., March 1932, Vol. 51.

24. Attwood, S. S., W. C. Dow and W. Krausnick, Reignition of Metallic A. C. Arcs in Air, A.I.E.E. Trans., Sept. 1931, Vol 50, p. 854.

25. Browne, T. E., Jr., Extinction of Short A. C. Arcs, A.I.E.E. Trans., Dec. 1931, Vol 50, p. 1461.

26. McCann, G. D. and J. J. Clark, Dielectric Recovery Characteristics of Large Air Gaps, A.I.E.E. Trans., 1943, Vol. 62, pp. 45-52.

27. Bellaschi and Rademacher, Dielectric Strength of Station and Line Insulation to Switching Surges, A.I.E.E. Trans., 1946, Vol. 65.

28. Craggs, J. D., W. Hopwood and J. M. Meek, On the Localized After-glows Observed with Long Sparks in Various Gases, J. Appl. Phys., Oct. 1947, Vol. 18, 919-27.

29. Browne, T. E., Jr., and F. C. Todd, Extinction of Short A. C. Arcs, Phys. Rev., 1930, Vol. 36, p. 726.

30. Todd, F. C., and T. E. Browne, Jr., Restriking of Short Magnetic Arcs, Phys. Rev., 1930, Vol. 36, p. 732.

31. Felici, N. and Y. Marchal, New Investigations on Dielectric Strength of Gases, Rev. Gen. Elect., April 1948, Vol. 57, pp. 155-62.

32. Cobine, J. D., Effect of Oxides and Impurities on Metallic Arc Reignition, Phys. Rev., 1938, Vol. 53, p. 911.

33. Malter, Louis, Anomalous Secondary Electron Emission, A New Phenomenon, Phys. Rev., 1936, Vol. 49, p. 478.

34. Suits, C. G. and H. Poritsky, Application of Heat Transfer Data to Arc Characteristics, Phys. Rev., 1939, Vol. 55, p. 1184.

35. Slepian, J., Conduction of Electricity in Gases, Westinghouse Electric and Manufacturing Company, East Pittsburgh, Pennsylvania, 1933, p. 165.

36. McAdams, Heat Transmission, McGraw-Hill, New York, 1933, p. 248.

37. Suits, C. G., Convection Currents in Arcs in Air, Phys. Rev., 1939, Vol. 55, p. 198.

38. Perry, John H., Chemical Engineers' Handbook, Second Edition, McGraw-Hill, New York, 1941, pp. 974-84.

39. Bellaschi, P. L., Lightning and 60 Cycle Power Tests on Wood Pole Line Insulation, A.I.E.E. Trans., 1947, Vol. 66, pp. 838-50.

40. Browne, T. E., Jr., Dielectric Recovery of Turbulent Arcs, Physics, 1934, Vol. 5, pp. 103-113.

41. Townsend, Electrons in Gases, Hutchinson's Scientific, 1947, p. 108.

42. Schulz, P., and W. Weizel, Ionization and Temperature in High Pressure Electric Arcs, F. Phys., 1944, 122 (Nos. 9-12), pp. 697-705.

43. Cobine, J. D., Gaseous Conductors, McGraw-Hill, 1941, p. 520.

44. Benford, Frank, The Black Body, General Electric Review, July 1943, p. 377 and Aug. 1943, p. 433.

45. Perry, John H., Chemical Engineers' Handbook, Second Edition, McGraw-Hill, New York, 1941, pp. 974-984.